Adapting Land Use and Infrastructure for Automated Driving: Part A

Yafeng Yin

Adapting Land Use and Infrastructure for Automated Driving: Part A

by
Yafeng Yin
Donald Cleveland
Collegiate Professor of Engineering
University of Michigan

DISCLAIMER

Contacts

For more information:

Yafeng Yin
2350 Hayward Street
Ann Arbor, MI 48109
Phone: 734-647-4979
Email: yafeng@umich.edu

CCAT
University of Michigan Transportation Research Institute
2901 Baxter Road
Ann Arbor, MI 48152
umtri-ccat@umich.edu
(734) 763-2498

Technical Report Documentation Page

1. Report No. Final Report No. 8	2. Government Accession No.	3. Recipient's Catalog No.
4. Title and Subtitle Adapting Land Use and Infrastructure for Automated Driving: Part A DOI:10.7302/21950		**5. Report Date** 01/01/2028 – 01/04/2024
7. Author(s) Yafeng Yin: https://orcid.org/0000-0003-3117-5463		**8. Performing Organization Report No.**
9. Performing Organization Name and Address Center for Connected and Automated Transportation University of Michigan Transportation Research Institute 2901 Baxter Road Ann Arbor, MI 48109 University of Michigan Civil and Environmental Engineering Department 2350 Hayward Street Ann Arbor, MI 48109		**10. Work Unit No.**
		11. Contract or Grant No. Contract No. 69A3551747105
12. Sponsoring Agency Name and Address U.S. Department of Transportation Office of the Assistant Secretary for Research and Technology 1200 New Jersey Avenue, SE Washington, DC 20590		**13. Type of Report and Period Covered** Final Report (January, 2018 – January, 2024)
		14. Sponsoring Agency Code OST-R

15. Supplementary Notes

Conducted under the U.S. DOT Office of the Assistant Secretary for Research and Technology's (OST-R) University Transportation Centers (UTC) program.

16. Abstract

This project is concerned with adapting land use and transportation infrastructure for automated driving. Autonomous vehicles will likely yield a transformation of urban form, its land use and mobility system. We propose to establish quantitative modeling frameworks to analyze these impacts and implications. The frameworks will provide a quantifiable understanding of the tradeoffs, and reveal the underlying mechanism and identify key parameters that could shape the future of mobility systems and urban land use. Moreover, the proposed modeling frameworks will aid planning agencies with infrastructure adaptation planning and optimize a roadmap for shaping highway infrastructure towards automated mobility.

17. Key Words Infrastructure, highway infrastructure, autonomous vehicles, automated vehicles, mobility, planning, optimization quantitative modeling		**18. Distribution Statement** No restrictions.	
19. Security Classif. (of this report) Unclassified	**20. Security Classif. (of this page)** Unclassified	**21. No. of Pages** 88	**22. Price**

Form DOT F 1700.7 (8-72)   Reproduction of completed page authorized

Abstract

Automated vehicles (AVs) will likely yield a transformation of urban form, its land use and mobility system. This report is concerned with adapting land use and transportation infrastructure for automated driving. In the first part of the report, we propose an infrastructure-based approach to close the connectivity gap for connected and automated vehicles (CAVs) in a mixed traffic environment. It is envisioned that roadside units can be deployed to sense vehicles in their coverage areas and provide the beyond-line-of-sight motion information to CAVs to empower them to react proactively, as they would do when following other CAVs. We thus develop a quantitative modeling framework to analyze the impacts of this type of roadside units at the strategic planning level. In the second part, we analytically examine how the parking locations of AVs impact the morning and evening commuting pattern, and then investigate the optimal AV parking supply that minimizes the total system cost. We also offer some insights through numerical studies regarding relationship among traffic efficiency, tolling schemes and AV parking supply.

Table of Contents

List of Figures

List of Tables

1. Introduction

In the foreseeable future, the traffic stream will be likely mixed with connected automated vehicles (CAVs) and regular vehicles (RVs). In the mixed traffic environment, when following a RV, due to the lack of vehicle-to-vehicle communications, it may take longer time for a CAV sense and react than a human driver, which results in longer time headway and reduces highway throughput. To address such a connectivity gap, this project investigates an infrastructure-based solution, i.e., the deployment of roadside units to further improve the performance of CAVs in the heterogeneous traffic stream. Specifically, it is envisioned that these roadside units can sense vehicles in their coverage areas and provide the beyond-line-of-sight motion information to CAVs to empower them to react proactively, as they would do when following other CAVs. Chapter 2 of this study is devoted to the analysis of the impacts of this type of roadside units at a strategic planning stage. In doing so, we first derive an analytical link performance function to capture their impact on the link capacity and travel time, and then develop a network equilibrium model to gauge their effect on travelers' route choices and thus the flow distribution of both RVs and CAVs across the whole network. This modeling development will allow us to conduct a cost-benefit analysis for a given deployment plan of roadside units. For a fair analysis, we further develop an optimization model to determine the optimal deployment plan for a given budget, while focusing on the worst case of its impact, because the flow distribution resulting from our network equilibrium model is not unique. Such a model provides a conservative estimate of the benefit brought by roadside units. Lastly, we offer case studies to demonstrate the models and unveil the potential of such an infrastructure-based solution. Chapter 2 is a collaborative work with Ye Li, Central South University, China, and Zhibin Chen, NYU Shanghai, China.

Chapter 3 of this study is devoted to analytically investigate the traffic dynamics of the integrated morning and evening commutes when daily trips are completed with automated vehicles (AVs). Given the parking locations of AVs resulting from the morning commute, firstly we analyze the evening commuting pattern, at which no traveler can reduce the individual travel cost given other AVs' times of departures from the parking spaces. The equilibrium traffic pattern at the evening commute is then integrated with the morning commute, where equilibrium choices of departure time from home and parking location are derived and analyzed. We then study the integrated morning-evening commuting pattern at the system optimum and develop the first-best road tolling scheme to achieve the system optimum. Furthermore, this study analyses the optimal AV parking supply strategy to minimize the total system cost, which is comprised of the total social parking cost and the total daily travel cost under either user equilibrium or system optimum traffic pattern. We also illustrate the modelling insights through numerical studies regarding relationship among traffic efficiency, tolling schemes and AV parking supply plans. This study highlights the

differences in daily commuting and parking patterns between the AV situation and the non-AV situation, and sheds light on how traffic and parking should be managed or planned in the future. Chapter 3 is a collaborative work with Xiang Zhang, Wei Liu, S. Travis Waller, University of New South Wales, Sydney, Australia.

2. Deployment of Roadside Units to Overcome Connectivity Gap in Transportation Networks with Mixed Traffic

2.1 Introduction

Among many other benefits, CAVs are expected to improve safety and increase the throughput of highway facilities. Specifically, with vehicle-to-vehicle (V2V) communications, a CAV can receive the information from another CAV it follows and make decisions proactively. This yields much shorter sensing-perception-reaction time and consequently improves safety and throughput (Van et al., 2006; Shladover et al., 2012). However, as the popularization of CAV is expected to be a gradual process, the traffic steam will be mixed with CAVs and regular vehicles (RVs) for a long time. In a mixed traffic environment, when a CAV follows a RV, it may take longer time for the CAV to sense and react than a human driver, which can amplify speed variations and cause unstable traffic flow (Milanés and Shladover, 2014; Milanés et al., 2014). This is particularly true at the early deployment of CAVs when their market penetration is low and the technology is not sufficiently advanced. With a low market penetration of CAVs, the likelihood of a CAV following another CAV is low. More importantly, car manufacturers may likely configure their CAVs with a lower operation speed and excessive safety clearance, i.e., longer time headway, to ensure safety to avoid liability. Undoubtedly, the presence of these types of CAVs in the traffic stream will slow other vehicles down and thus compromise the efficiency of transportation systems, as recognized by recent studies such as Chen et al. (2017), Ghiasi et al. (2017), Seo and Asakura (2017) and Calvert et al., (2017). Such an efficiency degradation could last for a while until the market penetration of CAVs reaches a certain threshold. This period is referred as the "dark age" of CAV deployment by Luo et al. (2019).

A potential solution to the above issue is to designate CAV-only facilities so that CAVs can make full use of the V2V communications to form a platoon with much shorter headways. However, such a solution improves social welfare only if the market penetration is sufficiently large. Ye and Yamamoto (2018) established a three-lane heterogeneous flow model to explore the impact of dedicated CAV lanes on the traffic flow throughput, and found that at a low CAV penetration rate, setting CAV dedicated lanes reduces the overall traffic flow throughput. Recognizing this point, Chen et al. (2016) developed a model to optimally deploy dedicated lanes for CAVs while considering the diffusion process of CAVs. Their model specifies when, where, and how many CAV lanes should be deployed in a general transportation network. Later, Chen et al. (2017) further extended the idea to design dedicated CAV-only zones. Recently, Chen et al. (2019) and Ye and Wang (2018) further integrated the idea of CAV lanes

with economic instruments, such as purchase subsidy and congestion pricing, to further increase social welfare.

In this report, we suggest another infrastructure-based solution to close the connectivity gap for CAVs. The proposed solution is to deploy roadside units equipped with sensing and communications devices. It is envisioned that these roadside units can sense vehicles in their coverage areas, and communicate the beyond-line-of-sight motion information to CAVs. Such a real-time information provision enable CAVs to react proactively, as they would do when following another CAV. Note that the roadside units of interest are conceptually similar to those currently deployed for connected vehicles, but with one essential difference: the capability of direct sensing of vehicles via, e.g., cameras. We further note that such integrated roadside units have started to appear on the market. Our solution falls in line with the general concept of infrastructure-assisted automated driving, which has been recently explored by other researchers. For example, the Managing Automated Vehicles Enhances Network (MAVEN) project is developing traffic management schemes from the infrastructure side to better monitor and coordinate CAVs on signalized intersections and corridors (Lu and Blokpoel, 2016; MAVEN, 2019; Rondinone et al., 2018; Rondinone, 2019).

Clearly, the proposed infrastructure-based solution is costly to implement. An immediate question would be whether the benefit can justify its cost. To this end, this study conducts a cost-benefit analysis to validate the potential of such a solution. While the investment cost of roadside units can be easily estimated, their benefits are much more difficult to assess. The focus of the study is thus on the latter. Our objective is modest. We attempt to establish a modeling framework to offer a macroscopic, ballpark estimate of the impact of roadside units on the performance of a transportation network at the strategic planning stage. In doing so, we first start at a facility level and analytically derive a new link performance function to capture the impact of roadside units on link capacity and travel time. A network equilibrium model integrating the established link performance function is then proposed to estimate how roadside units will further impact travelers' route choice and thus the system performance. With the proposed equilibrium model, the mixed traffic flow distribution of both CAVs and RVs across the road network with the presence of roadside units can be delineated, enabling a cost-benefit analysis for a given deployment plan of roadside units. For a fair and sensible analysis, we further develop an optimization model to determine the optimal deployment plan for a given budget, while focusing on the worst case of its impact, because the flow distribution resulting from our network equilibrium model is not unique. Such a model provides a conservative estimate of the benefit brought by roadside units. The established

deployment model is a nonlinear minimax problem with complementarity constraints, and a heuristic procedure based on the cutting-plane scheme is developed to solve the model. Lastly, we offer two numerical examples to demonstrate the proposed models and solution algorithm, and more importantly, to conduct cost-benefit analyses to make a case for the proposed infrastructure-based solution.

The remaining of the chapter will be organized as follows. In Section 2.2, a new link performance function and a network equilibrium model are established to capture the impacts of roadside units on the link capacity/travel time and the network performance, respectively. Section 2.3 presents the deployment model that optimizes the deployment plan of roadside units whereby their benefit can be conservatively estimated. The solution algorithm is also discussed. The section is followed by case studies and cost-benefit analyses in Section 2.4.

2.2 Capturing the Impacts of Roadside Units

Figure 2.1 is a sketch on how roadside units work. The roadside units are used to sense multiple vehicles upstream and provide their motion information to the following CAV via vehicle-to-infrastructure (V2I) communication. The beyond-line-of-sight motion information will allow CAVs to respond proactively so as to improve the safety of CAVs and the traffic stream stability (Treiber et al., 2006; Ngoduy and Jia, 2017; Wang, 2018). It can also reduce the time headway of the following CAV and increase highway throughput. Below we propose mathematical models to capture the impacts of roadside units on the link travel time and the network efficiency respectively.
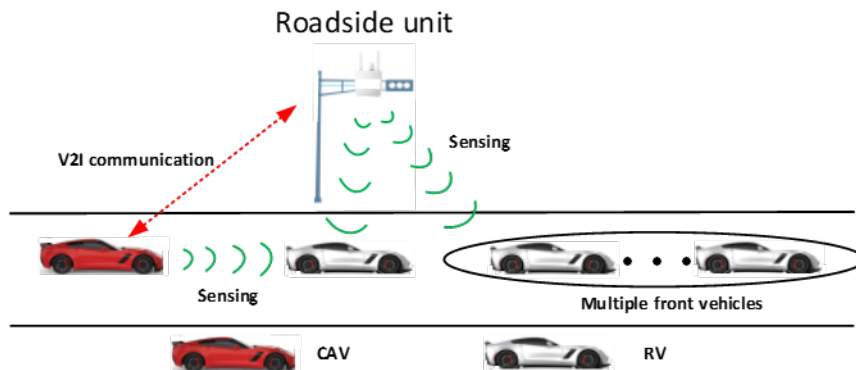
Figure 2.1: Illustration of the function of roadside units

2.2.1 Impact on the link travel time

The aim of this subsection is to capture the impact of roadside units on link capacity and travel time at the steady state for the planning purpose. Our derivation is in the same spirit as previous studies such as Chen et al. (2017) and Seo and Asakura (2017). As shown in Figure 2.2, there are totally four car-following scenarios in a heterogeneous traffic stream involving CAVs and RVs: CAV follows CAV or RV, and RV follows CAV or RV. As the critical headways are the same for a RV following a CAV or a RV, we use L_R to denote them. For the critical headway when a CAV following a CAV or a RV, we define them as L_C and L_A, respectively. Since roadside units provide the beyond-line-of-sight information to the CAV when it is following a RV, the critical headway for the CAV (denoted by L_I) can be shorten, i.e., $L_I < L_A$. Furthermore, considering the advancement level of existing technologies, we assume that the relation among L_A, L_R, L_I and L_C follows $L_A \geq L_R > L_I > L_C$ (Milanés and Shladover, 2014; Milanés et al., 2014).
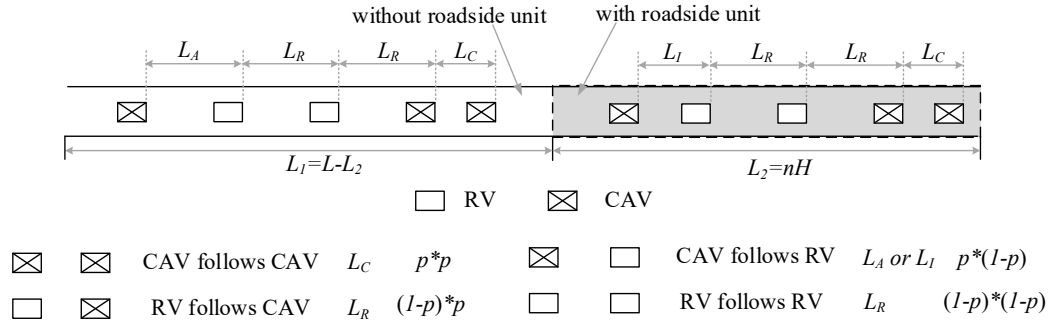
Figure 2.2: Illustration of car-following scenarios

We define the proportion of CAVs in the mixed traffic on a link as p, and the proportion of RVs is thus $1 - p$. The probability of occurrence for these four car-following scenarios in the traffic stream can be estimated as $P(\text{CAV follows CAV}) = p \cdot p$, $P(\text{CAV follows RV}) = p \cdot (1 - p)$, $P(\text{RV follows CAV}) = (1 - p) \cdot p$, and $P(\text{RV follows RV}) = (1 - p) \cdot (1 - p)$. Suppose the coverage or detected length of a roadside unit as H, then for a link deployed with n roadside units, the total length covered by roadside units is nH. To capture the effect of roadside units, the link can be conceptually divided into multiple sub-links, each of which is either covered by a roadside unit or not. As we assume that the deployment of roadside units will only affect the headway of CAVs following RVs, and we consider a steady state for the planning purpose

6

without capturing traffic dynamics, specific locations of these roadside units on a particular link will not affect the total travel time for traversing through the link. Therefore, all the roadside units on a link can be regarded as being deployed consecutively, such that the link is divided into only two sub-links, one without roadside units (denoted by sub-link 1), and the other one covered by roadside units (denoted by sub-link 2), as displayed in Figure 2.2. Suppose the length of the link is L, then the length of sub-link 2 (denoted by L_2), as previously mentioned, would be equal to nH. The length of sub-link 1 is $L_1 = L - nH$.

Given the proportion of CAVs, i.e., p, in the mixed traffic stream, the capacity of sub-link 1 can be derived as below:

$$q_{M1} = \frac{v_M}{(1-p)L_R + p^2 L_C + p(1-p)L_A}$$
$$= \frac{1}{(1-p)h_R + p^2 h_C + p(1-p)h_A} \tag{1}$$

where q_{M1} defines the capacity of sub-link 1; v_M defines the critical speed, which is assumed to be the same for both two sub-links (Chen et al., 2017); and h_R, h_C and h_A are the critical time headways corresponding to L_R, L_C and L_A, respectively. In Eq. (1), $(1-p)L_R + p^2 L_C + p(1-p)L_A$ represents the average space headway on sub-link 1.

Similarly, we can derive the capacity of sub-link 2:

$$q_{M2} = \frac{v_M}{(1-p)L_R + p^2 L_C + p(1-p)L_I}$$
$$= \frac{1}{(1-p)h_R + p^2 h_C + p(1-p)h_I} \tag{2}$$

where q_{M2} is the capacity of sub-link 2; and h_I is the critical time headway corresponding to L_I.

Without loss of generality, the link travel time is assumed to follow the Bureau of Public Roads (BPR) function, so the travel times of the two sub-links can be estimated as follows:

$$t_1 = \frac{L_1}{v_0}\left(1 + \alpha\left(\frac{x_A + x_R}{q_{M1}}\right)^\beta\right) \tag{3}$$

$$t_2 = \frac{L_2}{v_0}\left(1 + \alpha\left(\frac{x_A + x_R}{q_{M2}}\right)^\beta\right) \tag{4}$$

where v_0, x_A, x_R are respectively the free-flow speed, traffic flows of CAVs and RVs, which are the same for both sub-links; and α and β are positive coefficients.

Accordingly, the travel time of the whole link can be easily derived as follows:

$$t = \frac{L - nH}{v_0}\left(1 + \alpha\left(x\big((1-p)h_R + p^2 h_C + p(1-p)h_A\big)\right)^\beta\right)$$
$$+ \frac{nH}{v_0}\left(1 + \alpha\left(x\big((1-p)h_R + p^2 h_C + p(1-p)h_I\big)\right)^\beta\right)$$

where $x = x_A + x_R$ and $p = x_A/x$. Note that this travel time function is non-monotone and asymmetric.

2.2.2 Impact on the network efficiency

As mentioned in the above subsection, the presence of roadside units will impact the link capacity and travel time, and can thus potentially change the route choice of travelers of using a RV or CAV, yielding a different traffic flow distribution across the network. To capture such an effect, a network equilibrium model is presented in this subsection.

Let $Q(N, A)$ denote a general transportation network, where N and A are sets of nodes and links, respectively. The set of origin-destination (O-D) pairs is denoted by W. Let $M = \{1,2\}$ denote the set of classes, where class 1 corresponds to RVs and class 2 corresponds to CAVs. Let Δ be the node-link incidence matrix, and $E^{w,m}$ be a vector where $w \in W$ and $m \in M$. The vector has two non-zero components: one has a value of 1 corresponding to the origin of w and the other has a value of -1 corresponding to the destination of w. $x_a^{w,m}$ is the link flow of class $m \in M$ between O-D pair $w \in W$ on link a, and $t_a(\cdot)$ is the link travel time function defined by Equation (5).

At equilibrium, all utilized paths of the same travel mode between the same O-D pair share the same travel cost, while those unutilized ones possess equal or higher travel cost. Mathematically, the multiclass network equilibrium conditions can be written as follows:

$$\Delta x^{w,m} = E^{w,m} d^{w,m} \qquad\qquad \forall w \in W, m \in M \qquad (6)$$

$$x_a^{w,m} \geq 0 \qquad\qquad \forall a \in A, w \in W, m \in M \qquad (7)$$

$$t_a \left(\sum_{m \in M} \sum_{w \in W} x_a^{w,m} \right) \geq \rho_j^{w,m} - \rho_i^{w,m} \qquad\qquad \forall a \in A, w \in W, m \in M \qquad (8)$$

$$\left[t_a \left(\sum_{m \in M} \sum_{w \in W} x_a^{w,m} \right) - \rho_j^{w,m} + \rho_i^{w,m} \right] x_a^{w,m} = 0 \qquad\qquad \forall a \in A, w \in W, m \in M \qquad (9)$$

where ρ are auxiliary variables.

Define $\Omega = \{x | (6), (7)\}$. the above equilibrium conditions (6)-(9) are equivalent to finding $x^* \in \Omega$ that solves the following variational inequality (VI) problem (NE-VI):

$$\sum_{m \in M} \sum_{w \in W} \sum_{a \in A} t_a \left(\sum_{m \in M} \sum_{w \in W} x_a^{w,m*} \right) (x_a^{w,m} - x_a^{w,m*}) \geq 0 \qquad\qquad \forall x \in \Omega \qquad (10)$$

The equivalence is trivial to establish by comparing the optimality condition of NE-VI with the equilibrium conditions. The NE-VI has the following two properties: 1) There exists at least one solution. The feasible region of NE-VI is compact and convex, and all the functions are continuous. Therefore, the NE-VI problem has at least one solution as per Weierstrass' theorem (Bazaraa et al., 2013). 2) Due to the non-monotone link performance function, there may exist multiple equilibrium flow distribution, which is further illustrated by the following example.

Consider a toy network with only one O-D pair connected by two parallel links, and suppose the demand of CAVs and RVs between the O-D pair are 10 and 4, respectively. Assume L/v_0=1 hour, α=1, β=1, h_R=1.5 s, h_A=1.5 s, h_C=0.6 s and h_I=1.1 s, and suppose the two links are deployed with the same number of roadside units (denoted by n). Therefore, the link performance function of the two links can be simplified as:

$$\tilde{t}_1 = \left(1 - \frac{nH}{L}\right)\left(1 + x(1.5(1 - p_1^2) + 0.6p_1^2)\right)$$
$$+ \frac{nH}{L}\left(1 + x\left(1.5(1 - p_1) + 0.6p_1^2 + 1.1p_1(1 - p_1)\right)\right)$$

where x_{A1}, x_{A2}, x_{R1} and x_{R2} are the flows of CAVs and RVs on link 1 and link 2, respectively; and $p_1 = x_{A1}/(x_{A1} + x_{R1})$ and $p_2 = x_{A2}/(x_{A2} + x_{R2})$.

Suppose $n = 0.5L/H$, then it is easy to verify that $(x_{A1}, x_{R1}, x_{A2}, x_{R2}) = (10, 0, 0, 4)$ and $(5, 2, 5, 2)$ are both equilibrium flow distribution with $\tilde{t}_1 = \tilde{t}_2 = 7$, and $\tilde{t}_1 = \tilde{t}_2 = 9.575$. Actually, there is an infinite number of equilibrium flow patterns. Figure 2.3 illustrates the total travel times corresponding to different equilibrium flow patterns, given different value of n. The horizontal axis is x_{A1}, representing the CAV flow on link 1, and vertical axis represents the total system travel time. As evident in Figure 2.3, each roadside-unit deployment plan may yield an infinite number of equilibrium flow patterns in this toy network.
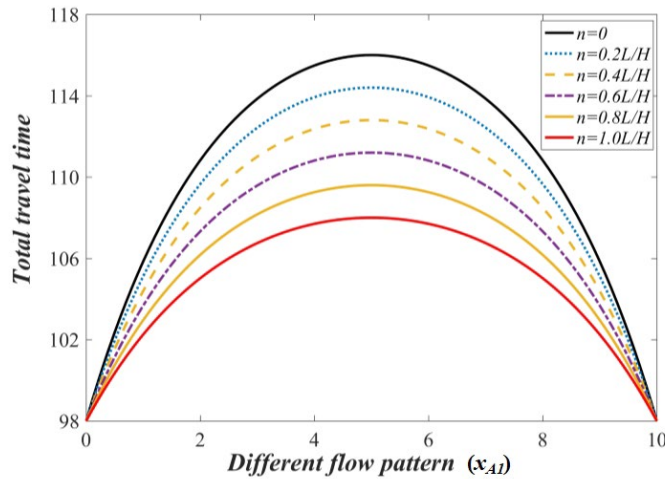
Figure 2.3: Total travel time of different equilibrium flow patterns

2.3. Deployment Model and Solution Algorithm

The non-uniqueness of the equilibrium flow distribution presents a challenge for conducting cost-benefit analysis for a specific deployment plan of roadside units. Planners have been

relying on the typically unique equilibrium flow distribution as the sole estimate or forecast of how traffic will react to changes in the transportation system. In contrast, our model produces a range of possible flow distributions corresponding to a deployment. To avoid overestimating the benefit, it is prudent to use the one with maximum total system travel time for cost-benefit analysis, as it yields the minimum savings. On the other hand, it is sensible to assume that the investment is well spent and thus consider an optimal deployment plan. These two points motivate us to develop a deployment model that provides a conservative estimate of the benefit brought by the roadside units while considering an optimal decision making process.

2.3.1 Deployment model

We develop an optimization model to determine a deployment plan whose worst-case system travel time (among all potential equilibrium flow distributions) is minimized. In the literature, some, e.g., Ban et al., (2009), refer to the solution to this type of models as a risk averse solution, while others, e.g., Lou et al. (2010), call it as a robust solution. The robust deployment (RD) model can be readily formulated as follows:

$$\min_{n} \max_{x,\rho} \sum_{a \in A} \sum_{m \in M} \sum_{w \in W} t_a \left(\sum_{m \in M} \sum_{w \in W} x_a^{w,m}, n_a \right) x_a^{w,m}$$

s.t. (6)-(9)

$$\sum_{a \in A} \pi n_a \leq B \tag{11}$$

$$n_a \in \{0,1,\dots,I_a\} \qquad\qquad \forall a \in A \tag{12}$$

where L_a is the length of link a; $I_a = \left\lceil \frac{L_a}{H} \right\rceil$, which is the minimum number of roadside units needed to fully cover the link; π is the cost of deploying one roadside unit; B is the budget limit; and n_a represents the number of roadside units deployed at link a. Note that, when $n_a = I_a$ and $n_a H > L_a$, Eq. (5) reduces to

$$t_a = \frac{L_a}{v_0} \left(1 + \alpha \left(x \big((1-p)h_R + p^2 h_C + p(1-p)h_I \big) \right)^\beta \right).$$

The objective of the above RD model is to minimize the worst-case system travel time.

Specifically, the inner problem identifies the worst case with the maximum total travel time among all possible equilibrium solutions that satisfy conditions (6)-(9); while the outer problem determines a deployment plan to minimize the worst-case travel time with the budget constraint (11) and considering the integral nature of n, i.e., constraint (12). The difficulty of solving the RD model is that the inner constraints (8) and (9) are affected by the decision variable n in the outer problem, which are coupled constraints. Moreover, the coupled constraints (8) and (9), together with constraint (7), constitute complementarity constraints, which make the above RD model very difficult to solve.

2.3.2 Cutting-plane scheme

Although previous studies have proposed a number of algorithms for solving the minimax problem, most of them deal with decoupled problems or coupled optimization with linear constraints (Shimizu and Aiyoshi, 1980; Stein, 2012; Zeng, 2015). In this study, we develop a heuristic procedure to solve the RD model based on a cutting-plane scheme, which has been used to solve semi-infinite optimization problem (Lawphongpanich and Hearn, 2004; Lou et al., 2010). The core idea is to solve a relaxed version of the original problem with a subset of feasible region, and then expand the subset until the optimal solution is achieved.

The RD model belongs to the coupled robust optimization problem, which has the following generic structure:

$$\min_{\psi \in \Lambda} \max_{\xi \in \Phi} f(\psi, \xi)$$

$$s.t. \ G(\psi, \xi) = 0$$

where the inner problem variable ξ is determined by outer problem variable ψ due to the constraints $G(\psi, \xi) = 0$. Let's assume at this moment that there is no joint constraints and the problem would have the following equivalent formulation:

CRO:

$$\min_{\psi,\theta} \theta$$

$$\text{s.t. } f(\psi, \xi) \leq \theta, \forall \xi \in \Phi$$

$$\psi \in \Lambda$$

Next, we consider to relax the CRO problem as follows:

CRO-R:

$$\min_{\psi,\theta} \theta$$

$$\text{s.t. } f(\psi, \xi) \leq \theta, \forall \xi \in \Phi^k$$

$$\psi \in \Lambda$$

where Φ^k is the subset of Φ at the kth iteration. Let ψ^k denote the optimal solution to the CRO-R model, then the inner problem turns out to be:

CIP:

$$\max_{\xi \in \Phi} f(\psi^k, \xi)$$

Solving CIP can generate an optimal solution, i.e., ξ^{k+1}, to $\max_{\xi \in \Psi} f(\psi^k, \xi)$ corresponding

to the current given decision in CRO-R, i.e., ψ^k. If the current objective value $f(\psi^k, \xi^{k+1}) \leq \theta$, then ψ^k and ξ^{k+1} are the optimal solution to the original CRO problem, as any action in the inner problem cannot worsen the outcome. Otherwise, extending Φ^k to Φ^{k+1} by adding ξ^{k+1}, and solving CRO-R based on Φ^{k+1} to figure out a better solution ψ^{k+1}. Repeat the above process until the object value of the inner problem is no greater than the one of the outer problem, i.e., θ.

However, with the presence of the coupled constraint, as the feasible set of the decision variable ξ in the inner problem is heavily affected by the value of ψ^k via the coupled constraints, the above cutting-plane algorithm is not readily applicable. Our remedy is to utilize a penalty function to remove the coupled constraint and reformulate the CRO problem as follows:

CRO-P:

$$\min_{\psi,\theta} \theta$$

$$s.t.\ f(\psi,\xi) - M\|G(\psi,\xi)\|_2 = \varphi(\psi,\xi) \leq \theta, \forall \xi \in \Phi$$

$$\psi \in \Lambda$$

where M is a sufficiently-large positive constant. Thus, when $\|G(\psi,\xi)\|_2 \neq 0$, the $\varphi(\psi,\xi)$ will be sufficiently small. Accordingly, the relaxation of CRO-P problem is:

CRO-P-R:

$$\min_{\psi,\theta} \theta$$

$$s.t.\ f(\psi,\xi) - M\|G(\psi,\xi)\|_2 = \varphi(\psi,\xi) \leq \theta, \forall \xi \in \Phi^k$$

$$\psi \in \Lambda$$

Consequently, the relaxed inner problem becomes:

CIP-R:

$$\max_{\xi \in \Phi} f(\psi^k,\xi) - M\|G(\psi^k,\xi)\|_2$$

As a result, the cutting-plane scheme can be used for the CRO-P problem. Below lists the completed solution process:

Step0: Initialization: $k = 1$, $\Phi^1 = \{\xi^1\}$.

Step1: Solve the CRO-P-R with Φ^k and let (ψ^k, θ^k) denote the optimal solution.

Step2: Solve the CIP-R with ψ^k and let ξ^{k+1} be the optimal solution.

Step3: If $f(\psi^k, \xi^{k+1}) \leq \theta^k$, then stop and ψ^k is the optimal solution of the original CRO problem; otherwise, set $\Phi^{k+1} = \Phi^k \cup \{\xi^{k+1}\}$, and go to **Step 1**.

In the RD problem, constraints (8) and (9) are the coupled constraints. To apply the process, we can replace the former with the following:

$$\rho_j^{w,m} - \rho_i^{w,m} + \eta_a^{w,m} = t_a\left(\sum_{m \in M}\sum_{w \in W} x_a^{w,m}\right) \qquad \forall a \in A, w \in W, m \in M \qquad (13)$$

$$\eta_a^{w,m} \geq 0 \qquad\qquad \forall a \in A, w \in W, m \in M \quad (14)$$

Consequently, $G_1(\boldsymbol{\psi}, \boldsymbol{\xi}) = \left[t_a (\sum_{m \in M} \sum_{w \in W} x_a^{w,m}) - \rho_j^{w,m} + \rho_i^{w,m} \right] x_a^{w,m}$ and $G_2(\boldsymbol{\psi}, \boldsymbol{\xi}) =$

$\rho_j^{w,m} - \rho_i^{w,m} + \eta_a^{w,m} - t_a (\sum_{m \in M} \sum_{w \in W} x_a^{w,m})$, and then the proposed solution algorithm

can be adopted to solve the RD problem.

Lastly, we note that, assuming that both $\boldsymbol{\psi}^k$ and $\boldsymbol{\xi}^{k+1}$ globally solve CRO-P-R and CIP-R at Step 1 and 2 respectively, if the above algorithm stops at some finite iteration, the process generates an optimal solution to the CRO-P problem. In our computational experiments, we did observe that the algorithm terminated in a finite number of steps. However, since it is difficult to ensure the global optimality for solving CRO-P-R and CIP-R problems, we do not claim that we can always find global optimal solutions. We essentially regard the above algorithm as heuristic.

2.4 Case Studies

In this section, two case studies are conducted to demonstrate the proposed models and solution algorithm. The primary objective of the first case study, based on a hypothetical nine-node network (Wu et al., 2011) is to validate the proposed solution algorithm while the second one is conducted on the South Florida network to showcase how the model can be applied to a realistic network. For both networks, cost-benefit analyses are offered to quantify the benefit-cost ratio (BCR) of the deployment of roadside units. For parsimony, we replace B/π in Eq. (11) with D, representing the maximum number of roadside units that could be deployed on the whole network given the limited budget. The common parameter settings include $\alpha = 0.15$, $\beta = 4$, $h_R = 1.5$ s, $h_A = 1.5$ s $h_C = 0.6$ s and $h_I = 1.1$ s (Milanés and Shladover, 2014; Milanés et al., 2014; Li et al., 2017).

2.4.1 Nine-node network

Tables 2.1 and 2.2 show the O-D demand and the network characteristic, respectively. Suppose the coverage length $H = 1$ km, Table 2.3 compares the objective function value of the proposed algorithm with the one resulting from enumeration, which is feasible when D is small and ensures global optimality. As we can see, the result gaps are both 0 with D equals 1 and 2, indicating that the proposed algorithm yields the global optimal

solution in these two cases. While D becomes larger than 2, as the total number of possible deployment plans increases exponentially, we cannot enumerate all the plans to verify the global optimality of the solution. Figure 2.4 illustrates the convergence pattern of the proposed solution algorithm for $D = 10$. The detailed optimal deployment plan and resultant flow distribution are presented in Table 2.4. Table 2.5 presents the comparison between the results corresponding to $D = 0$ and $D = 10$. It is evident that the travel times of the links deployed with roadside units, such as link 2-5, 5-7 and 9-8, can be reduced significantly. Correspondingly, the shortest path travel time for all the four O-D pairs decrease by 2.55% to 4.03%. Regarding the total system travel time, the optimal deployment plan can reduce it by 3.32%. More specifically, the total travel time of RVs and CAVs are both reduced by 3.32%. It implies that deploying roadside units can considerably benefit the system and both types of vehicles.

Table 2.1: O-D demand for the nine-node network

O-D	RV	CAV
1-3	6	3
1-4	12	6
2-3	18	9
2-4	24	12

Table 2.2: The characteristics of the nine-node network

Link	Number of Lanes	$\frac{L}{v_0}$ (min)	L (km)	I_a	Link	Number of Lanes	$\frac{L}{v_0}$ (min)	L (km)	I_a
1-5	2	5.00	10	10	6-9	5	7.00	14	14
1-6	3	6.00	12	12	9-7	4	4.00	8	8
2-5	6	3.00	6	6	9-8	3	2.00	4	4
2-6	6	9.00	18	18	7-3	4	3.00	6	6
5-6	3	9.00	18	18	7-4	4	6.00	12	12
5-7	2	2.00	4	4	7-8	3	2.00	4	4
5-9	4	8.00	16	16	8-3	6	8.00	16	16
6-5	2	4.00	8	8	8-4	6	6.00	12	12
6-8	5	6.00	12	12	8-7	6	4.00	8	8

Table 2.3: Optimality gap of different value of D

D	1	2
Objective value of proposed algorithm	6766.80	6736.08
Objective value by enumeration	6766.80	6736.08
Gap	0.00	0.00

Table 2.4: Equilibrium flow and travel time with D=10

Link	RV flow	CAV flow	Travel time (min)	Deployment (n_a)
1-5	6.85	3.31	16.58	0
1-6	11.15	5.69	26.26	0
2-5	23.79	10.91	**13.99**	**2**
2-6	18.21	10.09	23.67	0
5-6	3.94	2.84	9.68	0
5-7	13.51	4.21	**41.52**	**4**
5-9	13.19	7.16	25.82	0
6-5	18.69	11.09	4.00	0
6-8	14.61	7.54	30.11	0
6-9	13.27	9.14	16.13	0
9-7	14.53	5.56	15.71	0
9-8	12.59	6.26	**13.97**	**4**
7-3	14.19	7.09	8.09	0
7-4	11.41	5.74	22.48	0
7-8	21.81	10.91	2.00	0
8-3	6.85	3.31	9.83	0
8-4	11.15	5.69	24.21	0
8-7	0.00	0.00	4.00	0
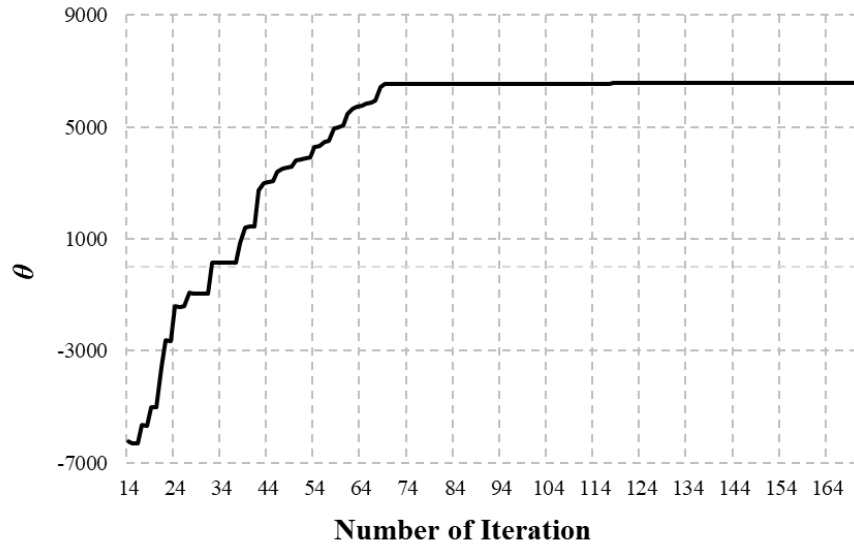
Figure 2.4 The iterative solution of proposed algorithm for nine-node network with D=10

Table 2.5 Comparison between the results corresponding to D=0 and D=10

Travel time	$D=0$	$D=10$	Reduction
1-3	68.30	66.20	**-3.08%**
1-4	82.69	80.58	**-2.55%**
2-3	66.28	63.61	**-4.03%**
2-4	80.67	77.99	**-3.32%**
Total travel time	6796.98	6571.33	**-3.32%**

2.4.2 South Florida network

In addition to the above small arbitrary network, the proposed roadside-unit deployment model is applied to a realistic network, i.e., the South Florida network. Specifically, it contains 82 nodes and 234 links, as shown in Figure 2.5. Demands of 12 O-D pairs are considered (see Table A1 in the appendix) and the network characteristics are given in Table A2 of the appendix. We first solve the R-RD problem with $D = 0$ and assume those 10 links with the largest flow to be candidates for the roadside-unit deployment. Then, the R-RD problem with $D = 10$ and $H = 1$ km is solved and the results are shown in Table 2.6. As we can observe, compared with $D = 0$, the optimal deployment of 10 roadside units can yield a 4.07% reduction on the total travel time, from 264,825.24 to

18

254,034.47. In particular, under the optimal deployment plan, all of the roadside units are deployed on link 64-63. It may imply that the concentrated deployment of roadside units could yield better outcome. Given such a concentrated deployment plan, the shortest path travel time of all O-D pairs with node 64 as origin have been reduced substantially (see Table 2.6).

Table 2.6: Result of deployment for the South Florida network

Path time	D=0	D=10
1-22	135.52	135.52
1-28	272.07	272.07
1-64	277.75	277.75
22-1	146.11	146.11
22-28	139.60	139.60
22-64	208.93	208.93
28-1	282.07	282.07
28-22	139.47	139.47
28-64	329.45	329.45
64-1	317.08	**280.75**
64-22	239.03	**202.70**
64-28	359.72	**323.39**
Total travel time	264,825.24	254,034.47
Reduction		-4.07%
Deployment plan		10 units on link 64-63

2.4.3 Cost-benefit analysis

The cost-benefit analysis is conducted for both nine-node and South Florida networks to answer the question of whether the benefit of deploying roadside units can justify its cost. To this end, we adopt the following parameter settings for the nominal case: (1) value of time (VOT) for RV and CAV: $0.5/min; (2) capital cost of roadside-unit deployment: $12,500/unit; (3) operating and maintenance cost: $3,000/unit/year; (4) lifetime: 10 year; (5) discount rate: 3% /year; (6) $D = 10$. The volume of peak hour is assumed to account for 10% of average daily volume. Based on the equilibrium network flow distributions on the nine-node and South Florida networks before and after the deployment of roadside units, and the above settings, the BCRs are calculated in Table 2.7. Specifically, the bold texts in the table represent the BCRs for the nominal case. As we can see, the BCRs on the nine-node and South Florida networks are 9.31 and

445.27, respectively. They are much higher than 1, indicating that the benefit of deploying roadside units is far more than its investment cost. Given that the costs for deploying, operating, and maintaining the roadside units are subject to uncertainty, a sensitivity analysis of the unit investment cost is presented in Table 2.7. We can observe that, although the BCRs will decrease with the increase in the investment cost of roadside units, they are still far larger than 1.

Similarly, as the roadside-unit coverage length (i.e., H) may vary as the technology advances, Table 2.7 also provides its sensitivity analysis on the BCR (see the 4th row). As expected, when the coverage length increases, the BCRs increase for both networks. Also, they are all much higher than 1.

Without concentrating on driving the vehicles, CAV travelers can engage on other activities, so their VOTs are expected to be lower than that of RV drivers. In view of this, another sensitivity analysis is conducted in Table 2.7 to investigate how the change of CAV travelers' VOT will affect the BCRs (see the 6th row). As we can see, when the value of VOT increases, the BCR will increase. The increasing VOT will not affect the flow distribution of CAVs or RVs but yield an increase in the value of travel time savings. Similar to roadside unit costs, the BCRs corresponding to various CAV travelers' VOT are all far greater than 1. All these results show that the benefit brought by the deployment of roadside units may far outweigh their investment costs.

Table 2.7: Sensitivity Analysis of Roadside-Unit Investment Costs, Coverage Length _H_ and VOT of CAV Users on the BCR

Change of the unit investment cost	**0%**		100%		150%		200%
BCR in Nine node	**9.31**		4.66		3.72		3.10
BCR in South Florida	**445.27**		222.64		178.11		148.42
_H_	0.25 km		0.5 km		0.75 km		**1 km**
BCR in Nine node	3.15		5.72		6.99		**9.31**
BCR in South Florida	78.86		222.64		333.96		**445.27**
VOT of CAV users	0.1	0.2	0.3	0.4	**0.5**	0.6	0.7
BCR in Nine node	6.83	7.45	8.07	8.69	**9.31**	9.93	10.55
BCR in South Florida	326.53	356.22	385.90	415.59	**445.27**	474.96	504.64

Note: The bold ones are results of the nominal cases.

3. Modelling and managing the integrated morning-evening commuting and parking patterns under the fully automated vehicle environment.

3.1 Backgrounds

Emerging technologies in communication and robotics have given rise to the prospect of AVs, which lead us to a new version of future transportation (Burns, 2013). Most major car manufacturers are racing to develop fully automated vehicles, and in the meantime, large metropolitan planning organizations are in the process of preparing for future automated transportation (Guerra, 2016). The advancements in AV technology will revolutionize motoring, aiming to reduce accident frequency, avert fatal crashes, achieve savings in travel time, relieve traffic congestion, increase fuel efficiency and improve transport accessibility. Since AVs can drive themselves on streets and automatically navigate multiple types of traffic environment contexts, direct human inputs may be no longer needed to complete daily trips. This means that former drivers are allowed to engage in other activities (e.g., studying or working) when driving, and such a dramatic transformation not only increases the utility of individual commutes, but also provides essential mobility to vulnerable groups, such as the disabled or elderly.

In addition to the abovementioned benefits, AVs may serve as a critical solution to parking-related problems, particularly for city centres where the level of human activity is high. In central business districts (CBDs) of cities, the space available for parking purposes is limited and costly, while a great deal of parking demand is generated by commuters every day (Van Ommeren et al., 2012). These traffic-related externalities impose a huge cost and inconvenience to commuters (Inci, 2015). Specifically, in a non-AV environment, travelers have to drive their cars to find a vacant parking space and walk from the parking location to the workplace in the morning, and then walk back to the parking location after work. In this process, commuters would worry about the arrival time to the workplace, given that finding a vacant parking space and walking to the workplace are both time-consuming in many cases. To resolve these issues, a large number of studies have been conducted, particularly in the areas of cruising for parking (Arnott and Inci, 2006; Inci and Lindsey, 2015; Liu and Geroliminis, 2016), parking reservation or permit schemes (Zhang et al., 2011; Yang et al., 2013; Liu et al., 2014; Chen et al., 2015), and parking pricing (Arnott et al., 1991; Qian et al, 2011; Qian et al, 2012; Qian and Rajagopal, 2014; He et al., 2015; Xiao et al., 2016; Ma and Zhang, 2017; Nourinejad and Roorda, 2017). However, all of these parking-related studies propose approaches for non-AV transportation systems, wherein AVs are not taken into account. With traditional vehicles, the limited land use for parking at CBDs and the walking

of commuters are two of the major concerns (e.g., Arnott et al., 1991). By contrast, in the context of AVs: (i) AVs can drop off commuters at the workplace and find a parking spot via self-driving, commuters no longer waste time on searching for parking; (ii) since AVs can drop off commuters at the workplace before finding a parking spot via self-driving, the parking location is not necessarily close to the city centre, resulting in reductions in social parking costs; (iii) the time spent in walking between the parking lot and the workplace can be completely eliminated. The above three behavior patterns may arise given the drastic development of communication technology and the aforementioned benefits of AVs. Indeed, it is predicted that owning a smart automated vehicle will become the norm for customers by the 2050s (Litman, 2018). We anticipate that the era of fully automated transportation will come up in the foreseeable future.

Although there is a surge of academic studies related to AVs (Duell et al., 2016; Krueger et al., 2016; Sparrow and Howard, 2017), few research efforts have been made to analytically investigate and identify the commuting and parking behaviour in the era of AVs, as well as the corresponding traffic efficiency and planning policy. Recently, under Vickrey's single-bottleneck setting, van den Berg and Verhoef (2016) and Lamotte et al. (2017) examined the commuting equilibrium with automated vehicles and incorporated the reduced value of time (for AVs) and/or improved road capacity from driver-less cars. Liu (2018) modelled the joint equilibrium of departure time and parking location choices when commuters travel with AVs in the morning. This study extends the literature by integrating the morning and evening commutes and exploring how AVs would reshape the integrated morning-evening commute. This is important and necessary since behaviours of AVs are significantly different from non-AVs during daily trips including both the morning and evening commutes. More importantly, morning and evening commutes are often correlated, e.g., where one parks in the morning would affect how one leaves in the evening, and the two commutes are not symmetric (e.g., Zhang et al., 2005; Zhang et al., 2008; Gonzales and Daganzo, 2013). In this context, the aims of this study are to answer the following two critical questions: (i) what are the key features of commuters' commuting and parking patterns when the daily travel process is considered in a fully automated environment? (ii) what are the optimal pricing and facility planning strategies (e.g., tolling, parking supply) to improve AV transport system efficiency?

To answer these questions, this study adopts a linear city modelling framework to analyze the AV-oriented commuting equilibrium, wherein the residential area and the city business centre are connected by a highway corridor (Arnott et al. 1991, Zhang et al., 2008, Li and Huang,

2017). The bottleneck model is adopted to capture traffic dynamics.[1] As compared to the non-AV case, the time of walking between the workplace and the parking lot will be eliminated and walking will be replaced by AVs' self-driving (Liu, 2018). Also, AVs will drop off commuters in the morning and can pick up commuters in the evening. These behavior changes will lead to the major changes in the commuting equilibrium when compared to the non-AV situation in Zhang et al. (2008). In addition, a feasible parking lot can be located far away from the workplace for AVs, while this will yield an unacceptable walking distance under non-AV environment.

It is noteworthy that the formulation of morning commute has accumulated a vaster literature than that of evening commute (De Palma and Arnott, 2012; Li and Huang, 2017). This is because of the assumption that the evening commuting trip is matched by a symmetric reverse process of the morning trip. However, the distinctions between the morning and evening traffic patterns have been highlighted in the relevant references, particularly in terms of departure/arrival patterns (De Palma and Lindsey, 2002; Zhang et al., 2008). In this study, we analyze bottleneck-constrained morning and evening commutes with AVs. Compared to the bottleneck model of non-AV trips, the location of the active bottleneck with congestion can be different for AV daily trips. Specifically, for AV commutes, the active bottleneck is on the way from home to the workplace in the morning but might be on the way from the parking location to the workplace during AVs' self-driving in the evening (rather than from workplace to home). Compared with a recent study on morning commute under AV environment by Liu (2018), this study further looks into the integrated morning-evening commuting problem and provides a more thorough and complete investigation of day-long commutes and planning policies for future automated transportation.

The remainder of this chapter is organized as follows. Section 3.2 and Section 3.3 analyze the morning-evening commute equilibrium under AV environment, where Section 3.2 formulates the equilibrium model for evening commutes given the parking locations of AVs resulting from the morning commute and Section 3.3 incorporates the obtained evening commute equilibrium from Section 3.2 into the user-equilibrium analysis considering daily travel costs. In Section 3.4, we analyze the AV traffic pattern at system optimum, and develop the time-dependent tolling schemes. In Section 3.5, we investigate the optimal AV parking supply

---

[1] Dynamic equilibrium analysis has received considerable theoretical attention over the past 50 years. The bottleneck model was initially proposed by Vickrey (1969), followed by numerous extensions (Lindsey, 2004; Li et al., 2017)). For recent comprehensive reviews, one can refer to Li et al. (2014) and Small (2015).

strategy under either user equilibrium or system optimum traffic patterns. Numerical results are presented in Section 3.6.

3.2 Equilibrium Analysis on Evening Commute with AVs

In this section, we analyze the equilibrium dynamic traffic pattern with regards to the time of departure from AV parking spots for evening commutes, given that parking locations have already been determined in the morning. At equilibrium, no commuter can further reduce the individual travel cost by changing his or her own AV departure time after work provided that all the others' departure times are given. The mathematical notations used throughout this study are summarised in Appendix B-1, unless otherwise specified.

The linear city network for morning-evening commute is described in Figure 3.1. We consider that along the linear corridor there exist two bottlenecks: one is on the way from the residential area to the workplace, which is termed as "inbound bottleneck"; the other one is on the way from the workplace to home, which is termed as "outbound bottleneck". Parking is located between the bottlenecks and home along the traffic corridor. We assume that AVs are owned privately by individual commuters (shared AV mobility systems are not considered here). Each AV will need a parking space along the corridor. We also assume that the capacities of the two bottlenecks are identical, which reduces the burden of tedious algebra due to asymmetric capacity.

As depicted in Figure 3.1, the travelling process of evening commute follows the procedure: Depart from parking spots → Pass the parking area (AV self-driving) → Pass the inbound bottleneck (AV self-driving) → Pick up commuters at the workplace → Pass the outbound bottleneck → Return back home. The "flow direction for morning commute" is also indicated in Figure 3.1, which will be discussed in Section 3.1. As a first step to examine the evening commute with AVs, it is assumed that during the pick-up process at the workplace, only short-term waiting is allowed at the city centre (i.e., only very short-term parking will be provided for AVs to pick up travelers) and tactical waiting of AVs is not allowed since it will be wasteful.[2] The pick-up time duration or waiting time is constant, which is assumed to be zero.

---

[2] Since AVs can drive themselves, some AVs may depart from parking much in advance and wait at the pick-up location for commuters (start to wait much earlier than the work closure time in order to pick up the commuter at the earliest time) if parking is allowed at the pick-up locations. This is similar to the tactical waiting or braking model in the literature (Lindsey et al., 2012; Xiao et al., 2012) for step tolls. Future study will incorporate the tactical waiting behaviors of AVs and quantify potential efficiency loss due to this type of waiting. However,

In this context, one can derive that in the evening commute, only the inbound bottleneck is activated. This is explained as follows. The AV traffic is firstly governed by the inbound bottleneck when AVs run from the parking lot to the workplace by self-driving, i.e., arrival rate to the city centre to pick up commuters is less than or equal to capacity s. This means that the departure rate from the city centre or the arrival rate to the outbound bottleneck is less than or equal to the bottleneck capacity s. Therefore, the outbound bottleneck from the workplace to home will not be activated. Congestion will not occur when commuters travel from the workplace to home in the evening.[3]
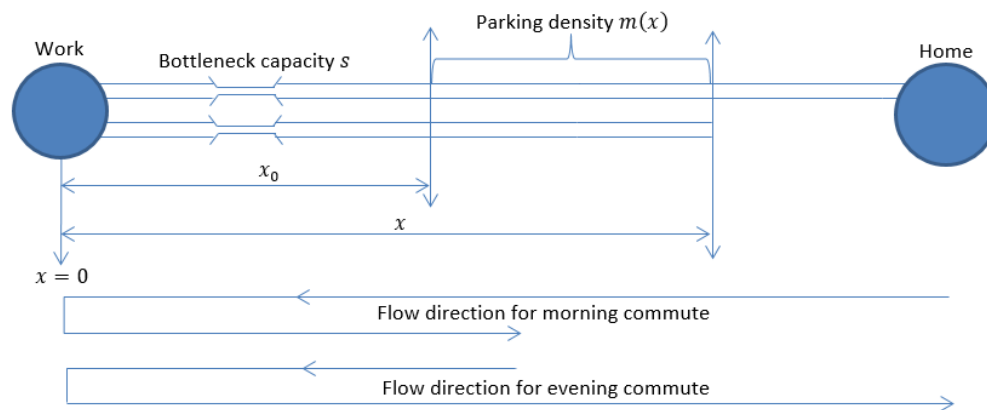
Figure 3.1 The linear city network for morning-evening commutes

For the evening commute, some travelers might choose to leave their office immediately after the work closure time and wait for their AVs to come to the city centre. We assume that the

---

AVs' waiting for commuters will be different from those tactical waiting to avoid toll (or avoid a higher toll) in the literature.

[3] In this study, the capacities of the inbound and outbound bottleneck are assumed to be identical, which is to avoid tedious algebra for identifying variations in equilibrium flow patterns due to asymmetric capacity. However, if asymmetric bottleneck capacities are incorporated, a tandem bottleneck approach similar to Kuwahara (1990) can be adopted. For example, if the inbound capacity is greater than the outbound capacity, queuing can arise at both the inbound and outbound bottlenecks, i.e., home to work and work to parking trips in the morning; parking to work and work to home in the evening commute. We then have to formulate two queues in the travel cost formulations in Eq. (1) for evening commute and later in Eq. (12) for morning commute.

cost of waiting out of the office building for a unit time is greater than the penalty cost for a unit time of late departure from the workplace. Under this assumption, everyone would wait in the office until their AVs arrive at the workplace and pick them up. Below we further summarise the main model assumptions (some are already mentioned and please refer to Appendix B-1 for the notations):

(i) The service capacities of the inbound and outbound bottlenecks in Figure 3.1 are identical.

(ii) For each AV, the parking location x remains the same throughout the day. The use of AVs for other trip purposes during the day is not considered in this study.

(iii) The parking density (i.e. number of available parking spaces per unit distance) along the linear traffic corridor is constant, i.e. $m(x) = m$. This allows analytical tractability. Note that a parking density of $m = 0.50$ (space per meter) means that on average for each 2-meter along the corridor there will be one parking space. Note that the parking density m at a location can be very large if a multi-story parking facility is considered.

(iv) All parking spots are off-street, so that the parking density has no impacts on the bottleneck's capacity.

(v) No parking spot is available at the workplace (only short-term parking for pick-up); No employer-provided parking or underground parking around the city centre is considered.

(vi) Early departure from the workplace is prohibited by employers. AVs' waiting at the city centre are not allowed due to Assumption (v). This means that all AVs will arrive at the workplace no earlier than the official work closure time in the evening.[4]

(vii) For early arrivals in the morning, the marginal savings in the early schedule delay cost by delaying a unit of time is greater than the marginal increase in the total cost of self-driving AV to find a parking spot in the morning and depart from the parking spot to pick up commuters in the evening, i.e. $\beta_1 > \frac{2\lambda ws}{m}$. This assumption is similar to that in Liu (2018) to ensure that congestion exists.

(viii) The headway of vehicles in motion is greater than the headway of parked vehicles in

---

[4] If early departure from work is allowed, due to the self-driving capability of AVs, AVs may pick up commuters earlier than the work closure time. This will create further complexity in modelling the integrated morning and evening commuting patterns. For simplicity and tractability, in this study, we assume that early departure from work is not allowed. A future study may allow early departure from work and more critically integrate this setting with tactical waiting of AVs discussed in footnote 2.

consideration of safe driving (Vogel, 2013), wherein the former can be calculated as $\frac{1}{s}$, and the latter as $\frac{w}{m}$, i.e. we have $\frac{1}{s} > \frac{w}{m}$.

(ix) Commuters are homogeneous, and have the same official work start and closure time. Their schedule penalties for morning and evening satisfy the following conditions: a) $\gamma_1 > \alpha_1 > \beta_1$ and $\alpha_1 > \lambda$, which are consistent with most empirical evidence in the literature; b) $\gamma_1, \gamma_2 > \lambda$, which means that the schedule delay penalty is more costly than the AV self-driving time; c) $\gamma_1 > 2\gamma_2$, which considers that late arrival to the workplace in the morning could cause a much greater loss to the company/employer than late departure from work in the evening.

(x) The cost for constant free-flow travel between home and the workplace and the cost for traversing the segment between $x = 0$ and $x = x_0$ without delay are assumed to be zero, considering that these two types of costs are the same to every commuter.

We now can formulate the individual travel cost for evening commuting, denoted as $c_2(t_2, x)$ (the subscript '2' is used to indicate 'evening commute'). For the commuter whose AV is parked at the location x and departs from the parking spot at time t_2, the travel cost is

$$c_2(t_2, x) = \lambda w(x - x_0) + \lambda \cdot \frac{q_2(t_2)}{s} + \gamma_2 \left(t_2 + w(x - x_0) + \frac{q_2(t_2)}{s} - t_2^* \right), \tag{1}$$

where λ is the cost for a unit-time of AV self-driving; w is the travel time spent in traversing a unit distance via AV self-driving without bottleneck congestion; and q_2 represents the queuing length experienced in the evening. From the right-hand side, the first term is the travel cost of traversing the parking area. The second term is the cost of queuing delay. The third term represents the penalty cost of late departure from the workplace. Note that it is not necessary to write down the queuing time at the outbound bottleneck since it will be zero.

We then can derive the first derivative of the individual travel cost with regards to the departure time t_2 as follows

$$\frac{\partial c_2(t_2, x)}{\partial t_2} = \gamma_2 + \frac{\lambda + \gamma_2}{s} \cdot \frac{dq_2(t_2)}{dt_2}. \tag{2}$$

The departure from the parking spot in the evening can be further divided into two stages,

which is analysed below (related to the first derivative of $c_2(t_2, x)$).

Stage 1:

At the very beginning of the evening commute, $\frac{dq_2(t_2)}{dt_2} \geq 0$ holds due to nonnegativity of the queue length, which results in the relationship $\frac{\partial c_2(t_2, x)}{\partial t_2} > 0$. This means that a postponed departure would cause an increase in individual travel cost with a larger queuing delay at the bottleneck. Some AVs will depart from their parking spots as early as possible to pick up commuters. However, AVs cannot arrive at the workplace earlier than t_2^* since waiting at the city centre is not allowed. Hence, some AVs will arrive at the inbound bottleneck immediately after t_2^* at equilibrium. However, the arrival rate of these AVs at the city centre will be constrained by the inbound bottleneck. These AVs will form a mass queue at the inbound bottleneck. We assume that AVs parked closer to the city centre will be in an advantageous position and they are in front of AVs parked further away in the pick-up process. This means that for two AVs parked at x_1 and x_2, with $x_1 < x_2$, if they arrive at the inbound bottleneck at the same time (which means that the AV parked further away must depart from the parking spot earlier under this circumstance), the AV parked at x_1 will be in front of the AV parked at x_2. Under this assumption, one can verify that only those parked relatively close will arrive at the bottleneck at t_2^* in order to pick up commuters. The order of AVs in the mass queue is determined by the parking locations of the AVs. Those AVs with a relatively far away parking location cannot compete to pick up commuters as early as t_2^*, since they will be in disadvantageous position (in the end of the queue with a long queuing time) even if they arrive at the city centre or inbound bottleneck at the same time. For those AVs arriving at the inbound bottleneck at time t_2^*, one can verify that a delayed departure from parking (as well as arrival at the inbound bottleneck) will increase individual travel cost, and an earlier departure (resulting in arriving earlier than t_2^*) is prohibited.

In particular, the arrival rate to the inbound bottleneck in the evening commute is denoted as r_2, where a further subscript (1 or 2) is added to reflect the stage. At stage 1, for AVs parked relatively close to the workplace, we denote the range of their parking location as $[x_0, \tilde{x}]$, where $\tilde{x}$ represents the location of the AV that is the furthest away from the workplace among all the AVs arriving at the bottleneck at time t_2^* in the evening. Since AVs can depart the parking earlier than t_2^*, as mentioned in the above, they will try to pick up commuters at t_2^*. However, during the pick-up process, arrival rate to the city centre will be constrained by

the inbound bottleneck (to arrive at the city centre), while arrival rate to the bottleneck at time t_2^* denoted as $r_{2,1}$ will approach infinity (i.e., a queue will form quickly once the evening peak begins at the inbound bottleneck). This is different from the literature where commuters have to walk. Based on our assumption that AVs parked closer to the city centre will be in an advantageous position, after reaching the bottleneck at t_2^*, the queueing length experienced by the AV parked at the location x is $m(x - x_0)$. One can verify that none of the AVs parked within $[x_0, \tilde{x}]$ can further reduce the individual evening travel cost by unilaterally arriving earlier/later than t_2^* at the inbound bottleneck (i.e., arriving earlier than t_2^* is not allowed and arriving later will increase cost).[5]

Stage 2:

AVs that are parked far from the workplaces, due to a disadvantageous parking location, would wait at the parking place to avoid the long queue. For these commuters, the equilibrium queue length will decrease over time (a trade-off between queueing delay cost and schedule delay cost),

$$\frac{\partial c_2(t_2, x)}{\partial t_2} = 0 \Longrightarrow \gamma_2 + \frac{\lambda + \gamma_2}{s} \cdot \frac{dq_2(t_2)}{dt} = 0 \Longrightarrow \frac{dq_2(t_2)}{dt_2} = -\frac{\gamma_2 \cdot s}{\lambda + \gamma_2}. \tag{3}$$

We denote the arrival rate to the inbound bottleneck (for pick-up) for the AVs parking far from the workplace as $r_{2,2}$. Since $r_{2,2} - s = \frac{dq_2(t_2)}{dt_2}$, we have an arrival rate less than s, i.e.,

$$r_{2,2} = \frac{\lambda}{\lambda + \gamma_2} \cdot s. \tag{4}$$

In summary, we have following results. For AVs with a parking location $x \leq \tilde{x}$, they arrive at the inbound bottleneck immediately after t_2^* (departure times from parking will be different for AVs); Otherwise, they depart from the parking space to produce an arrival rate to the inbound bottleneck equal to $r_{2,2} = \frac{\lambda}{\lambda + \gamma_2} \cdot s$. With the above results in mind and based on equilibrium condition and flow conservation constraint, we can determine the individual travel cost for the evening commute as follows. For $x \leq \tilde{x}$, we have $t_2 = t_2^* - w(x - x_0)$, and

---

[5] If AVs parked closer to the city centre will NOT be in an advantageous position during the evening pick-up process, all AVs arriving at the city centre at the same time may form a mass queue with a random order, which is similar to that in Arnott et al. (1990) for step tolling. An expected cost for AVs in the mass similar to Arnott et al. (1990) might be utilized to model this case. This deserves a future study, and if possible, should be examined and compared to the case with tactical waiting or braking for AVs (just like Lindsey et al. (2012) did for the step tolling problem).

$q_2(t_2) = m(x - x_0)$, and

$$c_2(t_2, x) = \lambda w(x - x_0) + (\lambda + \gamma_2)\frac{m(x - x_0)}{s}; \qquad (5)$$

For $x > \tilde{x}$, we have $t_2^* - w(x - x_0) < t_2 \le t_2^* + \frac{IV}{s} - w(x - x_0)$, and $q_2(t_2) =$

$(\tilde{x} - x_0)m + \left(t_2 - t_2^* + w(x - \tilde{x})\right)\left(-\frac{\gamma_2 \cdot s}{\lambda + \gamma_2}\right)$, and

$$c_2(t_2, x) = \lambda w(x - x_0) + (\lambda + \gamma_2)\frac{m(\tilde{x} - x_0)}{s}, \qquad (6)$$

where the critical location $\tilde{x}$ is as follows:

$$\tilde{x} = x_0 + \frac{N\gamma_2}{m(\lambda + \gamma_2)}. \qquad (7)$$

It can be easily verified that when $x \to \tilde{x}$, the cost in Eq. (5) is equal to the cost in Eq. (6). It is obvious that in $c_2(t_2, x)$, the first part is related to the self-driving from parking to the inbound bottleneck, and the second part is a cost governed by the trade-off between queuing delay and scheduling delay. Eq. (5) and Eq. (6) also indicate that the parking location has non-trivial impacts on the equilibrium travel cost for evening commute. This highlights the importance of integrating morning and evening commutes in the analysis. More specifically, it can be seen that when $x \le \tilde{x}$, the parking location has impacts on queuing delay costs, penalty costs for late departure commuters, and cost of AV-self driving to leave the parking area. By contrast, if $x > \tilde{x}$, at equilibrium, the parking location can only influence the time spent in traversing the parking area by AV self-driving, but cannot make any difference to the sum of the queuing delay cost and the schedule delay cost. Therefore, AVs of these commuters do not necessarily depart strictly in the order that the AVs are parked. Their departure times (from parking) only need to produce an arrival curve QR in Figure 3.2. The above analysis is similar to Zhang et al. (2008) with non-AVs in the sense that there is a critical parking location $\tilde{x}$ for the evening commute. However, the behaviour patterns of AVs are significantly different from the behaviour patterns of non-AVs.
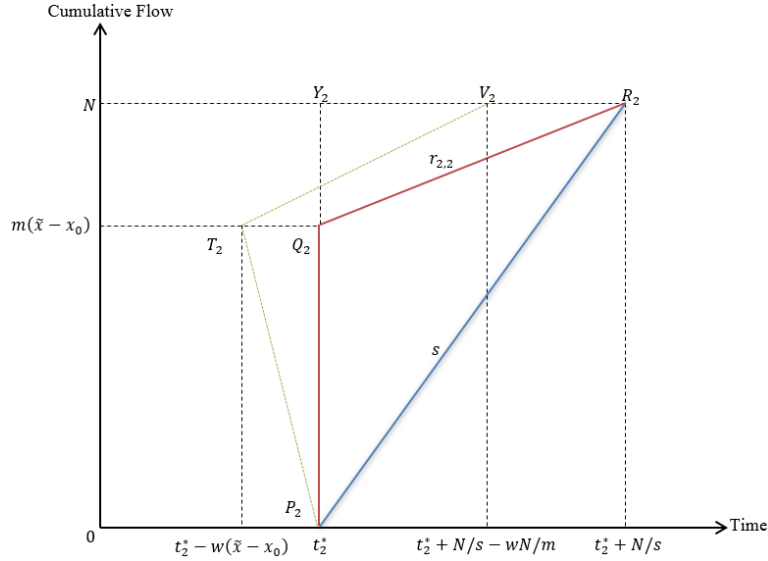
Figure 3.2 Equilibrium traffic flow pattern for evening commute

The equilibrium flow pattern for the evening commute is depicted in Figure 3.2. The red curve $P_2Q_2R_2$ describes the time of arrival to the entrance of the bottleneck. The blue curve P_2R_2 represents the time of departure from the bottleneck (the time of arrival at the workplace). The horizontal difference between $P_2T_2V_2$ and $P_2Q_2R_2$ represents the time of AV-self driving to leave the parking area; the difference in the y-coordinate between P_2T_2 and the line $y = m(\tilde{x} - x_0)$ represents the cumulative early departure from the parking space, while the difference in the y-coordinate between T_2V_2 and the line $y = m(\tilde{x} - x_0)$ indicates the cumulative late departure. As mentioned, for these commuters, they do not necessarily depart strictly in the order that the AVs are parked. Figure 3.2 only illustrates the case where an AV parked further away is departing later from the parking (please refer to the departure curve T_2V_2).

In Figure 3.2, the area of the triangle PQR represents the total time delay at the bottleneck. Then, the total cost of queuing delay experienced by AV self-driving, $TQ_2(AV)$, can be calculated as follows

$$TQ_2(AV) = 0.5 \frac{\gamma_2 \lambda N^2}{s(\lambda + \gamma_2)}. \tag{8}$$

In addition, the total cost for departing from the parking space and leaving the parking area

by AV self-driving is

$$TP_2(AV) = 0.5\lambda w \frac{N^2}{m}. \tag{9}$$

In Figure 3.2, the area of the triangle PYR represents the total time that is to be penalised for late departure from the workplace. Then, the total schedule delay cost for late departure, TS_2, can be calculated as follows:

$$TS_2 = 0.5\gamma_2 \frac{N^2}{s}. \tag{10}$$

The total evening travel cost at equilibrium then can be expressed as follows:

$$TETC_{UE} = TQ_2(AV) + TP_2(AV) + TS_2 = 0.5 \frac{\gamma_2 \lambda N^2}{s(\lambda + \gamma_2)} + 0.5\lambda w \frac{N^2}{m} + 0.5\gamma_2 \frac{N^2}{s}. \tag{11}$$

Note that if people were allowed to depart for home before t_2^* with the penalty for early departure applied, the equilibrium flow pattern would change, as well as the equilibrium cost. Specifically, if the traffic pattern for on-time and late departures still follow Figure 3.2, the equilibrium cost is expected to decrease since departure times of commuters will be more concentrated around t_2^*, i.e., a proportion of AVs might choose early departure from work at equilibrium.

3.3. Equilibrium Analysis on Integrated Morning-Evening Commute under AV Environment

As discussed in Section 3.2, the parking location of AVs indeed can affect the departure time decision and travel cost of commuters in the evening commute. The parking location also affects commuters' cost in the morning. For example, a closer parking to the city centre means a less AV self-driving time cost. In this section, we investigate the joint user-equilibrium in terms of departure time from home and choice of AV parking locations for the morning commute, considering the daily travel cost (the costs of the morning and evening commutes are both included). At user equilibrium, each commuter has the same individual daily travel cost, and no one can reduce his or her own travel cost by unilaterally adjusting the departure time and/or the parking location. Section 3.1 formulates the individual daily travel cost for the integrated morning-evening commute. Section 3.2 conducts analysis on the user-equilibrium traffic pattern considering the daily travel cost with regards to the departure time and the parking location in the morning commute.

3.3.1 Individual daily travel cost for AV commute

We first discuss the travel process for morning commute with AVs, which follows the procedure as depicted in Figure 3.1: Depart from home → Pass the inbound bottleneck

→ Arrive at the workplace and drop off commuters → Pass the outbound bottleneck (AV self-driving) → Find an appropriate parking spot (AV self-driving). In the morning commute, the traffic is governed by the first bottleneck encountered during the travel process, i.e., the inbound bottleneck. This means that after the AVs pass the inbound bottleneck and drop off the commuters, the traffic rate is less than or equal to the outbound bottleneck capacity, and there is no congestion at the outbound bottleneck. It can be seen that the processes for morning commute and evening commute are not simple mirror symmetries. Particularly, in the morning, traffic congestion occurs at the inbound bottleneck when travelers are driving their AVs, while in the evening, the congestion happens when AVs drive themselves from the parking lot to the workplace. Also, the outbound bottleneck is used for two types of trips: by empty AVs in the morning to access parking after dropping people off at work, and by occupied AVs in the evening to take people from the workplace to home. Based on the above analysis, yet the outbound bottleneck is never congested. However, if parking at the city centre is allowed, this could shift the road capacity constraint from the inbound bottleneck to the outbound bottleneck, or cause both bottlenecks to become active (depending on the number of parking at different locations). This is because AVs parked at the CBD are incentivised to depart from the workplace and drive people back home immediately after the business closure time, in order to minimise their penalty cost for late departure, which can lead to traffic congestion at the outbound bottleneck. These cases will be analysed in a follow-up study to further identify optimal parking supply strategies for AVs.

We consider that in the morning, commuters have a desired arrival time at the workplace, which is t_1^* (we use subscript '1' to indicate morning commute). Early and late arrival at the workplace will be penalized. The morning commute cost $c_1(t_1, x)$ for commuters who leave home at time t_1 in the morning and park the AV at location x can be calculated as follows:

$$c_1(t_1, x) = \alpha_1 \frac{q_1(t_1)}{s} + \beta_1 \left[t_1^* - t_1 - \frac{q_1(t_1)}{s} \right]^+ + \gamma_1 \left[t_1 + \frac{q_1(t_1)}{s} - t_1^* \right]^+ + \tag{12}$$
$$\lambda w(x - x_0),$$

where $[\cdot]^+ \equiv max\{\cdot, 0\}$. From the right-hand side of Eq. (12), the first term is the cost of queuing delay. The second and the third terms represent the penalty costs caused by early and late arrival to the workplace respectively. The fourth term is the cost of finding a parking space via AV self-driving. Note that in the cost formulation $c_1(t_1, x)$, we take all combinations of (t_1, x) into account, which means that x and t_1 are independent (how

they are related at equilibrium will be discussed later on).

We now formulate the individual daily travel cost in a fully automated environment, which is denoted as $c(t_1, x)$ for commuters who leave home at time t_1 in the morning and park the AV at location x. Then, $c(t_1, x)$ which consists of both the morning and evening commuting costs can be given as follows:

$$c(t_1, x) = c_1(t_1, x) + c_2(t_2, x). \tag{13}$$

Based on the evening equilibrium cost in Section 3.2 and Eq. (12) and Eq. (13), we can derive the first derivative of the individual daily travel cost with regards to the parking location as follows: for $x \leq \tilde{x}$, $\frac{\partial c(t_1, x)}{\partial x} = 2 \cdot \lambda w + (\lambda + \gamma_2) \frac{m}{s} > 0$; and for $x > \tilde{x}$,

$\frac{\partial c(t_1, x)}{\partial x} = 2 \cdot \lambda w > 0$. The relationship $\frac{\partial c(t_1, x)}{\partial x} > 0$ always holds. This means that, for AVs departing at a specific time t_1, AVs would always choose to park as close to the workplace as possible after dropping off commuters, in order to reduce the individual daily travel cost. Hence, x is dependent on (or governed by) the departure time t_1 for morning commute. Let $x = x(t_1)$, we have

$$c(t_1, x) = \left\{ \alpha_1 \frac{q_1(t_1)}{s} + \beta_1 \left[t_1^* - t_1 - \frac{q_1(t_1)}{s} \right]^+ + \gamma_1 \left[t_1 + \frac{q_1(t_1)}{s} - t_1^* \right]^+ + \tag{14}$$
$$\lambda w(x(t_1) - x_0) \right\} + \left\{ c_2(t_2, x(t_1)) \right\}.$$

By denoting the departure rate from home as r_1 (arrival rate to the inbound bottleneck for morning commute) and the departure time of the first commuter as t_s, we then have (AVs will choose the closest parking available, which is reflected by $x = x(t_1)$)

$$\int_{t_s}^{t_1} r_1(u) du = \int_{x_0}^{x} m(y) dy. \tag{15}$$

Hence, $r_1(u) = m(x) \frac{dx}{dt_1}$ or $\frac{dx}{dt_1} = \frac{r_1(u)}{m(x)}$. Under the assumption $m(x) = m$, we have

$$\frac{dx}{dt_1} = \frac{r_1(u)}{m}. \tag{16}$$

From the above analysis, we can find that the departure-time choice in the morning and that in the evening are interrelated. Specifically, the parking location is dependent on the departure time for morning commute under the defined equilibrium, and the departure pattern for evening commute is significantly influenced by the parking location as discussed in Section 3.2. Note that later a subscript (1, 2, or 3) is further added to r_1 to

reflect the stage during the morning departure/arrival duration. With the above results in mind, we are now ready to derive the equilibrium of the integrated morning-evening commute.

3.3.2 User-equilibrium AV traffic pattern for morning commute considering daily travel cost

We now investigate the equilibrium traffic pattern with AVs in the morning when the daily travel cost is considered. We denote the departure time of the on-time-arrival commuters as $\bar{t}$, and the corresponding parking location as $\bar{x}$. We also define that the departure time for morning commute corresponding to the parking location $\tilde{x}$ as $\tilde{t}$. To ease the presentation of analysis, we categorise all the possible scenarios (for equilibrium traffic pattern) into two groups in terms of the relationship between $\bar{x}$ and $\tilde{x}$: for Scenario 1, $\tilde{x} < \bar{x}$; for Scenario 2, $\tilde{x} \geq \bar{x}$, and will discuss each scenario in the following subsections.

3.3.2.1 Scenario 1

Under the assumption $\tilde{x} < \bar{x}$, for early arrivals in the morning, some of the AVs arriving at the workplace early in the morning will arrive at the bottleneck immediately after t_2^* in the evening, while the others will depart later to avoid a long queue; For late arrivals in the morning, all AVs will delay their departure to balance schedule delay cost and queueing delay cost. Hence, the traffic pattern for AV morning commutes can be divided into three stages, namely Stage 1, Stage 2 and Stage 3, and the rates of departure from home at each stage, denoted as $r_{1,1}(t_1)$, $r_{1,2}(t_1)$ and $r_{1,3}(t_1)$, are summarised in Table 3.1. Furthermore, we can categorize Scenario 1 into two cases, depending on whether or not a queue exists in the first stage, of which the conditions are also presented in Table 3.1. As can be seen, these conditions are related to values of time and AV self-driving time, schedule penalties, parking density, AV self-driving speed, and bottleneck capacity. For the derivation process for the results shown in Table 3.1, see *Derivation. Scenario 1* in Appendix B-2.

Table 3.1 Summary of two cases under the Scenario 1 where $\tilde{x} < \bar{x}$

	Case 1	Case 2
Condition	$\dfrac{2\lambda ws}{m} < \beta_1 \leq \dfrac{2\lambda ws}{m} + \lambda + \gamma_2$	$\beta_1 > \dfrac{2\lambda ws}{m} + \lambda + \gamma_2$
$r_{1,1}(t_1)$	$\dfrac{\beta_1}{\dfrac{2\lambda ws}{m} + \lambda + \gamma_2} s \leq s$	$\dfrac{\alpha_1}{\alpha_1 - \beta_1 + \dfrac{2\lambda ws}{m} + \lambda + \gamma_2} s > s$
$r_{1,2}(t_1)$	$\dfrac{\alpha_1}{\alpha_1 - \beta_1 + \dfrac{2\lambda ws}{m}} s > s$	$\dfrac{\alpha_1}{\alpha_1 - \beta_1 + \dfrac{2\lambda ws}{m}} s > s$
$r_{1,3}(t_1)$	$\dfrac{\alpha_1}{\alpha_1 + \gamma_1 + \dfrac{2\lambda ws}{m}} s < s$	$\dfrac{\alpha_1}{\alpha_1 + \gamma_1 + \dfrac{2\lambda ws}{m}} s < s$

Case 1

For Case 1, the user-equilibrium AV traffic pattern in terms of departure time and parking location for morning-evening commutes is depicted in Figure 3.3. The curves for evening commute have the same physical meaning as those in Figure 3.2. For morning commute, the red curve $P_1 Q_1 R_1 W_1$ represents the cumulative departure from home, i.e. the cumulative arrival at the bottleneck; the blue curve $P_1 Q_1 W_1$ represents the cumulative flow arriving at the workplace, i.e. the cumulative departure from the bottleneck; the purple curve $P_1 Z_1 V_1$ represents the cumulative arrival at the parking lot in the morning.

Figure 3.3 indicates that in Case 1, the inbound bottleneck does not operate at capacity at Stage 1 of the travel period. This is one of the main distinctions between Case 1 and the other cases, which will be further discussed in the following sections. Roughly speaking, as the penalty for early arrival is relatively small in Case 1 as compared to the other cases, some commuters are motivated to depart far earlier to ensure an advantageous parking place close to the workplace and reduce the cost of empty AV trips for the parking purpose. This leads to less departure concentration over time, resulting in the unsaturated traffic at the early stage of AV morning commute. The condition of Case 1 differs from the case where the bottleneck is not used to capacity by conventional vehicles identified by Arnott et al. (1991). This is primarily due to that in this study walking is replaced by AV self-driving and morning and evening commutes have been integrated.
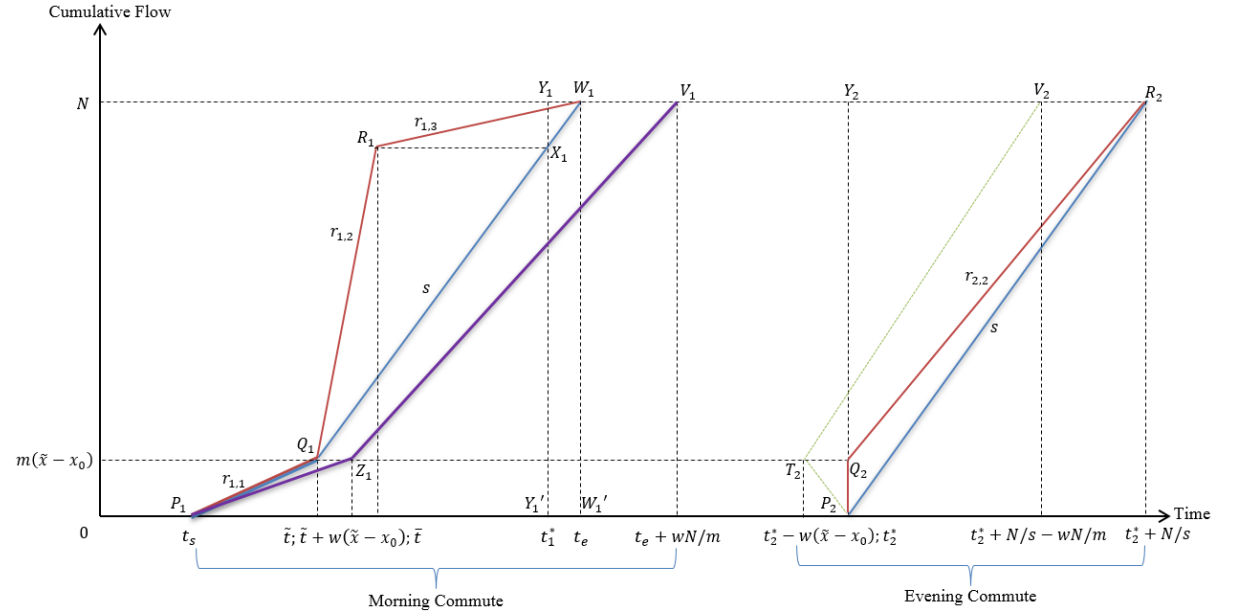
Figure 3.3 Daily equilibrium commute pattern for Case 1

From flow conservation and equilibrium conditions, we can determine the first and last departure times t_s and t_e as follows:

$$t_s = t_1^* - \frac{\gamma_1}{(\beta_1+\gamma_1)}\left(\frac{1}{r_{1,1}} - \frac{1}{s}\right)\frac{N\gamma_2}{(\lambda+\gamma_2)} - \frac{1}{(\beta_1+\gamma_1)}\left(2 \cdot \frac{\lambda w}{m} + \frac{\gamma_2}{s} + \frac{\gamma_1}{s}\right)N; \tag{17}$$

$$t_e = t_1^* + \frac{\beta_1}{(\beta_1+\gamma_1)}\left(\frac{1}{r_{1,1}} - \frac{1}{s}\right)\frac{N\gamma_2}{(\lambda+\gamma_2)} - \frac{1}{(\beta_1+\gamma_1)}\left(2 \cdot \frac{\lambda w}{m} + \frac{\gamma_2}{s} - \frac{\beta_1}{s}\right)N. \tag{18}$$

and we can also obtain the analytical expressions of $\tilde{t}$ and $\bar{t}$ as follows

$$\tilde{t} = t_1^* - \frac{2 \cdot \frac{\lambda w}{m} + \frac{\gamma_2}{s} + \frac{\gamma_1}{s}}{\beta_1+\gamma_1}N + \frac{N\gamma_2}{(\lambda+\gamma_2)}\left(\frac{\beta_1}{r_{1,1}(\beta_1+\gamma_1)} + \frac{\gamma_1}{s(\beta_1+\gamma_1)}\right); \tag{19}$$

$$\bar{t} = t_1^* - \frac{2 \cdot \frac{\lambda w}{m} + \frac{\gamma_2}{s} + \frac{\gamma_1}{s}}{\beta_1+\gamma_1}N + \frac{1}{r_{1,2}-r_{1,3}}\left(1 - \frac{r_{1,3}}{s}\right)N + \tag{20}$$

$$\left(\frac{1}{r_{1,2}-r_{1,3}}\left(\frac{r_{1,2}-r_{1,3}}{r_{1,1}} + \frac{r_{1,3}}{s} - 1\right) - \frac{\gamma_1}{\beta_1+\gamma_1}\left(\frac{1}{r_{1,1}} - \frac{1}{s}\right)\right)\frac{N\gamma_2}{(\lambda+\gamma_2)}.$$

We can calculate the total daily travel cost at equilibrium, denoted as $TDTC_{UE}$, for

37

Case 1 as follows:

$$TDTC_{UE} = \left[\frac{\gamma_1 \left(\frac{2\lambda ws}{m} + \lambda + \gamma_2 - \beta_1 \right)}{(\beta_1 + \gamma_1)s} \left(\frac{N\gamma_2}{\lambda + \gamma_2} \right) + \frac{\beta_1}{\beta_1 + \gamma_1} \left(2 \cdot \frac{\lambda w}{m} + \frac{\gamma_2}{s} + \frac{\gamma_1}{s} \right) N \right] N. \tag{21}$$

Particularly, the term in the square bracket represents the individual daily travel cost at equilibrium.

We can also evaluate different aggregate cost components for morning commuting when daily traffic reaches the user equilibrium condition. We denote the area of the polygon Ω as A_Ω, where Ω is represented by specific nodes in this section. Then, the total cost of queuing delay for morning commutes, denoted as TQ_1, is

$$TQ_1 = \alpha \cdot A_{Q_1 R_1 W_1}. \tag{22}$$

The total cost of schedule delay for morning commutes, denoted as TS_1, is

$$TS_1 = \left[\beta_1 \cdot A_{P_1 Y_1' X_1 Q_1} \right] + \left[\gamma_1 \cdot A_{X_1 Y_1 W_1} \right], \tag{23}$$

where the term in the first square bracket is the total schedule delay cost for early arrivals, and the term in the second square bracket for late arrivals. The total cost for finding an appropriate parking space by AV self-driving in the morning, denoted as $TP_1(AV)$, is

$$TP_1(AV) = \lambda \cdot A_{P_1 Q_1 W_1 V_1 Z_1}. \tag{24}$$

In addition, it is evident that the relationship $TP_1(AV) = TP_2(AV)$ must hold in this study. This is because, no matter where individual AV parks, from a system perspective, parking from x_0 to $x_0 + \frac{N}{m}$ will be occupied as they are the possible closest parking to serve all the demand.

We then investigate the relationship between the two critical time points $\bar{t}$ and $\tilde{t}$, by calculating the difference: $\bar{t} - \tilde{t} = \frac{1}{r_{1,2} - r_{1,3}} \left(\frac{s - r_{1,3}}{s} \right) \frac{m\lambda N}{m(\lambda + \gamma_2)}$.

Considering $r_{1,2} > s > r_{1,3}$, $\frac{1}{r_{1,2} - r_{1,3}} \left(\frac{s - r_{1,3}}{s} \right) \frac{m\lambda N}{m(\lambda + \gamma_2)} > 0$ always holds. This means that, in Case 1, $\bar{t}$ is always greater than $\tilde{t}$, and consequently, the condition $\tilde{x} < \bar{x}$ must hold. Hence, when $\frac{2\lambda ws}{m} < \beta_1 \leq \frac{2\lambda ws}{m} + \lambda + \gamma_2$, the equilibrium traffic pattern

must be Case 1.

Case 2

For Case 2, the user-equilibrium AV traffic pattern in terms of departure time and parking location for morning-evening commutes is depicted in Figure 3.4. For both morning and evening commutes, the physical meanings of curves highlighted in different colors are the same as Figure 3.3.

Similarly, we can determine t_s and t_e as follows:

$$t_s = t_1^* - \frac{\left(2 \cdot \frac{\lambda w}{m} + \frac{\gamma_2}{s} + \frac{\gamma_1}{s}\right)}{\beta_1 + \gamma_1} N; \quad t_e = t_1^* - \frac{\left(2 \cdot \frac{\lambda w}{m} + \frac{\gamma_2}{s} - \frac{\beta_1}{s}\right)}{\beta_1 + \gamma_1} N. \tag{25}$$

Based on equilibrium conditions, we can also determine $\tilde{t}$ and $\bar{t}$ as follows

$$\tilde{t} = t_1^* - \frac{\left(2 \cdot \frac{\lambda w}{m} + \frac{\gamma_2}{s} + \frac{\gamma_1}{s}\right)}{\beta_1 + \gamma_1} N + \frac{N \gamma_2}{r_{1,1}(\lambda + \gamma_2)}; \tag{26}$$

$$\bar{t} = t_1^* - \frac{\left(2 \cdot \frac{\lambda w}{m} + \frac{\gamma_2}{s} + \frac{\gamma_1}{s}\right)}{\beta_1 + \gamma_1} N + \frac{s - r_{1,3}}{(r_{1,2} - r_{1,3})s} N + \frac{(r_{1,2} - r_{1,1})N \gamma_2}{r_{1,1}(r_{1,2} - r_{1,3})(\lambda + \gamma_2)}. \tag{27}$$

We can calculate the total daily travel cost at equilibrium ($TDTC_{UE}$) for Case 2:

$$TDTC_{UE} = \left[\frac{\beta_1}{\beta_1 + \gamma_1}\left(2 \cdot \frac{\lambda w}{m} + \frac{\gamma_2}{s} + \frac{\gamma_1}{s}\right)N\right]N, \tag{28}$$

where the term in the square bracket represents the individual daily travel cost at equilibrium. In addition, different aggregate cost components for Case 2 can be evaluated as follows:

$$TQ_1 = \alpha \cdot A_{P_1Q_1R_1W_1}; TS_1 = \left[\beta_1 \cdot A_{P_1Y_1'X_1}\right] + \left[\gamma_1 \cdot A_{X_1Y_1W_1}\right]; TP_1(AV) = \lambda \cdot A_{PWV} = TP_2(AV). \tag{29}$$

We again investigate the relationship between the two critical time points $\bar{t}$ and $\tilde{t}$ by calculating the difference:

$$\bar{t} - \tilde{t} = \frac{N}{(r_{1,2} - r_{1,3})\left(\alpha_1 + \gamma_1 + \frac{2\lambda ws}{m}\right)}\left[\left(\gamma_1 + \frac{2\lambda ws}{m}\right) - \left(\frac{\gamma_2}{\lambda + \gamma_2}\right)(\beta_1 + \gamma_1 - \lambda - \gamma_2)\right]$$

The term in the first square bracket is always positive considering that $r_{1,2} > s > r_{1,3}$. To ensure that $\tilde{x} < \bar{x}$, the necessary and sufficient condition is $\bar{t} > \tilde{t}$, as x is a

monotonically increasing function of t. Hence, when $\beta_1 > \frac{2\lambda ws}{m} + \lambda + \gamma_2$, Case 2 will occur if in the meantime, the following condition is satisfied:

$$\left(\gamma_1 + \frac{2\lambda ws}{m}\right) > \left(\frac{\gamma_2}{\lambda + \gamma_2}\right)(\beta_1 + \gamma_1 - \lambda - \gamma_2)$$

This condition can be re-written as

$$\beta_1 < \frac{2\lambda ws}{m} + \lambda + \gamma_2 + \frac{\lambda}{\gamma_2}\left(\gamma_1 + \frac{2\lambda ws}{m}\right)$$

Therefore, the condition of Case 2 can be re-written as

$$\frac{2\lambda ws}{m} + \lambda + \gamma_2 < \beta_1 < \frac{2\lambda ws}{m} + \lambda + \gamma_2 + \frac{\lambda}{\gamma_2}\left(\gamma_1 + \frac{2\lambda ws}{m}\right)$$

By comparing between Case 1 and Case 2, two clear insights can be provided. First, the start time of departure from home is earlier for Case 1 than that for Case 2 in the morning. One of the reasons is that the parking density m tends to be relatively smaller for Case 1 according to the conditions of these two cases summarised in Table 3.1. This means that the difference in the distance of AV self-driving to find a parking space is larger between two consecutive arriving AVs. Furthermore, Case 1 has a smaller penalty cost for early arrival, indicated by β_1, than Case 2. Given the two reasons above, in Case 1, commuters are motivated to depart earlier to park their AVs closer to the workplace, resulting in an earlier start of morning commuting. Second, by comparing the formulations of total daily travel costs for Case 1 and Case 2, it can be seen that we have an additional term $\frac{\gamma_1\left(\frac{2\lambda ws}{m} + \lambda + \gamma_2 - \beta_1\right)}{(\beta_1 + \gamma_1)s}\left(\frac{\gamma_2}{\lambda + \gamma_2}\right)N^2$ for Case 1. This is primarily because the earlier start of morning commutes in Case 1 causes commutes to be less concentrated around t_1^*, and as a result, the corridor is not fully used at Stage 1 given that $r_{1,1}(t) \leq s$. By contrast, in Case 2, the service rate of the inbound bottleneck is always at capacity from the beginning of Stage 1 through the end of Stage 3, which is described in Figure 3.4. Hence, the 'wasted capacity' in Case 1 leads to the abovementioned additional cost term within the formulation of $TSDTC_{UE}$.

3.3.2.2 Scenario 2

In Scenario 2, we have $x_0 \leq \bar{x} \leq \tilde{x}$. AVs that arrive early in the morning all reach the inbound bottleneck immediately after the official work closure time t_2^* in the evening; For late arrivals in the morning, some AVs arriving relatively early will

depart from the parking spot early and arrive at the bottleneck immediately after the time t_2^* in the evening, while the others will depart later to avoid a long queue. Similar to Scenario 1, three stages are formed in the departure pattern. Different from Scenario 1, there is only one case in Scenario 2 under the condition $\beta_1 > \frac{\lambda ws}{m} + \lambda + \gamma_2$, which is referred to as Case 3 in this study. In Case 3, the departure rates at equilibrium are summarized as follows (see *Derivation. Scenario 2* in Appendix B-2):

$$r_{1,1}(t_1) = \frac{\alpha_1}{\alpha_1 - \beta_1 + \frac{2\lambda ws}{m} + \lambda + \gamma_2} s > s \; ; \; r_{1,2}(t_1) = \frac{\alpha_1}{\alpha_1 + \gamma_1 + \gamma_2 + \lambda + \frac{2\lambda ws}{m}} s < \tag{30}$$
$$s; r_{1,3}(t_1) = \frac{\alpha_1}{\alpha_1 + \gamma_1 + \frac{2\lambda ws}{m}} s < s.$$

Furthermore, the relationship $r_{1,1}(t_1) > s > r_{1,3}(t_1) > r_{1,2}(t_1)$ holds.

For Case 3, the user-equilibrium traffic pattern in terms of departure time and parking location for morning-evening commutes is depicted in Figure 3.5. For both morning and evening commutes, the physical meanings of curves in different colors are the same as Figure 3.3 and Figure 3.4.

Similarly, based on the flow conservation and equilibrium conditions, we can determine t_s and t_e as follows:

$$t_s = t_1^* - \frac{\left(2 \cdot \frac{\lambda w}{m} + \frac{\gamma_2}{s} + \frac{\gamma_1}{s}\right)}{\beta_1 + \gamma_1} N; t_e = t_1^* - \frac{\left(2 \cdot \frac{\lambda w}{m} + \frac{\gamma_2}{s} - \frac{\beta_1}{s}\right)}{\beta_1 + \gamma_1} N. \tag{31}$$

Similarly, we can determine $\tilde{t}$ and $\bar{t}$ as follows

$$\tilde{t} = t_1^* - \frac{\left(2 \cdot \frac{\lambda w}{m} + \frac{\gamma_2}{s} + \frac{\gamma_1}{s}\right)}{\beta_1 + \gamma_1} N + \left(\frac{1}{s} - \frac{1}{r_{1,3}}\right) N + \frac{1}{r_{1,3}} \frac{N\gamma_2}{(\lambda + \gamma_2)};$$

$$\bar{t} = t_1^* - \frac{\left(2 \cdot \frac{\lambda w}{m} + \frac{\gamma_2}{s} + \frac{\gamma_1}{s}\right)}{\beta_1 + \gamma_1} N - \frac{r_{1,2}}{(r_{1,1} - r_{1,2})}\left(\frac{1}{s} - \frac{1}{r_{1,3}}\right) N + \frac{1}{(r_{1,1} - r_{1,2})}\left(1 - \frac{r_{1,2}}{r_{1,3}}\right) \frac{N\gamma_2}{(\lambda + \gamma_2)}. \tag{32}$$

We can calculate the total daily travel cost at equilibrium for Case 3

$$TDTC_{UE} = \left[\frac{\beta_1}{\beta_1 + \gamma_1}\left(2 \cdot \frac{\lambda w}{m} + \frac{\gamma_2}{s} + \frac{\gamma_1}{s}\right) N\right] N. \tag{33}$$

Particularly, the term in the square bracket represents the individual daily travel cost at equilibrium for Case 3. Similar to Case 2, we can evaluate different aggregate cost

components for Case 3 based on Figure 3.5: $TQ_1 = \alpha \cdot A_{P_1 Q_1 R_1 W_1}$; $TS_1 = [\beta_1 \cdot A_{P_1 Y_1' X_1}] + [\gamma_1 \cdot A_{X_1 Y_1 W_1}]$; $TP_1(AV) = \lambda \cdot A_{P_1 W_1 V_1} = TP_2(AV)$.
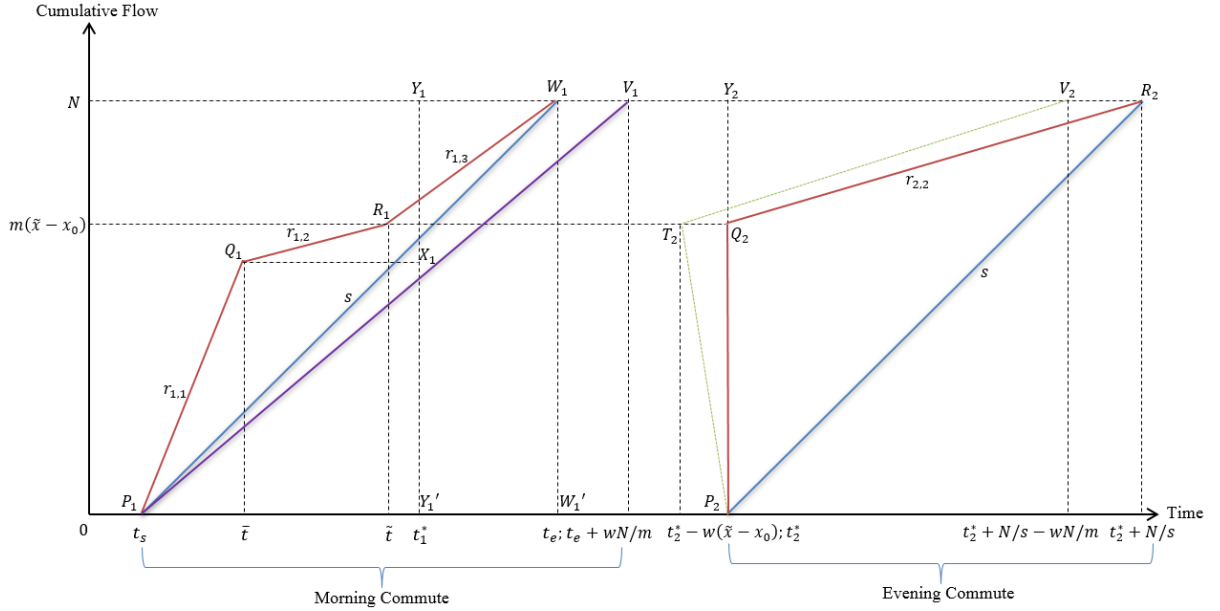
Figure 3.4 Daily equilibrium commute pattern for Case 3.

It can be easily observed that the formulations of t_s, t_e and $TDTC_{UE}$ are the same for Case 2 and Case 3. This is because, unlike Case 1, the bottleneck is always at capacity with traffic congestion throughout the morning commute in Case 2 and Case 3.

It is noteworthy that the identical mathematical formulations of t_s, t_e and $TDTC_{UE}$ for Case 2 and Case 3 do not mean that we can obtain the same computational results on the values of these metrics for the two cases. This is because these two cases have different conditions and there is no overlap in between. The condition of Case 2 has been explored in Section 3.3.2.1. We now further investigate the condition of Case 3. To do this, we analyze the relationship between the two critical time points $\bar{t}$ and $\tilde{t}$ in Case 3 by calculating the difference:

$$\tilde{t} - \bar{t} = \left[N \frac{\left(\alpha_1 + \gamma_1 + \gamma_2 + \lambda + \frac{2\lambda w s}{m}\right)}{(\beta_1 + \gamma_1)\alpha_1 s} \right] \left[-\left(\gamma_1 + \frac{2\lambda w s}{m}\right) + \frac{\gamma_2}{(\lambda + \gamma_2)}(\gamma_1 + \beta_1 - \lambda - \gamma_2) \right]$$

To ensure that $\tilde{x} \geq \bar{x}$ holds for Case 3, the necessary and sufficient condition is $\tilde{t} \geq \bar{t}$. Given that the term in the first square bracket in the above equation is always

42

positive, the additional condition $\left(\gamma_1 + \frac{2\lambda ws}{m}\right) \leq \frac{\gamma_2}{(\lambda+\gamma_2)}(\gamma_1 + \beta_1 - \lambda - \gamma_2)$ must hold.

This condition can be re-written as $\beta_1 \geq \frac{2\lambda ws}{m} + \lambda + \gamma_2 + \frac{\lambda}{\gamma_2}\left(\gamma_1 + \frac{2\lambda ws}{m}\right)$. Given that

$\beta_1 \geq \frac{2\lambda ws}{m} + \lambda + \gamma_2$ holds for Case 3, the condition of Case 3 is

$\beta_1 \geq \frac{2\lambda ws}{m} + \lambda + \gamma_2 + \frac{\lambda}{\gamma_2}\left(\gamma_1 + \frac{2\lambda ws}{m}\right)$. This condition is consistent with the condition

of Case 2 in terms of the critical point for β_1 valued at $\frac{2\lambda ws}{m} + \lambda + \gamma_2 + \frac{\lambda}{\gamma_2}\left(\gamma_1 + \frac{2\lambda ws}{m}\right)$

Furthermore, we can conclude that if $\beta_1 = \frac{2\lambda ws}{m} + \lambda + \gamma_2 + \frac{\lambda}{\gamma_2}\left(\gamma_1 + \frac{2\lambda ws}{m}\right)$, the two critical time points $\tilde{t}$ and $\bar{t}$ are the same (accordingly, the two critical parking locations $\tilde{x}$ and $\bar{x}$ are the same). Under such circumstance, for all the commuters who arrive early or on time in the morning, their AVs will depart from parking spots early and arrive at the bottleneck immediately after the work closure time, while for all the commuters who arrive late in the morning, their AVs will delay the departure time after work to avoid a long queue for evening commutes. This is the boundary case between Case 2 and Case 3. To summarize, the conditions of all the three possible cases at user equilibrium are listed in Table 3.2.

Table 3.2 Summary of conditions for Cases 1, 2 and 3.

Case	Condition
Case 1	$\frac{2\lambda ws}{m} < \beta_1 \leq \frac{2\lambda ws}{m} + \lambda + \gamma_2$
Case 2	$\frac{2\lambda ws}{m} + \lambda + \gamma_2 < \beta_1 < \frac{2\lambda ws}{m} + \lambda + \gamma_2 + \frac{\lambda}{\gamma_2}\left(\gamma_1 + \frac{2\lambda ws}{m}\right)$
Case 3	$\beta_1 \geq \frac{2\lambda ws}{m} + \lambda + \gamma_2 + \frac{\lambda}{\gamma_2}\left(\gamma_1 + \frac{2\lambda ws}{m}\right)$

The comparison between Case 1 and Case 2 has been analyzed in the last section. We now further discuss the conditions for Case 2 and Case 3. Table 3.2 implies that changes of the penalty costs for early arrival and late arrival, indicated by β_1 and γ_1, can cause the switch between Case 2 and Case 3. Specifically, if β_1 increases, Case 3 is more likely to occur; if γ_1 increases, Case 2 is more likely to occur. The reason is explained as follows. Regardless of β_1 and γ_1, the numbers of early departure and

delayed departure for evening commute are respectively $\frac{\gamma_2 N}{\lambda+\gamma_2}$ and $\frac{\lambda}{\lambda+\gamma_2}N$. For Case 2, the number of early arrivals equals the number of early departures plus a proportion of delayed departure for evening commute. By contrast, for Case 3, the number of early arrivals is less, which merely equals a proportion of early departure. Hence, when late arrival incurs more severe punishment, i.e. γ_1 becomes larger, more commuters would choose early arrival, and therefore, Case 2 will be more likely. On the other hand, if early arrival becomes more costly, i.e. β_1 becomes larger, commuters would be less likely to arrive early, which makes Case 3 more likely.

It is noteworthy that β_1 should be greater than λ and γ_2 (for Case 2 and Case 3). Whether this will occur or not should rely on case-by-case empirical studies for a city or community, which is beyond the scope of this study. As per Vickrey (1973), β_1 and γ_2 can be determined as the utility of home-based activities minus that of working for employers. The former depends on people's productivity, while the latter can be regarded as a fixed value given that people usually get paid at a constant rate. Intuitively, $\beta_1 > \lambda$ and $\beta_1 > \gamma_2$ might happen in the sense that morning time is valuable given that a majority of people are energetic in the morning. In this sense, early arrival might indicate inefficient use of valuable morning time, which can be more costly than AV self-driving time or waiting time caused by late departure in the evening when people value time less after work.

3.3.3 Variation of user-equilibrium AV traffic pattern against the parking density

In Section 3.3.2, we investigate the user-equilibrium traffic patterns under three different cases. The conditions for the occurrence of each case are related to the parking density. This means that parking supply could potentially affect the UE traffic pattern and its efficiency. To investigate the influences of m, we first identify the feasible region of m.

It can be verified that $m > \frac{2\lambda ws}{\beta_1}$ (based on Assumption (vii) in Section 3.2) and $m > ws$ (based on Assumption (viii) in Section 3.2). One can further verify that we should have

$m \in \Omega_m = (ws, +\infty)$ if $\beta_1 > 2\lambda$; or $m \in \Omega_m = \left(\frac{2\lambda ws}{\beta_1}, +\infty\right)$ if $\frac{2\lambda ws}{m} < \beta_1 \leq 2\lambda$.

We further summarize how the equilibrium flow pattern will change with respect to m and how it is related to the range of β_1 in Table 3.3 (this can be verified by checking the

conditions in Table 3.2).

Table 3.3 Flow patterns change with parking density

Situation	Range of β_1	Range of m	Cases
(i)	$\dfrac{2\lambda ws}{m} < \beta_1 < \lambda + \gamma_2$	$m \in \Omega_m$	Case 1
(ii)	$\lambda + \gamma_2 \le \beta_1 < 3\lambda + \gamma_2$	$m \le \dfrac{2\lambda ws}{\beta_1 - \lambda - \gamma_2}$	Case 1
		$m > \dfrac{2\lambda ws}{\beta_1 - \lambda - \gamma_2}$	Case 2
(iii)	$3\lambda + \gamma_2 \le \beta_1 < \lambda + \gamma_2 + \dfrac{\lambda\gamma_1}{\gamma_2}$	$m \in \Omega_m$	Case 2
(iv)	$\lambda + \gamma_2 + \dfrac{\lambda\gamma_1}{\gamma_2} \le \beta_1 < 3\lambda + \gamma_2 + \dfrac{\lambda}{\gamma_2}(\gamma_1 + 2\lambda)$	$m \le \left(1 + \dfrac{\lambda}{\gamma_2}\right)\dfrac{2\lambda ws}{\beta_1 - \left(\lambda + \gamma_2 + \frac{\lambda}{\gamma_2}\gamma_1\right)}$	Case 2
		$m > \left(1 + \dfrac{\lambda}{\gamma_2}\right)\dfrac{2\lambda ws}{\beta_1 - \left(\lambda + \gamma_2 + \frac{\lambda}{\gamma_2}\gamma_1\right)}$	Case 3
(v)	$\beta_1 \ge 3\lambda + \gamma_2 + \dfrac{\lambda}{\gamma_2}(\gamma_1 + 2\lambda)$	$m \in \Omega_m$	Case 3

As can be seen in Table 3.3, the equilibrium traffic pattern varies with the AV parking density m in different manners under the abovementioned five situations (each situation has a different range of β_1). We have several observations in Table 3.3. Firstly, when β_1 increases, i.e., Situation (i) → Situation (ii) → Situation (iii) → Situation (iv) → Situation (v), generally speaking, the flow pattern tends to change from Case 1 to Case 2 and then to Case 3. This is briefly explained as follows. When β_1 is small (early arrival in the morning commute is relatively costless), some commuters may depart sufficiently early (even with no congestion delays) to secure a better parking location, i.e., Case 1. When β_1 becomes relatively large (early arrival is relatively costly), even those commuters with a relatively close parking location $(x < \tilde{x})$ will arrive late in the morning, i.e., Case 3. And Case 2 is in-between where β_1 is neither too large nor too small. These results are consistent with our discussions for Table 3.2 (comparison of the three cases). Secondly, when m increases, the flow pattern tends to change from Case 1 to Case 2 or from Case 2 to Case 3. This is because, when m is relatively small, i.e., parking is relatively sparse, commuters are more incentivised to compete for a good parking location, which results in Case 1 (some commuters depart sufficiently early even without congestion). When m is relatively large, i.e., parking is more densely distributed, departing later may still lead to a not very far away parking location, commuters are less incentivized to compete for a

closer parking, which results in Case 3 (some with a relatively close parking location $(x < \tilde{x})$ still arrive late in the morning). Again, Case 2 is in-between.

While the flow pattern may change with m, the total daily travel cost at equilibrium always decreases with the increase of m, when all the other parameters are considered given. This is primarily due to the savings in the time cost for AV self-driving to find a parking spot in the morning and to return to the workplace in the afternoon, given that a larger m results in a smaller $\frac{N}{m}$. This can also be verified mathematically: the relationship

$\frac{dTDTC_{UE}}{dm} < 0$ holds for Case 1, Case 2 and Case 3; meanwhile, for Situation (ii) and Situation (iii), the evaluation of $TDTC_{UE}$ goes smoothly at the transition point of m.

It can be seen that the equilibrium daily traffic pattern of AVs is different from that of non-AVs (Zhang et al., 2005, 2008). We now summarize some of the major characteristics of commuting equilibriums with AVs. First, the walking time between the office and the parking spot for morning-evening commuting is eliminated when people travel with AVs, which can influence the arrival and departure time for work as well as the schedule delay cost. This leads to the different time-dependent equilibrium traffic pattern than the literature with non-AVs. Second, this study integrates the correlated morning and evening commutes. Compared to Zhang et al. (2008), for morning commuting, the proposed model considers both early arrival and late arrival in the morning. This raises three different cases for the morning traffic pattern depending on the value of time, schedule penalties, and parking supply (as discussed in Table 3.2 and Table 3.3). Third, as AVs can park far away from the workplace in the morning, they must drive themselves back to the workplace to pick up commuters after work due to the unacceptable walking distance. This leads to an active inbound bottleneck on the way from parking lots to the city centre for evening commute with AVs, which is different from the non-AV situation where commuters experience congestions on the way from the workplace to home after work. Furthermore, in comparison to the equilibrium analysis considering AV morning commuting only (Liu, 2018), this study further highlights the importance of integrating asymmetric morning commute and evening commute for modelling traffic dynamics in a fully automated environment.

Overall, the adoption of AVs substantially reshapes both the morning and evening commutes, which involves when, where and how congestion will occur. With such a distinctive AV traffic pattern derived, it is expected that the optimal tolling scheme and parking supply strategy for the AV daily commute will be different from those under the

non-AV environment and those when only the morning commute is considered for AVs. Based on the presented equilibrium analysis, the tolling scheme and the AV parking supply plan will be discussed in the following sections.

3.4 System Optimum and Time-dependent Tolling Scheme for AV Traffic Behavior

In this section, we first discuss the traffic pattern at system optimum (SO). Then, we investigate the congestion tolling scheme to achieve the system optimal traffic pattern. Generally speaking, for both morning and evening commutes, at system optimum, the following conditions should be satisfied: (i) traffic congestion at the bottleneck must be completely eliminated, i.e. the queuing delay is always zero; (ii) the schedule delay cost should be minimized to the largest extent, i.e. the times of arrival at and departure from the workplace should be respectively close to the official work start time and closure time as far as possible; (iii) the time cost for AV-self driving should be minimized, i.e. the selected parking location should be as close to the workplace as possible. Given these conditions in mind, we can then investigate the first-best tolling schemes for morning and evening commutes.

3.4.1 System optimum for evening commute and tolling scheme

For evening commute, under the system optimum conditions, the traffic pattern should be formed in the way that: (i) the arrival rate to the bottleneck r_2 should always be equal to the service capacity of the bottleneck s, which means that the bottleneck capacity is fully utilised without any congestion; (ii) the first AV arrives at the workplace to pick up commuters at the official work closure time t_2^*. We need to emphasise that under the SO flow pattern, the order of departures from the parking lot is not unique, which means that a parking location closer to the workplace does not necessarily correspond to an earlier departure time. An illustrative SO flow pattern for the evening commute is depicted in Figure 3.6(a), where AVs parked closer to the workplace will depart earlier in the evening. The blue solid line PR reflects both the arrival at and departure from the bottleneck. The green curve PW represents the time of departure from parking spots under the assumption that AVs parked closer to the workplace will depart earlier in the evening.
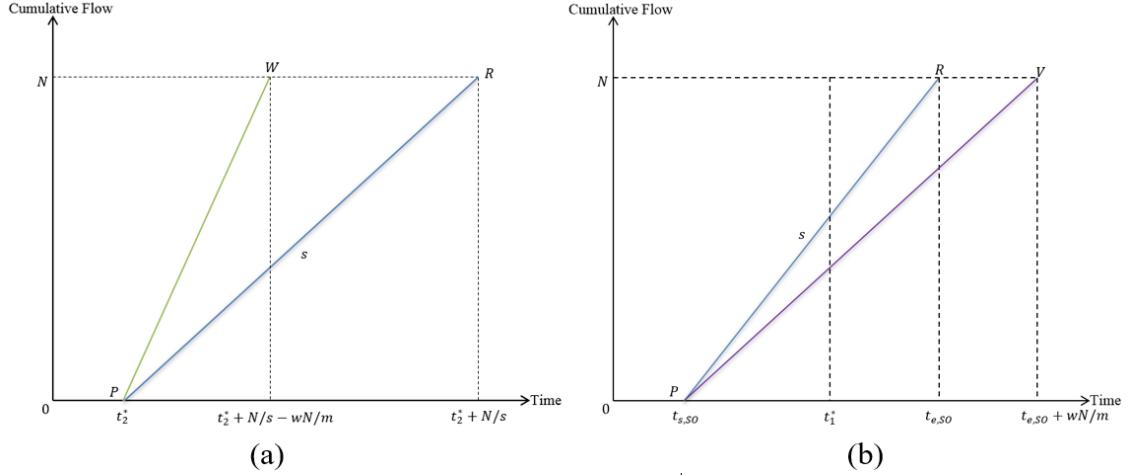
Figure 3.5 SO traffic pattern for (a) evening commute and (b) morning commute

We denote the tolling fee for evening commute at time t as $\sigma_2(t)$, where t represents the time of arrival at the inbound bottleneck. We can derive the following tolling scheme to achieve the SO for the evening commute depicted in Figure 3.6(a):

$$
\sigma_2(t) = \begin{cases} \gamma_2 \cdot \dfrac{N}{s} + \varepsilon_0 & t \in (0, t_2^*) \\ -\gamma_2 \cdot t + \gamma_2 \cdot \left(t_2^* + \dfrac{N}{s}\right) + \varepsilon_0 & t \in \left[t_2^*, t_2^* + \dfrac{N}{s}\right] \\ \varepsilon_0 & t \in \left(t_2^* + \dfrac{N}{s}, +\infty\right) \end{cases}
\tag{34}
$$

where the last AV arriving at the inbound bottleneck pays the tolling fee ε_0. Note that this evening toll is imposed at the inbound bottleneck based on the arrival time at the bottleneck to eliminate congestion during the pick-up process. At the SO, the individual travel cost for evening commute including the toll is

$$
c_2^\sigma(t_2, x)_{SO} = \lambda w(x - x_0) + \frac{\gamma_2 N}{s} + \varepsilon_0.
\tag{35}
$$

The individual travel cost under the SO conditions increases linearly with regards to the parking location x, which is because the self-driving cost is proportional to the distance to the city centre. At system optimum, the total evening travel cost including road tolls is

$$
TETC^\sigma{}_{SO} = 0.5\lambda w \frac{N^2}{m} + \frac{\gamma_2 N^2}{s} + \varepsilon_0 N.
\tag{36}
$$

The $TETC^\sigma{}_{SO}$ is comprised of the total toll revenue for evening commute TR_2 and the total evening travel cost excluding tolls $TETC_{SO}$, which are given as follows:

$$TR_2 = 0.5\frac{\gamma_2 N^2}{s} + \varepsilon_0 N; \; TETC_{SO} = 0.5\lambda w\frac{N^2}{m} + 0.5\frac{\gamma_2 N^2}{s}. \tag{37}$$

It is obvious that $TETC_{UE} - TETC_{SO} = 0.5\frac{N^2\gamma_2(m-ws)\lambda}{ms(\lambda+\gamma_2)-\lambda s^2 w} > 0.$

3.4.2 System optimum for morning commute considering daily travel cost

For morning commute, under the system optimum conditions, the traffic pattern should be formed in the way that: (i) the departure rate from home (arrival rate to the bottleneck) is equal to the bottleneck service capacity s; (ii) the parking area is fully occupied from the parking location x_0 outwards, in order to minimise the system-level time cost of AV self-driving. It is worth noting that the parking order of AVs within the parking area has no impact on system efficiency. For simplicity, similar to the evening commute case, we target a SO where AVs with an earlier departure time is parked closer to the workplace. In addition, according to the standard conclusion from the literature, we have the first departure time $t_{s,SO} = t_1^* - \frac{\gamma_1}{\beta_1+\gamma_1} \cdot \frac{N}{s}$ and the last departure time $t_{e,SO} = t_1^* + \frac{\beta_1}{\beta_1+\gamma_1} \cdot \frac{N}{s}$ for morning commuting at system optimum. The SO traffic pattern for morning commuting is shown in Figure 3.6(b). The blue curve PR represents the cumulative departure from home as well as the cumulative arrival at the workplace. The purple curve PV represents the cumulative arrival at the AV parking lot.

We denote that the tolling fee for arrival time to the inbound bottleneck t (departure time from home) in the morning as $\sigma_1(t)$. The following toll scheme can be derived to support the SO in the morning commute:

$$\sigma_1(t) = \begin{cases} \varepsilon_0 & t \in (0, t_{s,SO}) \\ \left(\beta_1 - \frac{2\lambda ws}{m}\right)\left(t - t_1^* + \frac{\gamma_1 N}{(\beta_1+\gamma_1)s}\right) + \varepsilon_0 & t \in [t_{s,SO}, t_1^*) \\ -\left(\gamma_1 + \frac{2\lambda ws}{m}\right)(t - t_1^*) + \left(\beta_1 - \frac{2\lambda ws}{m}\right)\frac{\gamma_1 N}{(\beta_1+\gamma_1)s} + \varepsilon_0 & t \in [t_1^*, t_{e,SO}] \\ \varepsilon_0 - \frac{2\lambda wN}{m} & t \in (t_{e,SO}, +\infty) \end{cases} \tag{38}$$

where ε_0 is the constant toll for the commuters arriving at the inbound bottleneck earlier than or equal to $t_{s,SO}$. It can be observed from Equation (39) that the toll at the beginning of the travel period is higher than that at the end. This is to compensate the late arrival commuters with a larger AV-self driving distance so that they have no incentive to compete for closer parking and additional schedule delay cost is avoided.

At system optimum, the total daily travel cost, denoted as $TDTC_{SO}$ can be determined as

follows

$$TDTC_{SO} = 0.5 \frac{\beta_1 \gamma_1}{\beta_1 + \gamma_1} \frac{N^2}{s} + \frac{\lambda w N^2}{m} + 0.5 \frac{\gamma_2 N^2}{s}. \tag{39}$$

We can further determine the total toll revenue for morning commutes TR_1 as follows

$$TR_1 = N \left[\varepsilon_0 + 0.5 \frac{\beta_1 \gamma_1 N}{(\beta_1 + \gamma_1)s} - \frac{\lambda w N}{m} \right]. \tag{40}$$

By comparing the total toll revenue for morning and evening commutes, it can be easily seen that TR_1 is dependent on the AV parking density m wherein we have $\frac{dTR_1}{dm} > 0$, while m has no influence on TR_2. The total toll revenue for daily commutes TR can be determined as follows

$$TR = TR_1 + TR_2 = N \left[2\varepsilon_0 + 0.5 \frac{\gamma_2 N}{s} + 0.5 \frac{\beta_1 \gamma_1 N}{(\beta_1 + \gamma_1)s} - \frac{\lambda w N}{m} \right]. \tag{41}$$

3.5 Optimal AV Parking Supply Strategy

3.5.1 Evaluation of total system cost of automated transportation system

Following Liu (2018), we further investigate the optimal AV parking supply strategies under either the no-toll equilibrium or system optimum traffic pattern. The objective is to minimise the total system cost, denoted as TSC in this study, which is comprised of the total daily travel cost (toll excluded) and the total social parking cost. As will be shown later, integrating morning and evening commutes significantly complicates the optimal parking supply solutions, and provides additional findings against a recent study by Liu (2018) where only morning commute is considered.

We consider that the social cost of a parking space is dependent on the distance between the parking location and the city centre, and hereby define the social cost of a unit parking spot at location x as $\rho(x)$. $\rho(x)$ is a monotonic decreasing function of x, which indicates that the social parking cost becomes larger when the parking location is closer to the city centre. We can then calculate the total social parking cost ($TSPC$) as follows

$$TSPC = \int_{x_0}^{x_0 + \frac{N}{m}} \rho(x) m(x) dx. \tag{42}$$

Under the assumption $m(x) = m$, the above equation can be re-written as

$$TSPC = \int_{x_0}^{x_0 + \frac{N}{m}} \rho(x) m \, dx. \tag{43}$$

Hence, we can determine the total system cost at user equilibrium TSC_{UE} and at system optimum TSC_{SO} as follows

$$TSC_{UE} = TDTC_{UE} + TSPC; TSC_{SO} = TDTC_{SO} + TSPC.$$

3.5.2 Optimal AV parking supply for user equilibrium

In this section, we investigate the optimal AV parking density m for all the five situations discussed in Section 3.3.3: Situation (i), $\frac{2\lambda ws}{m} < \beta_1 < \lambda + \gamma_2$; Situation (ii), $\lambda + \gamma_2 \leq \beta_1 < 3\lambda + \gamma_2$; Situation (iii), $3\lambda + \gamma_2 \leq \beta_1 < \lambda + \gamma_2 + \frac{\lambda\gamma_1}{\gamma_2}$; Situation (iv), $\lambda + \gamma_2 + \frac{\lambda\gamma_1}{\gamma_2} \leq \beta_1 < 3\lambda + \gamma_2 + \frac{\lambda}{\gamma_2}(\gamma_1 + 2\lambda)$; and Situation (v), $\beta_1 \geq 3\lambda + \gamma_2 + \frac{\lambda}{\gamma_2}(\gamma_1 + 2\lambda)$. In different situations, how the commuting equilibrium and system efficiency change with the parking density is different.

3.5.2.1 Situation (i)

In Situation (i) when $\frac{2\lambda ws}{m} < \beta_1 < \lambda + \gamma_2$, only Case 1 occurs even if parking density m can vary. We derive and examine the first derivative of TSC_{UE} with respect to the parking density:

$$\frac{dTSC_{UE}}{dm} = \left[-\frac{\gamma_1}{(\beta_1+\gamma_1)}\left(\frac{N^2\gamma_2}{\lambda+\gamma_2}\right)\left(\frac{2\lambda w}{m^2}\right) - \frac{2\beta_1\lambda wN^2}{\beta_1+\gamma_1}\left(\frac{1}{m^2}\right) \right] + \left[\int_{x_0}^{x_0+\frac{N}{m}} \rho(x)dx - \rho\left(x_0 + \frac{N}{m}\right)\frac{N}{m} \right].$$ (45)

The term in the first square bracket is the marginal increase in the total daily travel cost under the user equilibrium conditions (negative, as discussed in Section 3.3.3). The term in the second square bracket is the marginal increase in the total social parking cost, which is positive given $\rho(x) \geq \rho\left(x_0 + \frac{N}{m}\right), \forall x \in \left[x_0, x_0 + \frac{N}{m}\right]$. This is because of the decreasing function of $\rho(x)$, which implies that the dense parking facility deployment closer to the city centre corresponds to higher land values and greater social costs. To allow for

analytical tractability, we assume a constant $\rho'(x)$, i.e., $\rho'(x) = \rho'$.

We further calculate the second derivative of TSC_{UE}:

$$\frac{d^2 TSC_{UE}}{dm^2} = \left[\frac{4\lambda w \gamma_1 \gamma_2}{(\beta_1+\gamma_1)(\lambda+\gamma_2)} + \frac{4\beta_1 \lambda w}{\beta_1+\gamma_1} + \rho'\left(x_0 + \frac{N}{m}\right)\right]\frac{N^2}{m^3}, \qquad (46)$$

where $\rho'(x) = \frac{d\rho(x)}{dx}$ $x \in \left[x_0, x_0 + \frac{N}{m}\right]$. When $\frac{d^2 TSC_{UE}}{dm^2} = 0$, we have $\rho'\left(x_0 + \frac{N}{m}\right) =$

$-\frac{4\lambda w \gamma_1 \gamma_2}{(\beta_1+\gamma_1)(\lambda+\gamma_2)} - \frac{4\beta_1 \lambda w}{\beta_1+\gamma_1} < 0$. Based on $\frac{dTSC_{UE}}{dm}$ and $\frac{d^2 TSC_{UE}}{dm^2}$, we found that to minimize

TSC_{UE} (total system cost including parking social cost), we have the optimal parking supply as follows.

Firstly, if $\rho' > -\frac{4\lambda w \gamma_1 \gamma_2}{(\beta_1+\gamma_1)(\lambda+\gamma_2)} - \frac{4\beta_1 \lambda w}{\beta_1+\gamma_1}$, the optimal solution m_{UE} is set to approach

infinity, or an upper bound if set; Secondly, if $\rho' < -\frac{4\lambda w \gamma_1 \gamma_2}{(\beta_1+\gamma_1)(\lambda+\gamma_2)} - \frac{4\beta_1 \lambda w}{\beta_1+\gamma_1}$, the optimal

solution m_{UE} is to approach the lower bound of the feasible region, i.e. $\frac{2\lambda w s}{\beta_1}$ if $\frac{2\lambda w s}{m} <$

$\beta_1 \leq 2\lambda$, or ws if $2\lambda < \beta_1 < \lambda + \gamma_2$; Thirdly, if $\rho' = -\frac{4\lambda w \gamma_1 \gamma_2}{(\beta_1+\gamma_1)(\lambda+\gamma_2)} - \frac{4\beta_1 \lambda w}{\beta_1+\gamma_1}$: if

$\frac{dTSC_{UE}}{dm} > 0$, the optimal solution is to approach the lower bound; if $\frac{dTSC_{UE}}{dm} < 0$, the

optimal solution is to approach infinity, or an upper bound if set; if $\frac{dTSC_{UE}}{dm} = 0$, the

optimal m_{UE} can be equal to any value within the feasible region.

The above results are in line with Liu (2018). When the social cost of parking varies with distance to the city centre relatively sharp or relatively flat, we have corner solutions for the parking density. In particular, when parking cost decreases with the distance to the city centre relatively flat (a less negative ρ'), we should provide all the parking in the city centre (a larger m) to save AV self-driving cost. When the parking cost decreases sharply with the distance to city centre (a more negative ρ'), we should provide parking further away (a smaller m) to save the social cost of parking supply. However, the exact conditions to identify the optimal parking density are different, since the impacts of parking density on the morning and evening commutes are both incorporated. For

example, the critical value of ρ' is equal to $-\frac{4\lambda w \gamma_1 \gamma_2}{(\beta_1+\gamma_1)(\lambda+\gamma_2)} - \frac{4\beta_1 \lambda w}{\beta_1+\gamma_1}$, which is equal to

twice of that in Liu (2018) plus an additional term $-\frac{4\lambda w \gamma_1 \gamma_2}{(\beta_1+\gamma_1)(\lambda+\gamma_2)}$. This will be further explained when we compare Situation (i) with other situations in Section 3.5.2.3 (for short, "twice" is related to integrated consideration of evening and morning commute, and the "additional" is related to the capacity waster at Case 1 in the beginning of the morning commute).

3.5.2.2 Situation (ii)

Under Situation (ii), the UE traffic pattern changes from Case 1 to Case 2 with the increase of m. It can be easily verified that the evaluation of TSC_{UE} changes smoothly around the transition point $m = \frac{2\lambda ws}{\beta_1-\lambda-\gamma_2}$, at which we have $TSC_{UE} = \frac{\beta_1}{\beta_1+\gamma_1}\left(\frac{\beta_1+\gamma_1-\lambda}{s}\right)N^2 + \int_{x_0}^{x_0+\frac{N}{m}}\rho(x)mdx$. Similar to Section 3.5.2.1, we can determine the optimal AV parking density m as follows.

Firstly, if $\rho' > -\frac{4\beta_1\lambda w}{\beta_1+\gamma_1}$, the optimal solution m_{UE} is to approach infinity, or an upper bound if set; Secondly, if $-\frac{4\lambda w\gamma_1\gamma_2}{(\beta_1+\gamma_1)(\lambda+\gamma_2)}-\frac{4\beta_1\lambda w}{\beta_1+\gamma_1} < \rho' < -\frac{4\beta_1\lambda w}{\beta_1+\gamma_1}$, the optimal solution is $m_{UE} = \frac{2\lambda ws}{\beta_1-\lambda-\gamma_2}$; Thirdly, if $\rho' < -\frac{4\lambda w\gamma_1\gamma_2}{(\beta_1+\gamma_1)(\lambda+\gamma_2)}-\frac{4\beta_1\lambda w}{\beta_1+\gamma_1}$, the optimal solution m_{UE} is to approach the lower bound of the feasible region, i.e. ws; Fourthly, if $\rho' = -\frac{4\beta_1\lambda w}{\beta_1+\gamma_1}$, we have: if $\frac{dTSC_{UE}}{dm} > 0$, the optimal solution is $m_{UE} = \frac{2\lambda ws}{\beta_1-\lambda-\gamma_2}$; if $\frac{dTSC_{UE}}{dm} < 0$, the optimal solution is to approach infinity, or an upper bound if set; if $\frac{dTSC_{UE}}{dm} = 0$, the optimal m_{UE} can be equal to any value within the region $\left(\frac{2\lambda ws}{\beta_1-\lambda-\gamma_2}, +\infty\right)$; Fifthly, if $\rho' = -\frac{4\lambda w\gamma_1\gamma_2}{(\beta_1+\gamma_1)(\lambda+\gamma_2)}-\frac{4\beta_1\lambda w}{\beta_1+\gamma_1}$, we determine the $\frac{dTSC_{UE}}{dm}$ by using Eq. (46) and then have: if $\frac{dTSC_{UE}}{dm} > 0$, the optimal solution is to approach the lower bound, i.e. ws; if $\frac{dTSC_{UE}}{dm} < 0$, the optimal solution is $m_{UE} = \frac{2\lambda ws}{\beta_1-\lambda-\gamma_2}$; if $\frac{dTSC_{UE}}{dm} = 0$, the optimal m_{UE} can be equal to any value within the region $\left(ws, \frac{2\lambda ws}{\beta_1-\lambda-\gamma_2}\right)$

The above results also share some similarities with Liu (2018). For example, when the social cost of parking varies with distance to the city centre relatively sharp or relatively flat, we have corner solutions for the parking density. This is because, when social cost of parking varies over space significantly (ρ' is more negative, and thus $\rho' < -\frac{4\lambda w \gamma_1 \gamma_2}{(\beta_1+\gamma_1)(\lambda+\gamma_2)} - \frac{4\beta_1 \lambda w}{\beta_1+\gamma_1}$), to minimise the total system cost we should minimise social cost of parking as much as possible. Instead, the ρ' is less negative (closer to zero), parking costs at different locations differ very little, we should provide more dense parking at city centre to reduce total travel cost of all commuters. However, different from Liu (2018), when ρ' is neither too small or too large, we have an interior optimal solution for m. For example, when $-\frac{4\lambda w \gamma_1 \gamma_2}{(\beta_1+\gamma_1)(\lambda+\gamma_2)} - \frac{4\beta_1 \lambda w}{\beta_1+\gamma_1} < \rho' < -\frac{4\beta_1 \lambda w}{\beta_1+\gamma_1}$, the optimal parking density is $m_{UE} = \frac{2\lambda w s}{\beta_1-\lambda-\gamma_2}$ where the UE traffic pattern will be at the transition case between Case 1 and Case 2.

3.5.2.3 Situation (iii), Situation (iv) and Situation (v)

Despite that the UE traffic pattern varies with the parking density m in different manners under Situation (iii), Situation (iv) and Situation (v) as discussed in Section 3.3.3 (Case 2 and Case 3 might arise), the total cost formulations are identical. Therefore, we combine these three situations for consideration here. Similar to Section 3.5.2.1 and Section 3.5.2.2, we can derive the following results.

Firstly, if $\rho' > -\frac{4\beta_1 \lambda w}{\beta_1+\gamma_1}$, the optimal solution m_{UE} is set to approach infinity, or an upper bound if set; Secondly, if $\rho' < -\frac{4\beta_1 \lambda w}{\beta_1+\gamma_1}$, the optimal solution m_{UE} is to approach the lower bound of the feasible region, i.e. ws; Thirdly, if $\rho' = -\frac{4\beta_1 \lambda w}{\beta_1+\gamma_1}$: if $\frac{dTSC_{UE}}{dm} > 0$, the optimal solution is $m_{UE} = ws$; if $\frac{dTSC_{UE}}{dm} < 0$, the optimal solution is to approach infinity, or an upper bound if set; if $\frac{dTSC_{UE}}{dm} = 0$, the optimal m_{UE} can be

equal to any value within the feasible region $(ws, +\infty)$.

For Situation (iii), Situation (iv) and Situation (v), the results and reasoning are similar to those for Situation (i), which are also consistent with Liu (2018). However, a critical value of ρ' is now equal to $-\frac{4\beta_1\lambda w}{\beta_1+\gamma_1}$, which is exactly twice of that in Liu (2018) due to consideration of both morning and evening trips. However, in Situation (i), the critical value of ρ' is equal to $-\frac{4\lambda w\gamma_1\gamma_2}{(\beta_1+\gamma_1)(\lambda+\gamma_2)}-\frac{4\beta_1\lambda w}{\beta_1+\gamma_1}$. This is due to that when Case 1 (the equilibrium traffic pattern) arises, there is a period with costly capacity waste, i.e., $r_{1,1} = \frac{\beta_1}{\frac{2\lambda ws}{m}+\lambda+\gamma_2}s \leq s$, which is further explained as follows. By setting the parking density to the upper bound (or infinity), we would have the largest $r_{1,1}$ (under the largest m), indicating $r_{1,1}$ is as close to s as possible in Case 1, and the efficiency loss due to capacity waste in Case 1 will be smaller. This means that there is an additional gain of setting a larger m in Case 1 when compared to other cases. Therefore, for Situation (i) (only Case 1 can arise), for a larger range of ρ', we should set m to be infinity or the upper bound. Moreover, for Situation (ii), since both Case 1 and Case 2 might arise, two critical values of ρ' are involved, and the determination of optimal parking density is more tedious.

We need to acknowledge that, in certain situations, the AV parking density may increase with the distance x from the city centre. The consideration of a varying $m(x)$ could affect the results on the optimal parking supply strategy, because: (i) the user-equilibrium traffic pattern will be modified, as late departure would have a less disadvantageous parking location with the increased parking density; (ii) the gradient of m is to be added as an unknown to the above derivation process, leading to potential analytical intractability. These cases can be numerically solved for real-world problems, while this study focuses on analytical insights.

3.5.3 Optimal AV parking supply for system optimum

In this section, we investigate the optimal parking supply scheme under the system optimum conditions. The total system cost at system optimum TSC_{SO} can be calculated

as follows

$$TSC_{SO} = TDTC_{SO} + TSPC = \left[0.5\frac{\beta_1\gamma_1}{\beta_1+\gamma_1}\frac{N^2}{s} + \frac{\lambda w N^2}{m} + 0.5\frac{\gamma_2 N^2}{s}\right] +$$
$$\int_{x_0}^{x_0+\frac{N}{m}}\rho(x)m(x)dx. \tag{47}$$

We then take the first and the second derivatives of TSC_{SO}:

$$\frac{dTSC_{SO}}{dm} = \left[-\frac{\lambda w N^2}{m^2}\right] + \left[\int_{x_0}^{x_0+\frac{N}{m}}r(x)dx - \rho\left(x_0+\frac{N}{m}\right)\frac{N}{m}\right]; \tag{48}$$

$$\frac{d^2TSC_{SO}}{dm^2} = \left[2\lambda w + \rho'\left(x_0+\frac{N}{m}\right)\right]\frac{N^2}{m^3}. \tag{49}$$

From $\frac{dTSC_{SO}}{dm}$ and $\frac{d^2TSC_{SO}}{dm^2}$, it can be verified that to minimize the TSC_{SO}, we have the following results. Firstly, when $\rho' > -2\lambda w$, the optimal solution of m, denoted as m_{SO}, is to approach infinity, or an upper bound if set; Secondly, when $\rho' < -2\lambda w$, the optimal solution m_{SO} is to approach the lower bound, which is equal to ws if $\beta_1 > 2\lambda$, or $\frac{2\lambda ws}{\beta_1}$ if $\frac{2\lambda ws}{m} < \beta_1 \leq 2\lambda$; Thirdly, when $\rho' = -2\lambda w$: if $\frac{dTSC_{SO}}{dm} > 0$, the optimal solution is to approach the lower bound; if $\frac{dTSC_{SO}}{dm} < 0$, the optimal solution is to approach infinity or upper bound if set; if $\frac{dTSC_{SO}}{dm} = 0$, the optimal solution m_{SO} can be set as any feasible value for m.

The above results for the optimal parking density under system optimum traffic pattern are in line with those under user equilibrium traffic pattern and also compatible with those in Liu (2018), where only morning commute is considered. Furthermore, by comparing the optimal parking densities under UE and SO flow patterns, one can readily identify that the optimal solutions under UE and SO are often not identical. Particularly, when ρ' has a medium value, where optimal solutions under UE and SO differ, the details are discussed as follows. Before providing detailed discussion, it should be noted that the following condition holds: $-\frac{4\lambda w\gamma_1\gamma_2}{(\beta_1+\gamma_1)(\lambda+\gamma_2)} - \frac{4\beta_1\lambda w}{\beta_1+\gamma_1} < -2\lambda w < -\frac{4\beta_1\lambda w}{\beta_1+\gamma_1}$ (this can be verified based on assumptions on the schedule delay penalties).

For Situation (i), if $-\frac{4\lambda w\gamma_1\gamma_2}{(\beta_1+\gamma_1)(\lambda+\gamma_2)} - \frac{4\beta_1\lambda w}{\beta_1+\gamma_1} < \rho' < -2\lambda w$, we should let m approach the

upper bound to minimise TSC_{UE}, but approach the lower bound to minimize TSC_{SO}. This means, it is more likely (for a larger range of ρ'), we should let m to be the upper bound to minimise TSC_{UE} than to minimise TSC_{SO}. This is explained in the following. For TSC_{UE}, an increasing m (parking concentration over space) can cause the arrivals to be more concentrated around the official work start time and consequently, reduce the schedule delay for morning commute. Moreover, an increasing m would reduce the efficiency loss due to capacity waste (in Case 1) under user equilibrium traffic pattern, as discussed before.

For Situation (iii), Situation (iv) and Situation (v), if $-2\lambda w < \rho' < -\frac{4\beta_1\lambda w}{\beta_1+\gamma_1}$, we should let m approach the lower bound to minimize TSC_{UE}, but approach the upper bound to minimise TSC_{SO}. This means that it is more likely (for a larger range of ρ') we should set m to be the lower bound to minimise TSC_{UE}. This is because, under user equilibrium, a decreasing parking density can lead to less concentrated departure rates over time for morning at equilibrium (smaller $r_{1,1}, r_{1,2}, r_{1,3}$), which would lead to smaller queuing delays at the bottleneck. In contrast to UE traffic, the queueing delay is completely eliminated at system optimum, so a decreasing m cannot result in reductions in congestion levels. Note that for Situation (iii), Situation (iv) and Situation (v) since there is no period with a capacity waste, the additional gain of setting a larger m for Situation (i) does not apply here.

For Situation (ii), if $-\frac{4\lambda w\gamma_1\gamma_2}{(\beta_1+\gamma_1)(\lambda+\gamma_2)} - \frac{4\beta_1\lambda w}{\beta_1+\gamma_1} < \rho' < -\frac{4\beta_1\lambda w}{\beta_1+\gamma_1}$, we have a medium optimal solution for UE (i.e. $m_{UE} = \frac{2\lambda ws}{\beta_1-\lambda-\gamma_2}$). By comparison, the optimal solution m_{SO} is to approach either the lower bound or the upper bound, depending on the relationship between ρ' and $-2\lambda w$, which is a mix of that for Situation (i) and for Situation (iii), Situation (iv) and Situation (v).

3.6 Numerical Studies

In this section, we present some numerical results to illustrate our analysis with AV day-long commuting and parking. Specifically, we analyze different aggregate cost components, tolling schemes and AV parking supply strategies under the no-toll user equilibrium and system optimum. As discussed in Section 3.3, we find that the user-equilibrium traffic pattern varies against the AV parking density, and we analyze five situations. To save space, only Situation (ii) and/or Situation (iv) are selected for numerical illustration. This is because these two

situations involve switching of user equilibrium traffic patterns (switching of cases), which are more complicated than the other situations. The parameters used for the numerical studies are summarized in Table 3.4.

Based on the analysis in Section 3.3.3, with the increase in the AV parking density, the traffic pattern switches from Case 1 to Case 2 at the transition point $m = 3000$ for Situation (ii); while for Situation (iv), the traffic pattern switches from Case 2 to Case 3 at the transition point $m = 2400$ (refer to Table 3.3).

Table 3.4 Parameters used for numerical studies

Parameter	Situation (ii)	Situation (iv)
α_1 ($/h)	9.91	9.91
β_1 ($/h)	6.6	6.84
γ_1 ($/h)	17.00	10.00
γ_2 ($/h)	3.50	4.00
λ ($/h)	3.00	0.80
s (veh/h)	2000	2000
w (h/km)	0.025	0.025
N (veh)	3,500	3,500
m (space/km)	50~5000	50~5000

3.6.1 Aggregate cost component

This section investigates the impacts of the AV parking density on different aggregate cost components. We analyze how the total cost of queuing delay, the total cost of schedule delay and the total cost of AV self-driving to find a parking space in the morning and leave the parking area in the evening vary with the parking density. As the results for Situation (ii) and Situation (iv) are similar, to save space, we present the former only in Figure 3.7. We have the following observations.

First, for morning commute, the TQ_1 is an increasing function of the parking density m, while the TS_1 is a decreasing function. This is explained as follows. A larger m indicates a more concentrated distribution of parking space, which means that the difference in the distance between the city centre and different parking spaces is less significant. Under this circumstance, a commuter is less motivated to depart from home earlier to obtain a parking space closer to the city centre, but would try to reach the workplace as punctually as possible to minimize the schedule delay instead, resulting in an increase in the total queuing delay cost and a decrease in the total schedule delay cost for morning commutes.

Second, unlike morning commute, both the total queuing delay cost and the total schedule

delay cost for evening commute is independent of the AV parking density m. For the total queuing delay cost, this is because, the arrival rate to the inbound bottleneck always follows the red curve PQR as shown in Figure 3.2, whatever the distribution of AV parking spaces is. In other words, the arrival rates for evening commute, $r_{2,1}$ and $r_{2,2}$, are independent of the AV parking density m, while the total queuing delay cost depends on $r_{1,1}$, $r_{2,2}$ and the total travel demand N only (see Figure 3.2). For the total schedule delay cost, the reason is that the AV arrival rate to the workplace to pick up commuters is always equal to the bottleneck capacity s from the official work closure time t_2^* onwards, until all the N commuters are picked up at the city centre. In this process, the pick-up time and frequency at the workplace have nothing to do with the AV parking distribution. Hence, m has no impact on the total schedule delay cost for evening commute.

Furthermore, Figure 3.7 shows that the total travel cost for finding a parking in the morning (AV self-driving from x_0 to the parking location x) and the cost for leaving the parking area in the evening (AV self-driving from the parking location x to x_0) to pick up commuters are equal, and both are decreasing over m. This is expected as a more concentrated parking distribution will decrease the total distance between the location x_0 and all other parking locations x.

(a) Queuing delay cost (b) Schedule delay cost (c) Time cost of finding parking space (morning) and leaving parking area (evening)
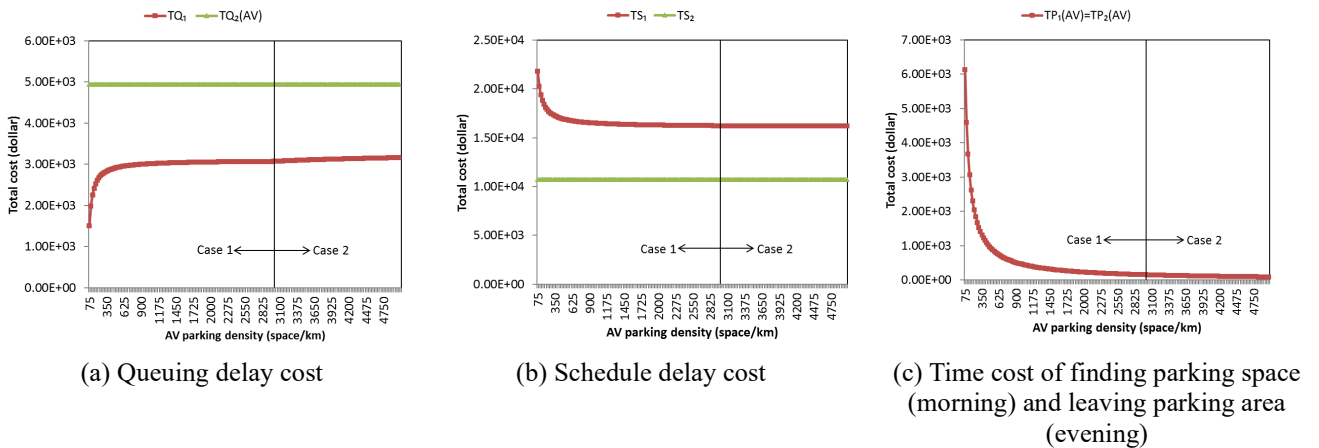
Figure 3.6 Evaluation of aggregate cost components against AV parking density under Situation (ii)

3.6.2 Tolling scheme

In this Section, we apply the first-best tolling scheme and show how the toll revenue varies with the AV parking density. For numerical illustration, we let $\varepsilon_0 = 10$. In particular, Figure 3.8 shows the change of total toll revenues against the AV parking

density under the introduced first-best toll schemes for morning-evening commutes. It is evident that the total toll revenue for evening peak is not influenced by the AV parking density, while the toll revenue increases with m for morning commute and consequently, the daily commute. In addition, Figure 3.8(a) shows that in Situation (ii), the traffic pattern in Case 2 can drive a greater total daily toll revenue than that in Case 1. Similarly, Figure 3.8(b) indicates that a more concentrated parking distribution can lead to a switch from Case 2 to Case 3 in Situation (iv), and as a result, the total daily toll revenue increases over m.

(a)   Situation (ii)   (b)   Situation (iv)
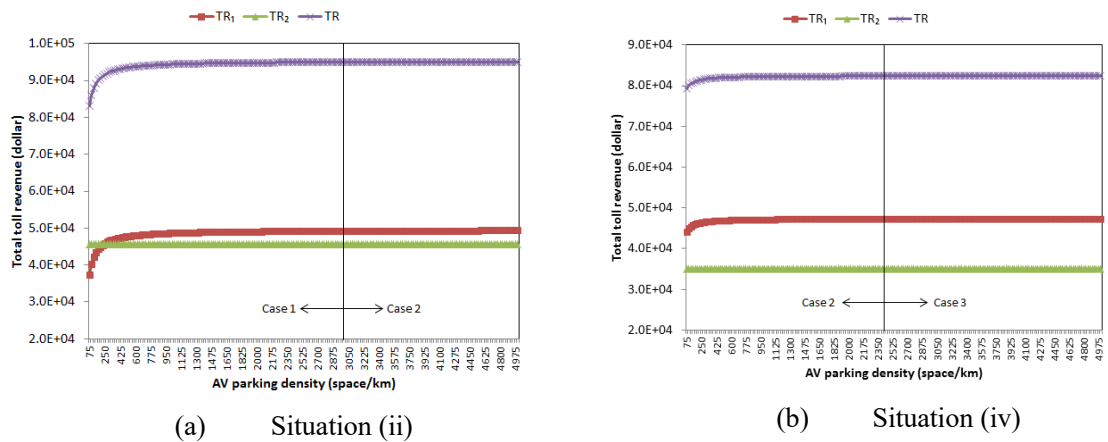
Figure 3.7 Toll revenue against the AV parking density

3.6.3 AV parking supply

In this section, we investigate the sensitivity of the system-level cost to the AV parking supply. Specifically, we examine the total social parking cost $TSPC$, the total system cost at equilibrium TSC_{UE} and the total system cost at system optimum TSC_{SO}, and analyse how these metrics are influenced by the AV parking density m. For the social cost of parking units, we use the function $\rho(x) = -\varphi(x - x_0) + 20$ in this case study. For demonstration purposes, we set $\varphi = 0.25, 0.18, 0.145, 0.05$ (i.e. $\rho'(x) = -0.25, -0.18, -0.145, -0.05$) for Situation (ii), and $\varphi = 0.1, 0.035, 0.02$ (i.e. $\rho'(x) = -0.1, -0.035, -0.02$) for Situation (iv). Figure 3.9 shows the evaluations of $TSPC$, TSC_{UE} and TSC_{SO} under different values of $\rho'(x)$ for Situation (ii), and Figure 3.10 depicts the results for Situation (iv).

It is shown in Figure 3.9 that the total social parking cost always increases with the AV parking density, because the social cost of parking spaces close to the city centre is relatively high. Figures 3.9(a) and 3.9(d) show that when $\rho'(x)$ is sufficiently small or large, the functions of TSC_{UE} and TSC_{SO} are both monotonic with respect to the AV

60

parking density. Specifically, as shown in Figure 3.9(a), both TSC_{UE} and TSC_{SO} is increasing with the small $\rho'(x)$ (more negative) causing the optimal solution to approach the lower bound, which is equal to $ws = 50$ for both UE and SO in this numerical illustration. Similarly, both TSC_{UE} and TSC_{SO} is decreasing with the large $\rho'(x)$ (more positive), which drives the optimal solutions $m_{UE} = m_{SO} \rightarrow +\infty$ (or the upper bound if prescribed).

By contrast, as shown in Figure 3.9(b) and Figure 3.9(c), when $\rho'(x)$ has a medium value, the situation is not as straightforward as the cases in Figure 3.9(a) and Figure 3.9(d). For both figures, we have the relationship $-\frac{4\lambda w \gamma_1 \gamma_2}{(\beta_1+\gamma_1)(\lambda+\gamma_2)} - \frac{4\beta_1 \lambda w}{\beta_1+\gamma_1} < \rho'(x) < -\frac{4\beta_1 \lambda w}{\beta_1+\gamma_1}$.

Because of $\rho'(x) > -\frac{4\lambda w \gamma_1 \gamma_2}{(\beta_1+\gamma_1)(\lambda+\gamma_2)} - \frac{4\beta_1 \lambda w}{\beta_1+\gamma_1}$, the TSC_{UE} decreases under the UE traffic pattern of Case 1 until m reaches line l. Then, the traffic pattern changes to Case 2, where we have $\rho'(x) < -\frac{4\beta_1 \lambda w}{\beta_1+\gamma_1}$, resulting in an increase in TSC_{UE}. Hence, the optimal solution m_{UE} is equal to the value of m at line l, which is equal to 3000. For both figures, m_{SO} is different from m_{UE}. Specifically, for Figure 3.9(b), TSC_{SO} is monotonic increasing because of $\rho'(x) < -2\lambda w$, resulting in the optimal solution $m_{SO} \rightarrow 50$; for Figure 3.9(c), the optimal parking density approaches infinity or the upper bound if set, because $\rho'(x) > -2\lambda w$ holds.

In practice, we may have an additional constraint on the parking density, i.e., m is both bounded from below and above and $m \in [m_l, m_u]$. The optimal m is then further constrained by $[m_l, m_u]$. In Figure 3.9, for example, when $\rho'(x) = -0.18$ (see Figure 3.9(b)), if we set the domain of m, denoted as $[m_l, m_u]$, to the right hand of line l, the TSC_{UE} is increasing, and the optimal solution of m should be equal to m_l. If we set the domain of m to the left of line l, the TSC_{UE} is decreasing, and we have the optimal solution $m_{UE} = m_u$. If the domain of m is across line l, the TSC_{UE} is first decreasing and then increasing, and the optimal solution is the value of m at line l, which is equal to 3000 in this example.
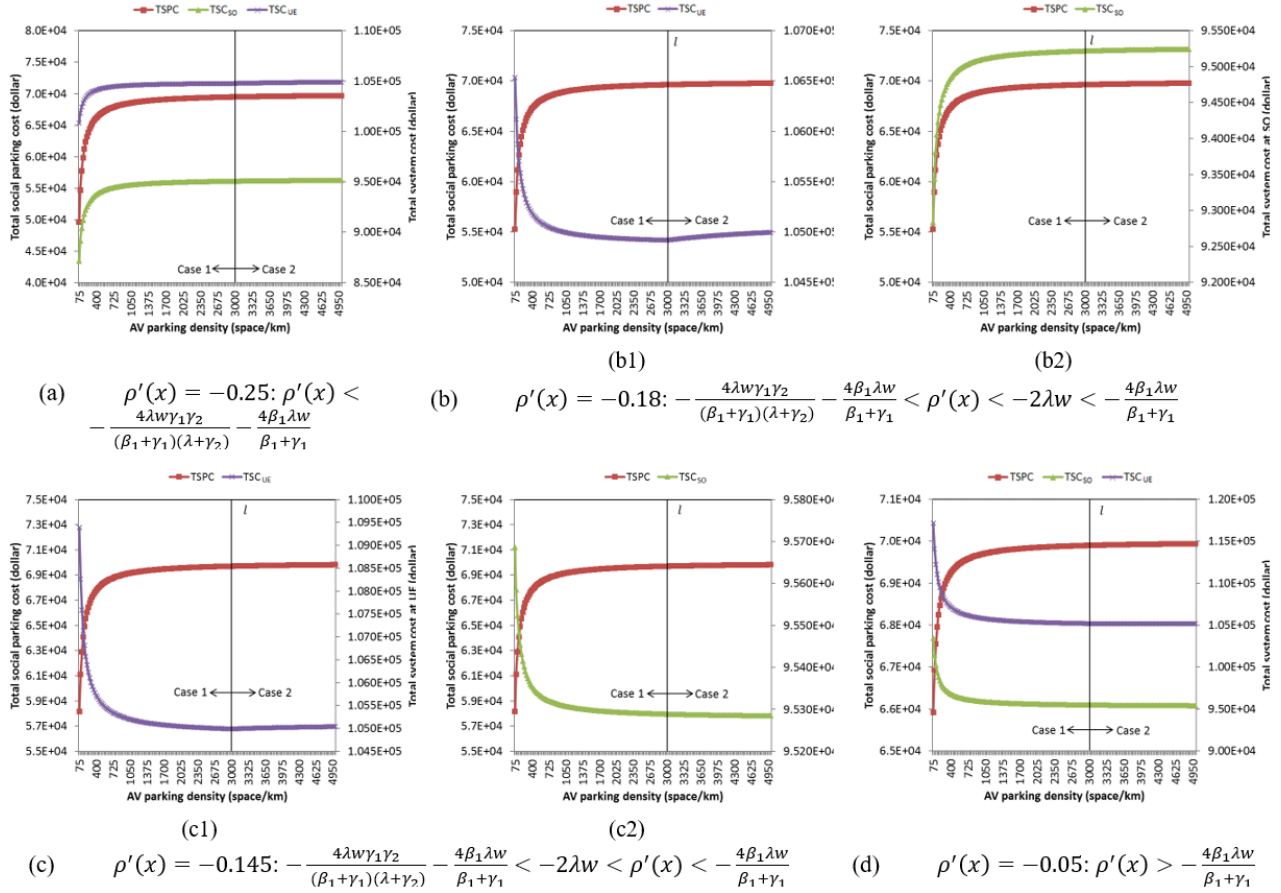
Figure 3.8 Social parking cost and system cost against AV parking density under Situation (ii)

In Figure 3.10, each curve is divided into two segments by line l, where we have $\beta_1 = f_3(m)$. It shows that with the increase of m, the traffic pattern can change from Case 2 to Case 3. Similar to Figure 3.9, the total social parking cost expands with the increase of m, because AV parking spaces closer to the city centre are more socially costly. It can be easily seen from Figure 3.10(a) that when $\rho'(x) < -2\lambda w$, the total system costs at equilibrium and at system optimum are both increasing with m. The optimal solutions of m for UE and SO are $m_{UE} = m_{SO} \rightarrow ws = 50$ in this numerical illustration. Similarly, as per Figure 3.10(c), we can obtain the optimal solutions $m_{UE} = m_{SO} \rightarrow +\infty$ (or the upper bound if set) when $\rho'(x) > -\dfrac{4\beta_1\lambda w}{\beta_1+\gamma_1}$. Figure 3.10(b) shows that when $-2\lambda w < \rho'(x) < -\dfrac{4\beta_1\lambda w}{\beta_1+\gamma_1}$, the TSC_{UE} decreases while the TSC_{SO} increases with the AV parking density. As a result, we have different optimal solutions for UE and SO traffic patterns,

62

which is consistent with the analysis in Section 3.5.3.

(a) $\rho'(x) = -0.1: \rho'(x) < -2\lambda w$

(b) $\rho'(x) = -0.035: -2\lambda w < \rho'(x) < -\frac{4\beta_1 \lambda w}{\beta_1 + \gamma_1}$

(c) $\rho'(x) = -0.02: \rho'(x) > -\frac{4\beta_1 \lambda w}{\beta_1 + \gamma_1}$
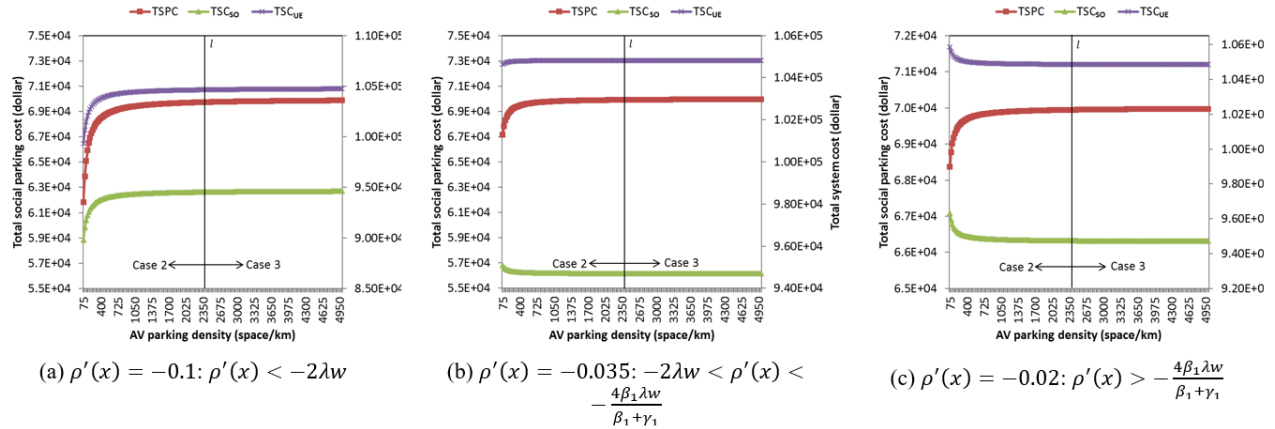
Figure 3.9 Social parking cost and system cost against AV parking density under Situation (iv)

The above numerical results suggest that the parking supply problem examined here is much more complicated than that in Liu (2018) after integrating both the morning and evening commutes. In particular, with the increase in the gradient of the social cost for a parking unit, the system-level cost might fluctuate in different manners under diverse situations, which is not observed when only morning commute is considered in the previous study. Specifically, by comparing between Situation (ii) and Situation (iv), we find that the total system cost at equilibrium is monotonically increasing or decreasing over the parking density under Situation (iv), while this change is not monotonic when the value of $\rho'(x)$ is moderate under Situation (ii). Furthermore, with a moderate $\rho'(x)$, the total system cost at system optimum is always decreasing under Situation (iv), while it can be either increasing or decreasing under Situation (ii). Such diversity in the cost pattern leads to different optimal parking supply solutions for the two studied situations. The finding highlights the importance of integrating the morning and evening commutes for management and planning issues related to AVs. This also indicates that parking supply strategies should be carefully determined considering parameters for the city (this determines the situation, where five situations can arise as discussed in Section 3.3 and Section 3.5) and traffic management strategies (e.g., whether tolling is implemented or not).

4. Findings and Conclusions

This study investigates the potential of an infrastructure-based solution, i.e., the deployment of roadside units, to close the connectivity gap for CAVs in a mixed traffic environment, and thus improve the performance of the road network. The solution is evaluated at a macroscopic level for the strategic planning purpose. To capture the impact of roadside units on the capacity of highway segments, a new link performance function is firstly derived. In particular, with the presence of roadside units, a link can be divided into two sub-links, one deployed with roadside units while the other does not; the effect of roadside units on reducing the space or time headway between CAVs and RVs on the former sub-link can be captured by modifying the capacity of the sub-link. As a result, the travel time function of the whole link can be described by simple mathematical derivation. Integrating the established link performance function, a network equilibrium model is developed to delineate how the deployment of the roadside units will affect travelers' route choices and thus the flow distribution across the network. As the resultant equilibrium flow distribution may not be unique, a deployment model is proposed to optimize the location of roadside units such that the total travel time under the worst scenario can be minimized. Such a deployment model enables a conservative benefit estimation for the roadside-unit deployment. As the deployment model is a minimax problem with coupled constraints, a heuristic procedure based on cutting-plane scheme is presented to solve the model. Case studies on two networks are conducted, and results illuminate the effectiveness of the proposed algorithm for solving the RD model and the significant impact of the deployment of roadside units on reducing the system travel time. In particular, the optimal location of 10 roadside units can reduce the system travel time on nine-node network and South Florida network by 3.32% and 4.07%, respectively. Furthermore, cost-benefit analyses are conducted to evaluate the potential of the deployment of roadside units. Specifically, the BCRs of deploying roadside units on these two networks are estimated to be 9.31 and 445.27, respectively. Sensitivity analyses are conducted to capture the impacts of the change of roadside-unit investment cost and coverage length, and CAV travelers' VOT on the BCRs. Although the BCRs change as the above parameters change, they are all far greater than 1, revealing that the benefit brought by the deployment of roadside units far outweighs the corresponding investment cost.

We conclude Chapter 2 by highlighting the importance of infrastructure adaptation planning for achieving automated mobility. While thus far the development of the CAV technology appears to be primarily driven by the private sector, the public sector has begun taking actions to change laws, policies and practices to encourage and promote the development and deployment of the technology. It is critical for planning agencies to modify and equip transportation infrastructure to support automated driving to promote the deployment of CAVs. There is a lack of systematic

methodology to support such policy making and planning practice. More research efforts are needed to fill this critical void.

In addition, this study analyzed the morning-evening commuting and parking problem when people complete daily trips with AVs. Specifically, we first model the equilibrium traffic pattern for the evening commute, where the parking locations are considered given as they have been decided in the morning commute. Then, in the second stage, by incorporating the obtained equilibrium travel cost for the evening commute, we model the integrated user equilibrium of departure time and parking location choices in the morning, considering the individual daily travel cost. Based on equilibrium analysis, we investigate the time-dependent tolling scheme and the AV parking supply strategy.

This study is the first to integrate the daily commuting and parking patterns in the context of AVs. It provides insights regarding strategic infrastructure planning and management with automated traffic. We differentiate our study from the existing literature on equilibrium commute by three aspects. Firstly, this study identifies the different daily travel and parking pattern for AVs against the literature with non-AVs (e.g., Zhang et al., 2008). For example, where and how congestion might occur have significantly changed. Secondly, when compared to Zhang et al. (2008), we have incorporated flexible morning arrival (both early arrival and late arrival are allowed) while we assume no early departure in the evening, and we have identified that much more complicated commuting pattern might arise than the case when only early arrival in the morning is considered. During the morning commute, there might exist a period with a capacity waste. Thirdly, by integrating the morning and evening commutes with AVs, we have identified new insights regarding the commuting pattern and the optimal parking supply that are ignored by Liu (2018) with the morning commute only.

5. Recommendations

This study can be extended in multiple directions. First, the refueling activity can be incorporated into the proposed framework of equilibrium with AVs, and optimally locating refueling stations will be investigated (Chen et al., 2017; Zhang et al., 2018). Second, future research will consider the volatility in the travel demand and the highway capacity in the context of AV commutes, and explore the sensitivity of system efficiency to these uncertainties (Ng and Waller, 2010; Wen et al., 2018). Also, the AV demand variability can be influenced by the governmental policy (for instance, license plate restriction, AV subsidies), which will be considered in the AV system analysis. Third, given that a traveler might need to complete another trip in the daytime (for example, having lunch outside the office), inter-peak commutes with AVs can also be accounted for in future studies. Fourth, the constraints on the amount of time spent at work as well as the corresponding parking fee will be analyzed, and their significance to the equilibrium traffic pattern will be extensively studied. Fifthly, it is noteworthy that a mix-vehicular traffic environment consisting of both AVs and conventional vehicles might arise. Moreover, there may be privately-owned and shared AVs. Commuters could have different mode choices and behavior patterns, such as driving privately owned AVs, taking public transit (with AVs or with traditional vehicles) and combining multiple modes in a trip (e.g., park-and-ride). These possibilities will be investigated in future studies, while this study serves as a basis for later studies to be built upon.

6. Outputs, Outcomes and Impacts

This study investigates the potential of an infrastructure-based solution, i.e., the deployment of roadside units, to close the connectivity gap for CAVs in a mixed traffic environment, and thus improve the performance of the road network. The proposed modeling framework can be utilized to support the planning of the deployment of roadside units to support automated driving automation.

This study highlights the importance of infrastructure adaptation planning for achieving automated mobility. While thus far the development of the CAV technology appears to be primarily driven by the private sector, the public sector has begun taking actions to change laws, policies and practices to encourage and promote the development and deployment of the technology. It is critical for planning agencies to modify and equip transportation infrastructure to support automated driving to promote the deployment of CAVs. There is a lack of systematic methodology to support such policy making and planning practice. More research efforts are needed to fill this critical void.

The following outputs were generated during the performance of this project:

- Li, Y., Chen, Z., Yin, Y. and Peeta, S. Deployment of Roadside Units to Overcome Connectivity Gap in Transportation Networks with Mixed Traffic. Transportation Research Part C, 111, 496-512, 2020

- Zhang, X, Liu, W., Waller, S.T. and Yin, Y. Modelling and managing the integrated morning-evening commuting and parking patterns under the fully autonomous vehicle environment. Transportation Research Part B, 128, 380-407, 2019

7. References

Arnott, R., De Palma, A. & Lindsey, R. (1990). Economics of a bottleneck. Journal of Urban Economics, 27(1), 111-130.

Arnott, R., De Palma, A., & Lindsey, R. (1991). A temporal and spatial equilibrium analysis of commuter parking. Journal of Public Economics, 45(3), 301-335.

Arnott, R., & Inci, E. (2006). An integrated model of downtown parking and traffic congestion. Journal of Urban Economics, 60(3), 418-442.

Ban, X. J., Lu, S., Ferris, M., & Liu, H. X., 2009. Risk averse second best toll pricing. In Transportation and Traffic Theory 2009: Golden Jubilee.197-218. Springer, Boston, MA.

Bazaraa, M. S., Sherali, H. D., & Shetty, C. M., 2013. Nonlinear programming: theory and algorithms. John Wiley & Sons.

Burns, L. D. (2013). Sustainable mobility: a vision of our transport future. Nature, 497(7448), 181.

Calvert, S. C., Schakel, W. J., & Van Lint, J. W. C., 2017. Will automated vehicles negatively impact traffic flow? Journal of Advanced Transportation.

Chen, Z., He, F., Zhang, L., & Yin, Y., 2016. Optimal deployment of autonomous vehicle lanes with endogenous market penetration. Transportation Research Part C: Emerging Technologies. 72, 143-156.

Chen, Z. , He, F. , Yin, Y. , & Du, Y., 2017. Optimal design of autonomous vehicle zones in transportation networks. Transportation Research Part B: Methodological. 99, 44-61.

Chen, D. , Ahn, S. , Chitturi, M. , & Noyce, D. A., 2017. Towards vehicle automation: roadway capacity formulation for traffic mixed with regular and automated vehicles. Transportation Research Part B: Methodological. 100, 196-221.

Chen, S., Wang, H., & Meng, Q., 2019. Designing autonomous vehicle incentive program with uncertain vehicle purchase price. Transportation Research Part C: Emerging Technologies. 103, 226-245.

Chen, Z., Liu, W., & Yin, Y. (2017). Deployment of stationary and dynamic charging infrastructure for electric vehicles along traffic corridors. Transportation Research Part C: Emerging Technologies, 77, 185-206.

Chen, Z., Yin, Y., He, F., & Lin, J. L. (2015). Parking reservation for managing downtown curbside parking. Transportation Research Record: Journal of the Transportation Research Board, (2498), 12-18.

De Palma, A., & Lindsey, R. (2002). Comparison of morning and evening commutes in the Vickrey bottleneck model. Transportation Research Record: Journal of the Transportation Research Board, (1807), 26-33.

De Palma, E., & Arnott, R. (2012). Morning commute in a single-entry traffic corridor with no late arrivals. Transportation Research Part B: Methodological, 46(1), 1-29.

Duell, M., Levin, M. W., Boyles, S. D., & Waller, S. T. (2016). Impact of autonomous vehicles on traffic management: Case of dynamic lane reversal. Transportation Research Record: Journal of the Transportation Research Board, (2567), 87-94.

Ghiasi, A., Hussain, O., Qian, Z. S., & Li, X., 2017. A mixed traffic capacity analysis and lane management model for connected automated vehicles: A Markov chain method. Transportation Research Part B: Methodological. 106, 266-292.

Gonzales, E. J., & Daganzo, C. F. (2013). The evening commute with cars and transit: Duality results and user equilibrium for the combined morning and evening peaks. Transportation Research Part B: Methodological, 57, 286-299.

Guerra, E. (2016). Planning for cars that drive themselves: metropolitan planning organizations, regional transportation plans, and autonomous vehicles. Journal of Planning Education and Research, 36(2), 210-224.

He, F., Yin, Y., Chen, Z., & Zhou, J. (2015). Pricing of parking games with atomic players. Transportation Research Part B: Methodological, 73, 1-12.

Inci, E. (2015). A review of the economics of parking. Economics of Transportation, 4(1-2), 50-63.

Inci, E., & Lindsey, R. (2015). Garage and curbside parking competition with search congestion. Regional Science and Urban Economics, 54, 49-59.

Krueger, R., Rashidi, T. H., & Rose, J. M. (2016). Preferences for shared autonomous vehicles. Transportation Research Part C: Emerging Technologies, 69, 343-355.

Kuwahara, M. (1990). Equilibrium queueing patterns at a two-tandem bottleneck during the morning peak. Transportation Science, 24(3), 217-229.

Lamotte, R., De Palma, A., & Geroliminis, N. (2017). On the use of reservation-based autonomous vehicles for demand management. Transportation Research Part B: Methodological, 99, 205-227.

Lawphongpanich, S., & Hearn, D. W., 2004. An MPEC approach to second-best toll pricing. Mathematical Programming. 101(1), 33-55.

Li, C. Y., & Huang, H. J. (2017). Morning commute in a single-entry traffic corridor with early and late arrivals. Transportation Research Part B: Methodological, 97, 23-49.

Li, Z. C., Lam, W. H., & Wong, S. C. (2014). Bottleneck model revisited: An activity-based perspective. Transportation Research Part B: Methodological, 68, 262-287.

Li, Z. C., Lam, W. H., & Wong, S. C. (2017). Step tolling in an activity-based bottleneck model. Transportation Research Part B: Methodological, 101, 306-334.

Li, Y., Xu, C., Xing, L., & Wang, W., 2017. Integrated cooperative adaptive cruise and variable speed limit controls for reducing rear-end collision risks near freeway bottlenecks based on micro-simulations. IEEE transactions on intelligent transportation systems. 18(11), 3157-3167.

Lindsey, R. (2004). Existence, uniqueness, and trip cost function properties of user equilibrium in the bottleneck model with multiple user classes. Transportation Science, 38(3), 293-314.

Lindsey, C.R., van den Berg, V.A. & Verhoef, E.T. (2012). Step tolling with bottleneck queuing congestion. Journal of Urban Economics, 72(1), 46-59.

Litman, T. (2018) Autonomous Vehicle Implementation Predictions, Victoria Transport Policy Institute.

Liu, W. (2018). An equilibrium analysis of commuter parking in the era of autonomous vehicles. Transportation Research Part C: Emerging Technologies, 92, 191-207.

Liu, W., & Geroliminis, N. (2016). Modeling the morning commute for urban networks with cruising-for-parking: An MFD approach. Transportation Research Part B: Methodological, 93, 470-494.

Liu, W., Yang, H., & Yin, Y. (2014). Expirable parking reservations for managing morning commute with parking space constraints. Transportation Research Part C: Emerging Technologies, 44, 185-201.

Lou, Y., Yin, Y., & Lawphongpanich, S., 2010. Robust congestion pricing under boundedly rational user equilibrium. Transportation Research Part B: Methodological. 44(1), 15-28.

Lu, M., & Blokpoel, R. J., 2016. A sophisticated intelligent urban road-transport network and cooperative systems infrastructure for highly automated vehicles. In Proceedings: World Congress on Intelligent Transport Systems, Montreal.

Luo, Q., Saigal, R., Chen, Z. and Yin, Y., 2019. Accelerating the adoption of automated vehicles by subsidies: A dynamic games approach. Available at SSRN: https://ssrn.com/abstract=3275580 or http://dx.doi.org/10.2139/ssrn.3275580.

Ma, R., & Zhang, H. M. (2017). The morning commute problem with ridesharing and dynamic parking charges. Transportation Research Part B: Methodological, 106, 345-374.

Managing Automated Vehicles Enhances Network. MAVEN. http://www.maven-its.eu/. Accessed July 30, 2019.

Milanés, V., Shladover, S. E., Spring, J., Nowakowski, C., Kawazoe, H., & Nakamura, M., 2014. Cooperative adaptive cruise control in real traffic situations. IEEE Transactions on intelligent transportation systems. 15(1), 296-305.

Milanés, V., & Shladover, S. E., 2014. Modeling cooperative and autonomous adaptive cruise control dynamic responses using experimental data. Transportation Research Part C: Emerging Technologies. 48, 285-300.

Ng, M., & Waller, S. T. (2010). A computationally efficient methodology to characterize travel time reliability using the fast Fourier transform. Transportation Research Part B: Methodological, 44(10), 1202-1219.

Nourinejad, M., & Roorda, M. J. (2017). Impact of hourly parking pricing on travel demand. Transportation Research Part A: Policy and Practice, 98, 28-45.

Ngoduy, D., & Jia, D., 2017 Multi anticipative bidirectional macroscopic traffic model considering cooperative driving strategy. Transportmetrica B: Transport Dynamics. 5(1), 96-110.

Qian, Z. S., & Rajagopal, R. (2014). Optimal dynamic parking pricing for morning commute considering

expected cruising time. Transportation Research Part C: Emerging Technologies, 48, 468-490.

Qian, Z. S., Xiao, F. E., & Zhang, H. M. (2011). The economics of parking provision for the morning commute. Transportation Research Part A: Policy and Practice, 45(9), 861-879.

Qian, Z. S., Xiao, F. E., & Zhang, H. M. (2012). Managing morning commute traffic with parking. Transportation Research Part B: Methodological, 46(7), 894-916.

Shladover, S. E., Su, D., & Lu, X. Y., 2012 Impacts of cooperative adaptive cruise control on freeway traffic flow. Transportation Research Record. 2324(1), 63-70.

Small, K. A. (2015). The bottleneck model: An assessment and interpretation. Economics of Transportation, 4(1-2), 110-117.

Sparrow, R., & Howard, M. (2017). When human beings are like drunk robots: Driverless vehicles, ethics, and the future of transport. Transportation Research Part C: Emerging Technologies, 80, 206-215.

Rondinone, M., Walter, T., Blokpoel, R., & Schindler, J., 2018. V2X communications for infrastructure-assisted automated driving. Presented in the 19th International Symposium on" A World of Wireless, Mobile and Multimedia Networks"(WoWMoM).

Rondinone, M. Managing Automated Vehicles Enhances Network. http://adas.cvc.uab.es/maven/wp-content/uploads/sites/16/2018/09/MAVEN-D5.2_v1.0_final.pdf. Accessed July 30, 2019.

Seo, T. , & Asakura, Y., 2017. Endogenous market penetration dynamics of automated and connected vehicles: transport-oriented model and its paradox. Transportation Research Procedia. 27, 238-245.

Shimizu, K., & Aiyoshi, E., 1980. Necessary conditions for min-max problems and algorithms by a relaxation procedure. IEEE Transactions on Automatic Control. 25(1), 62-66.

Stein, O., 2012. How to solve a semi-infinite optimization problem. European Journal of Operational Research. 223(2), 312-320.

Treiber, M., Kesting, A., & Helbing, D., 2006. Delays, inaccuracies and anticipation in microscopic traffic models. Physica A: Statistical Mechanics and its Applications. 360(1), 71-88.

Van Arem, B., Van Driel, C. J., & Visser, R., 2006. The impact of cooperative adaptive cruise control on traffic-flow characteristics. IEEE Transactions on intelligent transportation systems. 7(4), 429-436.

Van den Berg, V. A. & Verhoef, E. T. (2016). Autonomous cars and dynamic bottleneck congestion: The effects on capacity, value of time and preference heterogeneity. Transportation Research Part B: Methodological, 94, 43-60.

Van Ommeren, J. N., Wentink, D., & Rietveld, P. (2012). Empirical evidence on cruising for parking. Transportation Research Part A: Policy and Practice, 46(1), 123-130.

Vickrey, W. S. (1969). Congestion theory and transport investment. The American Economic Review, 59(2), 251-260.

Vickrey, W. S. (1973). Pricing, metering, and efficiently using urban transportation facilities, Highway Research Record, 476.

Vogel, K. (2003). A comparison of headway and time to collision as safety indicators. Accident Analysis & Prevention, 35(3), 427-433.

Wang, M., 2018. Infrastructure assisted adaptive driving to stabilise heterogeneous vehicle strings. Transportation Research Part C: Emerging Technologies. 91, 276-295.

Wen, T., Cai, C., Gardner, L., Dixit, V., Waller, S. T., & Chen, F. (2018). A strategic user equilibrium for independently distributed origin-destination demands. Computer-Aided Civil and Infrastructure Engineering, 33(4), 316-332.

Wu, D., Yin, Y., & Lawphongpanich, S., 2011. Pareto-improving congestion pricing on multimodal transportation networks. European Journal of Operational Research. 210(3), 660-669.

Xiao, F., Shen, W., & Zhang, H.M. (2012). The morning commute under flat toll and tactical waiting. Transportation Research Part B: Methodological, 46(10), 1346-1359.

Xiao, L. L., Liu, T. L., & Huang, H. J. (2016). On the morning commute problem with carpooling behavior under parking space constraint. Transportation Research Part B: Methodological, 91, 383-407.

Yang, H., Liu, W., Wang, X., & Zhang, X. (2013). On the morning commute problem with bottleneck congestion and parking space constraints. Transportation Research Part B: Methodological, 58, 106-118.

Ye, Y., & Wang, H., 2018. Optimal Design of Transportation Networks with Automated Vehicle Links and Congestion Pricing. Journal of Advanced Transportation.

Ye, L., & Yamamoto, T., 2018. Impact of dedicated lanes for connected and autonomous vehicle on traffic flow throughput. Physica A: Statistical Mechanics and its Applications, 512, 588-597.

Zhang, X., Huang, H. J., & Zhang, H. M. (2008). Integrated daily commuting patterns and optimal road tolls and parking fees in a linear city. Transportation Research Part B: Methodological, 42(1), 38-56.

Zhang, X., Rey, D., & Waller, S. T. (2018). Multitype recharge facility location for electric vehicles. Computer-Aided Civil and Infrastructure Engineering, 33(11), 943-965.

Zhang, X., Yang, H., & Huang, H. J. (2011). Improving travel efficiency by parking permits distribution and trading. Transportation Research Part B: Methodological, 45(7), 1018-1034.

Zhang, X., Yang, H., Huang, H. J., & Zhang, H. M. (2005). Integrated scheduling of daily work activities and morning–evening commutes with bottleneck congestion. Transportation Research Part A: Policy and Practice, 39(1), 41-60.

Zeng, B., 2015. Easier than we thought-a practical scheme to compute pessimistic bilevel optimization problem. Available at SSRN: https://ssrn.com/abstract=2658342 or http://dx.doi.org/10.2139/ssrn.2658342.

8. Appendixes

TABLE A1. O-D demand for the South Florida network

O-D	RV	CAV
1-22	44	22
1-28	63.5	31.75
1-64	63.5	31.75
22-1	44	22
22-28	60	30
22-64	62.5	31.25
28-1	63.5	31.75
28-22	60	30
28-64	63.5	31.75
64-1	72	36
64-22	62.5	31.25
64-28	63.5	31.75

TABLE A2. South Florida network characteristics

Link	Number of Lanes	$\frac{L}{v_0}$ (min)	L (km)	I_a	Link	Number of Lanes	$\frac{L}{v_0}$ (min)	L (km)	I_a	Link	Number of Lanes	$\frac{L}{v_0}$ (min)	L (km)	I_a
1-2	3	3.08	6.16	0	31-5	3	8.24	16.48	0	55-35	3	2.67	5.34	0
1-29	2	5.64	11.28	0	31-30	2	9.00	18.00	0	55-54	3	2.16	4.32	0
2-1	3	3.00	6.00	6	31-32	2	4.71	9.42	0	55-56	3	10.08	20.16	0
2-3	3	10.89	21.78	0	31-51	1	2.40	4.80	0	56-11	3	3.56	7.12	0
3-2	3	10.00	20.00	20	32-31	2	4.71	9.42	0	56-55	3	10.08	20.16	0
3-4	5	1.33	2.66	0	32-33	3	5.06	10.12	0	56-57	3	4.00	8.00	0
3-30	2	7.92	15.84	0	32-52	1	2.29	4.58	0	57-12	3	2.67	5.34	0
4-3	5	1.33	2.66	0	32-82	2	1.76	3.52	0	57-56	3	4.00	8.00	0
4-5	3	7.48	14.96	0	33-8	3	4.36	8.72	0	57-58	3	3.33	6.66	0
5-4	3	7.48	14.96	0	33-32	3	5.06	10.12	0	58-13	4	2.29	4.58	0
5-6	5	4.43	8.86	0	33-34	3	4.42	8.84	0	58-37	3	1.00	2.00	0
5-31	3	8.24	16.48	0	33-53	3	2.67	5.34	0	58-38	2	8.10	16.2	0
6-5	5	4.43	8.86	0	34-9	2	4.15	8.30	0	58-57	3	3.33	6.66	0
6-7	5	2.56	5.12	0	34-33	3	4.42	8.84	0	59-38	3	10.60	21.20	0
6-82	3	5.60	11.2	0	34-35	3	2.63	5.26	0	59-40	4	3.90	7.80	0
7-6	5	2.56	5.12	0	34-54	2	2.10	4.20	0	59-65	4	5.35	10.70	0
7-8	4	3.93	7.86	0	35-10	3	3.73	7.46	0	60-54	2	5.45	10.90	0
8-7	4	3.93	7.86	0	35-34	3	1.99	3.98	0	60-61	2	6.11	12.22	0
8-9	4	4.08	8.16	0	35-36	3	5.43	10.86	0	61-60	2	6.11	12.22	0
8-33	3	4.36	8.72	0	35-55	3	2.67	5.34	0	61-62	3	6.29	12.58	0
9-8	4	4.08	8.16	0	36-35	3	5.43	10.86	0	62-61	3	6.29	12.58	0
9-10	4	1.94	3.88	0	36-37	3	6.21	12.42	0	62-63	4	1.85	3.70	0
9-34	2	4.15	8.30	0	37-36	3	6.21	12.42	0	63-37	3	7.58	15.16	0
10-9	4	1.94	3.88	0	37-38	3	8.37	16.74	0	63-62	4	1.85	3.70	0

10-11	5	8.86	17.72	0	37-58	3	1.00	2.00	0	63-64	3	6.00	12.00	**12**
10-35	3	3.73	7.46	0	37-63	3	7.58	15.16	0	63-65	5	2.34	4.68	0
11-10	5	8.86	17.72	0	38-37	3	8.37	16.74	0	64-63	3	6.00	12.00	**12**
11-12	6	2.87	5.74	0	38-39	3	2.82	5.64	0	65-59	4	5.35	10.70	0
11-56	3	3.56	7.12	0	38-58	2	8.10	16.20	0	65-63	5	2.34	4.68	0
12-11	6	2.87	5.74	0	38-59	3	10.60	21.20	0	66-40	1	3.42	6.84	0
12-13	4	2.46	4.92	0	39-17	3	4.27	8.54	0	66-41	1	3.50	7.00	0
12-57	3	2.67	5.34	0	39-38	3	2.82	5.64	0	66-67	5	1.55	3.10	0
13-12	4	2.46	4.92	0	39-40	2	7.62	15.24	0	67-17	5	9.68	19.36	0
13-14	5	2.18	4.36	0	40-39	2	7.62	15.24	0	67-66	5	1.55	3.10	0
13-58	4	2.29	4.58	0	40-41	3	3.43	6.86	0	67-68	3	2.45	4.90	0
14-13	6	2.18	4.36	0	40-59	4	3.90	7.80	0	67-72	4	7.38	14.76	0
14-15	6	3.99	7.98	0	40-66	4	3.42	6.84	0	68-67	3	2.45	4.90	0
15-14	6	3.99	7.98	0	41-40	3	3.43	6.86	0	68-69	3	2.62	5.24	0
15-16	5	1.32	2.64	0	41-42	3	2.15	4.30	0	69-18	3	4.76	9.52	0
16-15	5	1.32	2.64	0	41-66	1	3.50	7.00	0	69-68	3	2.62	5.24	0
16-17	4	4.00	8.00	0	42-41	3	2.15	4.30	0	69-70	2	7.50	15.00	0
17-16	4	4.00	8.00	0	42-43	4	6.10	12.20	0	70-69	2	7.50	15.00	0
17-18	5	3.38	6.76	0	43-42	4	6.10	12.20	0	70-71	3	3.70	7.40	0
17-39	3	4.27	8.54	0	43-44	4	1.73	3.46	0	71-21	3	4.21	8.42	0
17-67	5	9.68	19.36	0	43-73	3	4.47	8.94	0	71-70	3	3.70	7.40	0
18-17	5	3.38	6.76	0	43-81	2	2.67	5.34	0	71-73	3	3.97	7.94	0
18-19	5	2.98	5.96	0	44-43	4	1.73	3.46	0	72-67	4	7.38	14.76	0
18-69	3	4.76	9.52	0	44-45	3	5.23	10.46	0	72-73	6	2.15	4.30	0
19-18	5	2.98	5.96	0	44-74	3	5.33	10.66	0	73-43	3	4.47	8.94	0
19-20	5	3.72	7.44	0	45-44	3	5.23	10.46	0	73-71	3	3.97	7.94	0
20-19	5	3.72	7.44	0	45-46	3	2.64	5.28	0	73-72	6	2.15	4.30	0
20-21	6	1.80	3.60	0	45-77	3	3.20	6.40	0	73-74	5	1.69	3.38	0

21-20	6	1.80	3.60	0	45-78	3	2.36	4.72	0	74-44	3	5.33	10.66	0
21-22	4	2.00	4.00	**4**	46-45	3	2.64	5.28	0	74-73	5	1.69	3.38	0
21-71	3	4.21	8.42	0	46-47	2	2.67	5.34	0	74-75	4	3.02	6.04	0
22-21	4	2.00	4.00	**4**	46-48	5	2.00	4.00	**4**	75-74	4	3.02	6.04	0
22-23	3	1.08	2.16	0	47-46	2	2.67	5.34	0	75-76	2	2.62	5.24	0
23-22	3	1.08	2.16	0	47-77	4	1.50	3.00	0	75-77	2	3.12	6.24	0
23-24	3	10.00	20.00	0	48-26	3	3.00	6.00	**6**	76-24	3	0.76	1.52	0
24-23	3	10.00	20.00	0	48-46	5	2.00	4.00	**4**	76-75	2	2.62	5.24	0
24-25	3	1.09	2.18	0	48-79	3	3.23	6.46	0	76-77	3	2.80	5.60	0
24-76	3	0.76	1.52	0	49-26	2	3.72	7.44	0	77-45	3	3.20	6.40	0
25-24	3	1.09	2.18	0	49-28	2	8.74	17.48	0	77-47	4	1.50	3.00	0
25-26	3	10.01	20.02	0	50-30	2	2.93	5.86	0	77-75	2	3.12	6.24	0
25-76	2	0.56	1.12	0	50-51	3	11.45	22.90	0	77-76	3	2.80	5.60	0
26-25	3	10.01	20.02	0	51-31	1	2.40	4.80	0	78-45	3	2.36	4.72	0
26-27	2	8.05	16.1	0	51-50	3	11.45	22.90	0	78-79	3	8.16	16.32	0
26-48	3	3.00	6.00	**6**	51-52	2	5.45	10.90	0	78-80	2	7.74	15.48	0
26-49	2	3.72	7.44	0	52-32	1	2.29	4.58	0	79-48	3	3.23	6.46	0
27-26	2	8.05	16.1	0	52-51	2	5.45	10.90	0	79-78	3	8.16	16.32	0
27-28	3	7.76	15.52	0	52-53	2	7.77	15.54	0	80-78	2	7.74	15.48	0
28-49	2	8.74	17.48	0	53-33	3	2.67	5.34	0	80-81	1	2.28	4.56	0
29-1	2	5.64	11.28	0	53-52	2	7.77	15.54	0	81-43	2	2.67	5.34	0
29-30	2	10.11	20.22	0	53-54	3	5.54	11.08	0	81-80	1	2.28	4.56	0
30-3	2	7.92	15.84	0	54-34	2	2.10	4.20	0	82-6	3	5.60	11.20	0
30-29	2	10.11	20.22	0	54-53	3	5.54	11.08	0	82-32	2	1.76	3.52	0
30-31	2	9.00	18.00	0	54-55	3	2.16	4.32	0	28-27	3	7.76	15.52	0
30-50	2	2.93	5.86	0	54-60	2	5.45	10.90	0	76-25	2	0.56	1.12	0

1

Appendix B.1 Mathematical notations

Notation	Definition
N	The total travel demand
t_1	The time of departure from home in the morning
t_2	Time of departure from the parking space in the evening
t_1^*	The official work start time
t_2^*	The official work closure time
t_s, t_e	The time of departure from home in the morning for the first and the last commuters
α_1	The value of time when travellers are driving AVs
β_1	The penalty cost for a unit time of early arrival at the workplace for morning commutes
γ_1	The penalty cost for a unit time of late arrival at the workplace for morning commutes
γ_2	The penalty cost for a unit time of late departure from the workplace for evening commutes
λ	The value of a unit AV self-driving time
w	The travel time needed to cover a unit distance by AV self-driving without the bottleneck congestion
s	The service capacity at the bottleneck
x	The distance from the workplace to a parking space
x_0	The distance between the workplace and the nearest parking location
$\tilde{x}$	The location of the AV that is the furthest away from the workplace among all the AVs arriving at the bottleneck at time t_2^* in the evening
$\bar{x}$	The parking location for the on-time-arrival morning commute
$\tilde{t}, \bar{t}$	The departure time for morning commute corresponding to the parking locations $\tilde{x}$ and $\bar{x}$.
m	The parking density for autonomous vehicles
m_{UE}, m_{SO}	The optimal AV parking density for the UE and SO traffic patterns
$q_1(t_1)$	The queue length experienced by commuters departing from home at t_1 for morning commutes
$q_2(t_2)$	The queue length experienced by an AV departing from the parking location at time t_2 for evening commutes
$c(t_1, x)$	The individual daily travel cost for a representative commuter who departs from home at t_1 and parks at the location x
$\rho(x)$	The social cost of a unit parking space at location x
TR, TR_1, TR_2	The total toll revenue for daily commute, morning commute and evening commute
TQ_1, TS_1	The total cost of queuing delay and schedule delay for morning commutes
$TP_1(AV)$	The total cost for finding parking spaces via AV self-driving in the morning
$TQ_2(AV)$	The total cost of queuing delay via AV self-driving for evening commutes
$TP_2(AV)$	The total cost for departing from the parking space and leaving the parking area by AV self-driving for evening commutes
TS_2	The total schedule delay cost for late departure in the evening
$TETC_{UE}, TETC_{SO}$	The total evening travel cost at the user equilibrium and at the system optimum
$TDTC_{UE}, TDTC_{SO}$	The total daily travel cost at the user equilibrium and at the system optimum
TSC_{UE}, TSC_{SO}	The total system cost at the user equilibrium and at the system optimum
$TSPC$	The total social parking cost

Appendix B-2. Derivations

Derivation. Scenario 1

In Scenario 1, we have the following three stages:

Stage 1:

For early arrival in the morning and immediate arrival to the inbound bottleneck after work, the individual daily travel cost for a representative commuter who departs from home at t_1 and parks at the location x is

$$c(t_1, x) = \left\{ \alpha_1 \frac{q_1(t_1)}{s} + \beta_1 \left(t_1^* - t_1 - \frac{q_1(t)}{s} \right) + \lambda w(x - x_0) \right\} + \left\{ \lambda w(x - x_0) + (\lambda + \gamma_2)(x - x_0) \frac{m}{s} \right\}. \tag{50}$$

There are two subcases for Stage 1. Firstly, if $r_{1,1}(t_1) > s$, we have $\frac{dc(t_1, x)}{dt_1} = \alpha_1 \frac{r_{1,1}(t_1) - s}{s} - \beta_1 \frac{r_{1,1}(t_1)}{s} + 2\lambda w \frac{r_{1,1}(t_1)}{m} + (\lambda + \gamma_2) \frac{m}{s} \frac{r_{1,1}(t_1)}{m}$. At equilibrium, $\frac{dc(t_1, x)}{dt_1} = 0$. We then have

$$r_{1,1}(t_1) = \frac{\alpha_1}{\alpha_1 - \beta_1 + \frac{2\lambda ws}{m} + \lambda + \gamma_2} s. \tag{51}$$

In this case, $\beta_1 > \frac{2\lambda ws}{m} + \lambda + \gamma_2$ must hold. Hence, if $\beta_1 > \frac{2\lambda ws}{m} + \lambda + \gamma_2$, we have $r_{1,1}(t_1) = \frac{\alpha_1}{\alpha_1 - \beta_1 + \frac{2\lambda ws}{m} + \lambda + \gamma_2} s > s$. The queue length is increasing at Stage 1. Secondly, if $r_{1,1}(t_1) \leq s$, no queue will occur at the bottleneck, i.e. $q_1(t_1) = 0$. We have $\frac{dc(t_1, x)}{dt_1} = -\beta_1 + 2\lambda w \frac{r_{1,1}(t_1)}{m} + (\lambda + \gamma_2) \frac{m}{s} \frac{r_{1,1}(t_1)}{m}$. At equilibrium, $\frac{dc(t_1, x)}{dt_1} = 0$. We then have

$$r_{1,1}(t_1) = \frac{\beta_1}{\frac{2\lambda ws}{m} + \lambda + \gamma_2} s \leq s. \tag{52}$$

In this case, $\beta_1 \leq \frac{2\lambda ws}{m} + \lambda + \gamma_2$ must hold. Hence, if $\beta_1 \leq \frac{2\lambda ws}{m} + \lambda + \gamma_2$, we have $r_{1,1}(t_1) = \frac{\beta_1}{\frac{2\lambda ws}{m} + \lambda + \gamma_2} s \leq s$. The queue length remains zero at Stage 1.

Stage 2:

For early arrival in the morning and late departure after work, we have

$$c(t_1, x) = \left\{ \alpha_1 \frac{q_1(t_1)}{s} + \beta_1 \left(t_1^* - t_1 - \frac{q_1(t_1)}{s} \right) + \lambda w(x - x_0) \right\} + \left\{ \lambda w(x - x_0) + \frac{\gamma_2 N}{s} \right\}. \tag{53}$$

If $r_{1,2}(t_1) > s$, we have $\frac{dc(t_1, x)}{dt} = \alpha_1 \frac{r_{1,2}(t_1) - s}{s} - \beta_1 \frac{r_{1,2}(t_1)}{s} + 2\lambda w \frac{r_{1,2}(t_1)}{m}$. At equilibrium, $\frac{dc(t_1, x)}{dt_1} = 0$. We have

$$r_{1,2}(t_1) = \frac{\alpha_1}{\alpha_1 - \beta_1 + \frac{2\lambda ws}{m}} s. \tag{53}$$

Under the assumption $\beta_1 > \frac{2\lambda ws}{m}$, $r_{1,2}(t_1) = \frac{\alpha_1}{\alpha_1 - \beta_1 + \frac{2\lambda ws}{m}} s > s$ always holds, i.e., congestion exists in Stage 2.

Stage 3:

For late arrival in the morning and late departure after work, we have

$$c(t_1, x) = \left\{ \alpha_1 \frac{q_1(t_1)}{s} + \gamma_1 \left(t_1 + \frac{q_1(t_1)}{s} - t_1^* \right) + \lambda w(x - x_0) \right\} + \left\{ \lambda w(x - x_0) + \frac{\gamma_2 N}{s} \right\}. \tag{54}$$

Considering that the queue has been accumulated in the previous stage(s), the first derivative of $c(t_1, x)$ can then be determined as follows

$$\frac{dc(t_1, x)}{dt_1} = \alpha_1 \frac{r_{1,3}(t_1) - s}{s} + \gamma_1 \frac{r_{1,3}(t_1)}{s} + 2\lambda w \frac{r_{1,3}(t_1)}{m}. \tag{55}$$

At equilibrium, $\frac{dc(t_1, x)}{dt_1} = 0$. We then have

$$r_{1,3}(t_1) = \frac{\alpha_1}{\alpha_1 + \gamma_1 + \frac{2\lambda ws}{m}} s < s. \tag{56}$$

Derivation. Scenario 2

In Scenario 2, we have the following three stages:

Stage 1:

For early arrival in the morning and immediate arrival to the inbound bottleneck after work closure time in the evening, the departure rate $r_{1,1}(t)$ has the same formulation under the same condition as that of Stage 1 in Scenario 1, which is

$$r_{1,1}(t_1) = \begin{cases} \frac{\alpha_1}{\alpha_1 - \beta_1 + \frac{2\lambda ws}{m} + \lambda + \gamma_2} s > s & \text{if } \beta_1 > \frac{2\lambda ws}{m} + \lambda + \gamma_2 \\ \frac{\beta_1}{\frac{2\lambda ws}{m} + \lambda + \gamma_2} s \le s & \text{if } \frac{2\lambda ws}{m} < \beta_1 \le \frac{2\lambda ws}{m} + \lambda + \gamma_2 \end{cases}$$

Stage 2:

For late arrival in the morning and immediate arrival to the inbound bottleneck after work, the individual daily travel cost for a representative commuter who departs from home at t_1 and parks at the location x is

$$c(t_1, x) = \left\{ \alpha_1 \frac{q_1(t_1)}{s} + \gamma_1 \left(t_1 + \frac{q_1(t_1)}{s} - t_1^* \right) + \lambda w(x - x_0) \right\} + \left\{ \lambda w(x - x_0) + (\lambda + \tag{58} \right.$$
$$\left. \gamma_2)(x - x_0) \frac{m}{s} \right\}.$$

Assuming that $r_{1,2}(t_1) > s$, we have $\frac{dc(t_1, x)}{dt_1} = \alpha_1 \frac{r_{1,2}(t_1) - s}{s} + \gamma_1 \frac{r_{1,2}(t_1)}{s} + 2\lambda w \frac{r_{1,2}(t_1)}{m} + \frac{(\lambda + \gamma_2)}{s} r_{1,2}(t_1)$.

At equilibrium, $\frac{dc(t_1, x)}{dt_1} = 0$. Then, we have $r_{1,2}(t_1) = \frac{\alpha_1}{\alpha_1 + \gamma_1 + \gamma_2 + \lambda + \frac{2\lambda ws}{m}} s < s$. This equation contradicts with the assumption $r_{1,2}(t_1) > s$. Thus, we have $r_{1,2}(t_1) \le s$ at Stage 2 in Scenario 2. Then, we can re-

3

evaluate the individual daily travel cost as follows.

Firstly, if $\beta_1 > \frac{2\lambda ws}{m} + \lambda + \gamma_2$ at Stage 1, $q_1(t_1) > 0$. We have $\frac{dc(t_1,x)}{dt_1} = \alpha_1 \frac{r_{1,2}(t_1)-s}{s} + \gamma_1 \frac{r_{1,2}(t_1)}{s} + 2\lambda w \frac{r_{1,2}(t_1)}{m} + \frac{(\lambda+\gamma_2)}{s} r_{1,2}(t_1)$. At equilibrium, $\frac{dc(t_1,x)}{dt_1} = 0$. We then have $r_{1,2}(t_1) = \frac{\alpha_1}{\alpha_1 + \gamma_1 + \gamma_2 + \lambda + \frac{2\lambda ws}{m}} s < $

s. Secondly, if $\beta_1 \le \frac{2\lambda ws}{m} + \lambda + \gamma_2$ at Stage 1, $q_1(t_1) = 0$. We have $c(t_1,x) = \{\gamma_1(t_1 - t_1^*) + \lambda w(x - x_0)\} + \{\lambda w(x - x_0) + (\lambda + \gamma_2)(x - x_0)\frac{m}{s}\}$ and $\frac{dc(t_1,x)}{dt_1} = \gamma_1 + 2\lambda w \frac{r_{1,2}(t_1)}{m} + \frac{(\lambda+\gamma_2)}{s} r_{1,2}(t_1)$.

At equilibrium, $\frac{dc(t_1,x)}{dt_1} = 0$. We then have $r_{1,2}(t_1) = -\frac{\gamma_1}{\frac{2\lambda w}{m} + \frac{\lambda+\gamma_2}{s}} < 0$. However, $r_{1,2}(t_1)$ must be

nonnegative. This means that for Scenario 2, at equilibrium, the condition $\beta_1 > \frac{2\lambda ws}{m} + \lambda + \gamma_2$ must be satisfied. This is consistent with the conclusion drawn from the presented analysis in Section 3.3.2.1, which states that if $\frac{2\lambda ws}{m} < \beta_1 \le \frac{2\lambda ws}{m} + \lambda + \gamma_2$, Case 1 of Scenario 1 must occur.

Stage 3:

For late arrival in the morning and late departure after work, we have

$$c(t_1,x) = \left\{\alpha_1 \frac{q_1(t_1)}{s} + \gamma_1\left(t + \frac{q_1(t_1)}{s} - t_1^*\right) + \lambda w(x - x_0)\right\} + \left\{\lambda w(x - x_0) + \frac{\gamma_2 N}{s}\right\}. \qquad (58)$$

At equilibrium, there will be a queue at the inbound bottleneck at the end of Stage 2. For Stage 3, we have $\frac{dc(t_1,x)}{dt_1} = \alpha_1 \frac{r_{1,3}(t_1)-s}{s} + \gamma_1 \frac{r_{1,3}(t_1)}{s} + 2\lambda w \frac{r_{1,3}(t_1)}{m} = 0$. We then have

$$r_{1,3}(t_1) = \frac{\alpha_1}{\alpha_1 + \gamma_1 + \frac{2\lambda ws}{m}} s < s.$$